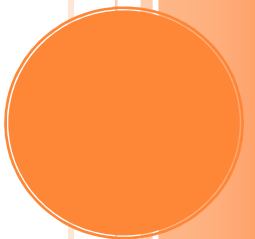


PPM 2011



INDEX: INVITED CONTRIBUTIONS

	pag
Javier Aizpurua (CSIC-UPV/EHU & DIPC, Spain) <i>"Plasmonic nanoantennas: building blocks for nanoscale control of optical fields"</i>	395
Harry Atwater (Caltech, USA) <i>"Artificial Photonic Materials to Challenge Conventional Limits to Light Trapping and Solar Energy Conversion"</i>	401
Nader Engheta (Univ of Pennsylvania, USA) <i>"Merging Electronics and Photonics Using Metamaterials"</i>	419
Shanhui Fan (Stanford University, USA) <i>"Title not available"</i>	-
Emmanuel Hadji (CEA, France) <i>"On chip light handling with single and twinned nanobeam cavities"</i>	433
Evelyn Hu (Harvard SEAS, USA) <i>"Gap-Mode Plasmonic Cavities: Engineering Light-Matter Interactions in Metallic Structures"</i>	435
Mitsuteru Inoue (Toyohashi Univ of Technology, Japan) <i>"Magnetophotonics and its applications"</i>	-
Thomas F Krauss (University of St. Andrews, UK) <i>"Photonic crystal nanocavities: Efficient light-matter interaction at the nanoscale"</i>	439
Luis M. Liz-Marzan (Universidad de Vigo, Spain) <i>"Hot spots and confinement in metal nanoparticles and assemblies"</i>	447
John Pendry (Imperial College London, UK) <i>"Transformation Optics at Optical Frequencies"</i>	455
Theo Rasing (Radboud Univ, The Netherlands) <i>"Ultrafast optical manipulation of magnetic order: challenges and opportunities"</i>	457
Alexei Tchelnov (CEA, France) <i>"Title not available"</i>	-
Paolo Vavassori (CIC nanoGUNE Consolider, Spain) <i>"Magnetic information in the Light Diffracted by Arrays of Nanometer-scale Magnets"</i>	473

INDEX: INVITED CONTRIBUTIONS (NANOMAGMA SESSION)

	pag
Bernard Dieny (SPINTEC, France) <i>"Title not available"</i>	-
Chiraz Frydman (HORIBA Scientific, France) <i>"Real time, multiplex and label-free Bio-interaction analysis by Surface Plasmon Resonance imaging"</i>	425
Harald Giessen (University of Stuttgart, Germany) <i>"Three-dimensional optical metamaterials and nanoantennas: Chirality, Coupling, and Sensing"</i>	429
Vasily Temnov (MIT, USA) <i>"Ultrafast acousto-magneto-plasmonics in hybrid metal-ferromagnet multilayer structures"</i>	469

INDEX: ORAL CONTRIBUTIONS

	pag
Pablo Alonso-González (CIC nanoGUNE, Spain) <i>"Mapping Near-Field Coupling Effects in Infrared Gap Antennas"</i>	397
Ashod Aradian (Centre de Recherche Paul Pascal, France) <i>"Unusual spectral response of loss-compensated plasmonic nanoparticles in active gain media"</i>	399
Patrice Baldeck (LIPhy CNRS, France) <i>"Two-photon laser fabrication of 3D silver nanowire microstructures and their plasmonic applications"</i>	403
Alvaro Blanco (Instituto de Ciencia de Materiales de Madrid (CSIC), Spain) <i>"Synthetic Opals and Sandcastles: Exploring Water at the Nanoscale"</i>	405
Jianing Chen (CIC nanoGUNE, Spain) <i>"Ferromagnetic Plasmonic Nanoantennas"</i>	409
Alexander Chizhik (Universidad del País Vasco, Spain) <i>"Magneto-optical study of magnetic microwires: domain structure, domain walls motion, magnetization reversal."</i>	411

INDEX: ORAL CONTRIBUTIONS

	pag
Alasdair Clark (University of Glasgow, United Kingdom) <i>"Nanogap Ring Antennae as Plasmon Coupled, Dichroic SERRS Substrates for Biosensing"</i>	413
Cesar de Julian Fernandez (INSTM - Univ. Firenze, Italy) <i>"Coupling between localized surface plasmon resonance and magnetic properties of nanoparticles, the effect in the reversal process"</i>	415
Anne Debarre (Lab. Aimé Cotton, France) <i>"Signature of the anisotropy of two-photon excited luminescence of nearly spherical gold particles diffusing in solution"</i>	417
Josep Ferré Borrull (Universitat Rovira i Virgili, Spain) <i>"Nanostructured silicon surfaces by self-assembled nanoporous anodic alumina for photonic applications"</i>	421
Luis S. Froufe-Pérez (UAM, Spain) <i>"Limits of light focusing through turbid media"</i>	423
Juan Galisteo-López (ICMM-CSIC, Spain) <i>"Light propagation in self-assembled hybrid metallodielectric structures"</i>	427
Raquel Gómez-Medina (Universidad Autónoma de Madrid, Spain) <i>"Interference between electric and magnetic dipoles in dielectric spheres: Scattering anisotropy and optical forces."</i>	431
Kuntheak Kheng (CEA-Grenoble and Univ. of Grenoble, France) <i>"Bright CdSe/ZnSe nanowire-quantum dots for single photons emission"</i>	437
Christoph Langhammer (Chalmers University of Technology, Sweden) <i>"Indirect Nanoplasmonic Sensing for Nanomaterials Science"</i>	441
Marco Leonetti (CSIC, Spain) <i>"Measuring light diffusion in thin leaky systems"</i>	443
Fred Lisdat (Technical University Wildau, Germany) <i>"Photobioelectrochemical sensors based on the combination of quantum dot electrodes with enzyme reactions"</i>	445
Enrique Macia (UCM, Spain) <i>"Exploiting aperiodic order in photonic devices"</i>	449
Maria Grazia Manera (CNR-IMM Lecce, Italy) <i>"Magneto-Plasmonic Nanostructured Materials For Gas Sensors Applications"</i>	451
Tetyana Nychporuk (Lyon Institute of Nanotechnology (INL), France) <i>"Strong photoluminescence enhancement of Si and SiC quantum dots by their resonant coupling with multi-polar plasmonic hot spots"</i>	453
Ida Ros (University of Padova, Italy) <i>"Surface Enhanced Raman Spectroscopy of different chain length PEP+ moiety bound to Nanorods"</i>	459
Jose A. Sánchez-Gil (CSIC, Spain) <i>"Designing plasmon nanoparticles tailored for applications in nanophotonics"</i>	463
Titus Sandu (National Institute for Research and Development in Microtechnologies, Romania) <i>"The effect of shape and structure variation of metallic nanoparticles on localized plasmon resonances"</i>	465
Thierry Taliercio (University Montpellier 2, France) <i>"Nanostructured arrays of doped semiconductors for IR nanophotonics"</i>	467
Veronica Toccafondo (Universidad Politécnica de Valencia, Spain) <i>"Development of high sensitivity biosensors using SOI photonic crystal waveguides"</i>	471

INDEX: ORAL CONTRIBUTIONS (NANOMAGMA SESSION)

	pag
Lionel Aigouy (LPEM-ESPCI-CNRS, France) <i>"Light Localization on a Gold Nanodisk Array Probed by Near-Field Optics"</i>	393
Alfonso Cebollada (IMM-CNM-CSIC, Spain) <i>"Internal electromagnetic field distribution and magneto-optical activity of metal and metal-dielectric magnetoplasmonic nanodisks"</i>	407
Juan Jose Saenz (Universidad Autonoma de Madrid, Spain) <i>"Magneto-Optical properties of nanostructured thin films"</i>	461
Rémi Vincent (Institut Langevin, ESPCI ParisTech, France) <i>"Controlling fluorescence resonant energy transfer with a magneto-optical nanoantenna"</i>	475

ALPHABETICAL ORDER

I: Invited / IN: Invited NANOMAGMA Session / O: Oral / ON: Oral NANOMAGMA Session

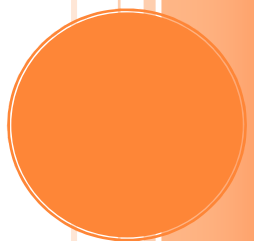
		pag
Lionel Aigouy (LPEM-ESPCI-CNRS, France) <i>"Light Localization on a Gold Nanodisk Array Probed by Near-Field Optics"</i>	ON	393
Javier Aizpurua (CSIC-UPV/EHU & DIPC, Spain) <i>"Plasmonic nanoantennas: building blocks for nanoscale control of optical fields"</i>	I	395
Pablo Alonso-González (CIC nanoGUNE, Spain) <i>"Mapping Near-Field Coupling Effects in Infrared Gap Antennas"</i>	O	397
Ashod Aradian (Centre de Recherche Paul Pascal, France) <i>"Unusual spectral response of loss-compensated plasmonic nanoparticles in active gain media"</i>	O	399
Harry Atwater (Caltech, USA) <i>"Artificial Photonic Materials to Challenge Conventional Limits to Light Trapping and Solar Energy Conversion"</i>	I	401
Patrice Baldeck (LIPhy CNRS, France) <i>"Two-photon laser fabrication of 3D silver nanowire microstructures and their plasmonic applications"</i>	O	403
Alvaro Blanco (Instituto de Ciencia de Materiales de Madrid (CSIC), Spain) <i>"Synthetic Opals and Sandcastles: Exploring Water at the Nanoscale"</i>	O	405
Alfonso Cebollada (IMM-CNM-CSIC, Spain) <i>"Internal electromagnetic field distribution and magneto-optical activity of metal and metal-dielectric magnetoplasmonic nanodisks"</i>	O	407
Jianing Chen (CIC nanoGUNE, Spain) <i>"Ferromagnetic Plasmonic Nanoantennas"</i>	O	409
Alexander Chizhik (Universidad del País Vasco, Spain) <i>"Magneto-optical study of magnetic microwires: domain structure, domain walls motion, magnetization reversal."</i>	O	411
Alasdair Clark (University of Glasgow, United Kingdom) <i>"Nanogap Ring Antennae as Plasmon Coupled, Dichroic SERRS Substrates for Biosensing"</i>	O	413
Cesar de Julian Fernandez (INSTM - Univ. Firenze, Italy) <i>"Coupling between localized surface plasmon resonance and magnetic properties of nanoparticles, the effect in the reversal process"</i>	O	415
Anne Debarre (Lab. Aimé Cotton, France) <i>"Signature of the anisotropy of two-photon excited luminescence of nearly spherical gold particles diffusing in solution"</i>	O	417
Bernard Diény (SPINTEC, France) <i>"Title not available"</i>	IN	-
Nader Engheta (Univ of Pennsylvania, USA) <i>"Merging Electronics and Photonics Using Metamaterials"</i>	I	419
Shanhui Fan (Stanford University, USA) <i>"Title not available"</i>	I	-
Josep Ferré Borrull (Universitat Rovira i Virgili, Spain) <i>"Nanostructured silicon surfaces by self-assembled nanoporous anodic alumina for photonic applications"</i>	O	421
Luis S. Froufe-Pérez (UAM, Spain) <i>"Limits of light focusing through turbid media"</i>	O	423
Chiraz Frydman (HORIBA Scientific, France) <i>"Real time, multiplex and label-free Bio-interaction analysis by Surface Plasmon Resonance imaging"</i>	IN	425
Juan Galisteo-López (ICMM-CSIC, Spain) <i>"Light propagation in self-assembled hybrid metallodielectric structures"</i>	O	427
Harald Giessen (University of Stuttgart, Germany) <i>"Three-dimensional optical metamaterials and nanoantennas: Chirality, Coupling, and Sensing"</i>	IN	429
Raquel Gómez-Medina (Universidad Autónoma de Madrid, Spain) <i>"Interference between electric and magnetic dipoles in dielectric spheres: Scattering anisotropy and optical forces."</i>	O	431

I: Invited / IN: Invited NANOMAGMA Session / O: Oral / ON: Oral NANOMAGMA Session

		pag
Emmanuel Hadji (CEA, France) <i>"On chip light handling with single and twinned nanobeam cavities"</i>	I	433
Evelyn Hu (Harvard SEAS, USA) <i>"Gap-Mode Plasmonic Cavities: Engineering Light-Matter Interactions in Metallic Structures"</i>	I	435
Mitsuteru Inoue (Toyohashi Univ of Technology, Japan) <i>"Magnetophotonics and its applications"</i>	I	-
Kuntheak Kheng (CEA-Grenoble and Univ. of Grenoble, France) <i>"Bright CdSe/ZnSe nanowire-quantum dots for single photons emission"</i>	O	437
Thomas F Krauss (University of St. Andrews, UK) <i>"Photonic crystal nanocavities: Efficient light-matter interaction at the nanoscale"</i>	I	439
Christoph Langhammer (Chalmers University of Technology, Sweden) <i>"Indirect Nanoplasmonic Sensing for Nanomaterials Science"</i>	O	441
Marco Leonetti (CSIC, Spain) <i>"Measuring light diffusion in thin leaky systems"</i>	O	443
Fred Lisdat (Technical University Wildau, Germany) <i>"Photobioelectrochemical sensors based on the combination of quantum dot electrodes with enzyme reactions"</i>	O	445
Luis M. Liz-Marzan (Universidad de Vigo, Spain) <i>"Hot spots and confinement in metal nanoparticles and assemblies"</i>	I	447
Enrique Macia (UCM, Spain) <i>"Exploiting aperiodic order in photonic devices"</i>	O	449
Maria Grazia Manera (CNR-IMM Lecce, Italy) <i>"Magneto-Plasmonic Nanostructured Materials For Gas Sensors Applications"</i>	O	451
Tetyana Nychporuk (Lyon Institute of Nanotechnology (INL), France) <i>"Strong photoluminescence enhancement of Si and SiC quantum dots by their resonant coupling with multi-polar plasmonic hot spots"</i>	O	453
John Pendry (Imperial College London, UK) <i>"Transformation Optics at Optical Frequencies"</i>	I	455
Theo Rasing (Radboud Univ, The Netherlands) <i>"Ultrafast optical manipulation of magnetic order: challenges and opportunities"</i>	I	457
Ida Ros (University of Padova, Italy) <i>"Surface Enhanced Raman Spectroscopy of different chain length PEP+ moiety bound to Nanorods"</i>	O	459
Juan Jose Saenz (Universidad Autonoma de Madrid, Spain) <i>"Magneto-Optical properties of nanostructured thin films"</i>	ON	461
Jose A. Sánchez-Gil (CSIC, Spain) <i>"Designing plasmon nanoparticles tailored for applications in nanophotonics"</i>	O	463
Titus Sandu (National Institute for Research and Development in Microtechnologies, Romania) <i>"The effect of shape and structure variation of metallic nanoparticles on localized plasmon resonances"</i>	O	465
Thierry Taliercio (University Montpellier 2, France) <i>"Nanostructured arrays of doped semiconductors for IR nanophotonics"</i>	O	467
Alexei Tchelnokov (CEA, France) <i>"Title not available"</i>	I	-
Vasily Temnov (MIT, USA) <i>"Ultrafast acousto-magneto-plasmonics in hybrid metal-ferromagnet multilayer structures"</i>	IN	469
Veronica Toccafondo (Universidad Politécnica de Valencia, Spain) <i>"Development of high sensitivity biosensors using SOI photonic crystal waveguides"</i>	O	471
Paolo Vavassori (CIC nanoGUNE Consolider, Spain) <i>"Magnetic information in the Light Diffracted by Arrays of Nanometer-scale Magnets"</i>	I	473
Rémi Vincent (Institut Langevin, ESPCI ParisTech, France) <i>"Controlling fluorescence resonant energy transfer with a magneto-optical nanoantenna"</i>	ON	475

PPM 2011

ABSTRACTS
ALPHABETICAL ORDER



LIGHT LOCALIZATION ON A GOLD NANODISK ARRAY PROBED BY NEAR-FIELD OPTICS

L. Aigouy¹, L. Lalouat¹, P. Prieto², A. Vitrey², A. Cebollada², M.U. González², A. García-Martín²

¹LPEM, UMR 8213 CNRS-ESPCI, 10 rue Vauquelin, 75231 Paris cedex 5, France

²IMM (CNM-CSIC), Isaac Newton 8, PTM, Tres Cantos, E-28760 Madrid, Spain

lionel.aigouy@espci.fr

By near-field optics, we have studied the localization of light on an array of metallic nanoparticles illuminated in a transmission mode. The array is made of 286 nm-wide and 50 nm-high gold nanodisks with a period of 500 nm. The SNOM probe is a fluorescent particle which detects the near-field on the surface. We will show that the measured local field is situated between adjacent nanodisks and in a direction parallel to the polarization of the incident light. By performing scans in a direction perpendicular to the surface, we have also observed that the light intensity strongly decays above the sample surface showing a 3D localization. All the experimental results are in very good agreement with numerical simulations performed by the FDTD method and by taking into account the size of the near-field probe.

Figures:

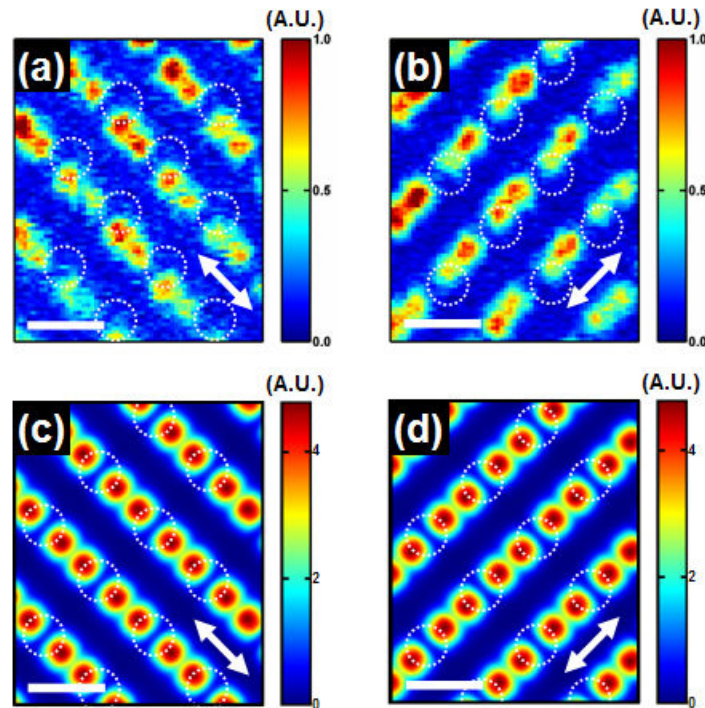


Figure 1: (a,b) SNOM images measured in a non-contact mode on the nanodisk array at a wavelength of 975 nm. The dotted circles indicate the position of the disks. (c,d) FDTD calculations of the near-field distribution on the structures. The calculation represents the square of the intensity of the total field which is the quantity measured with the near-field fluorescent probe used in the experiments. The calculations has been performed by taking into account of the probe size (a 160 nm large cube). The white arrows indicate the incident polarization direction. The scale bar is 500 nm-long.

PLASMONIC NANOANTENNAS: BUILDING BLOCKS FOR NANOSCALE CONTROL OF OPTICAL FIELDS

Javier Aizpurua

Center for Materials Physics CSIC-UPV/EHU and Donostia International Physics Center DIPC,
Paseo Manuel Lardizabal 5, Donostia-San Sebastián 20018, Spain
aizpurua@ehu.es

Optical antennas or plasmonic antennas are nanoscale metallic structures which act as effective receivers, transmitters and receivers of visible light. Different canonical nanostructures such as metallic nanorings [1], nanorods [2], nanowires [3], dimers [4] or nanoshells [5] are commonly used as optical nanoantennas. These nanoantennas show the ability to focus electromagnetic radiation into tiny spots of nanometer-scale dimensions allowing for more effective field-enhanced visible spectroscopies such as in surface-enhanced Raman spectroscopy (SERS) or in SEIRA. We will address here the optical response of these nanoantennas in a variety of configurations.

We will show theoretically and experimentally how the optical response of a nanoantenna can be engineered through the manipulation of the antenna gap, bridging together concepts of optics and circuit theory [6-9]. With use of similar concepts, we also analyze theoretically the concept of ultrafast optical switches based on nonlinear plasmonic nanoantennas. We explore the use of a photoconductive load at the antenna gap to act as an effective optical nanoswitcher. The principle of switching is based on the transition from capacitive to conductive coupling between two plasmon modes when bringing two nanoparticles into physical contact, as schematically shown in Fig. 1a. We show that photoexcited free carriers in a semiconductor material can be used as a load to short circuit the antenna arms, leading to a strong modification of both the spectral resonance structure (Fig 1b) and near-field mode-profile (Fig 1c-d). As the plasmonic antenna switch is based on a strong confinement of optical fields in space rather than in time, the nanoantenna switch can operate at very low switching energy while potentially reaching a much faster response than microphotonic switching devices.

Another spectroscopy where the role of plasmonic resonances plays an important role is Raman-Brillouin scattering of single metallic nano-objects [10]. The interaction between the vibrations of a metallic nano-object and the plasmons induced on it determine the activation and deactivation of certain vibrational modes in the Raman scattering. To illustrate the wide range of applications of plasmonic interactions in totally different systems, we will conclude by analysing the forces originated from the excitation of plasmons by the fast electron beam in Scanning Transmission Electron Microscopy (STEM) [11]. Our model calculations show that metallic nanoparticles experience attractive or repulsive forces as a function of the position of the electron beam. This ability to manipulate the forces on the particles can be used in gold nanoparticles for example to produce coalescence.

From the overview and the examples shown here, it is straightforward to conclude that an understanding of the interactions occurring at the optical nanoantennas in such a variety of systems, and the knowledge on the electromagnetic response occurring in the different spectroscopy and microscopy configurations are crucial to engineer and design plasmonic devices for improved detection and controlled optical response.

References:

[1] J. Aizpurua et al. Phys. Rev. Lett. 90 (2003) 057401.
 [2] J. Aizpurua et al. Phys. Rev. B. 71 (2005) 235420.
 [3] F. Neubrech et al. Appl. Phys. Lett. 89 (2006) 253104.
 [4] I. Romero et al. Optics Express 14, (2006) 9988.
 [5] B. Lassiter et al. Nano Letters 8, (2008) 1212.
 [6] A. Alù and N. Engheta, Nat. Phot. 2, (2008) 307-310.
 [7] M. Schnell et al. Nature Photonics 3, (2009) 287-291.
 [8] N. Large, M. Abb, J. Aizpurua, and O. Muskens, Nano Letters. (2010) 10, 1741-1746.
 [9] O. Pérez-González et al. Nano Letters. 10, (2010) 3090.
 [10] N. Large et al. Nano Letters 9 (2009) 3732.
 [11] A. Reyes-Coronado et al. Phys. Rev. B 82 (2010) 235429.

Figures:

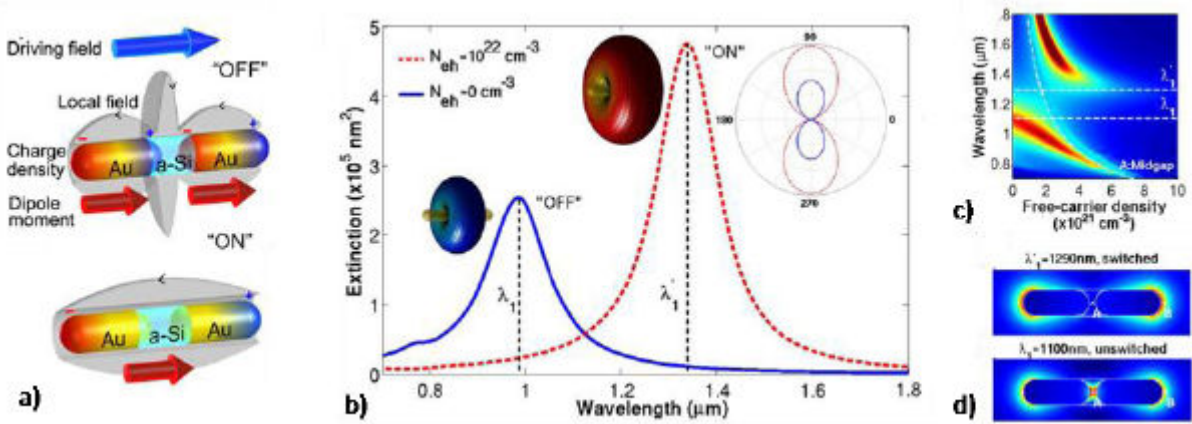


Figure 1: Figure: a) Schematics of the surface charge density in an "OFF" and "ON" nanoantenna switching situation. b) Extinction spectrum for "OFF" and "ON" switches. c) Near-Field peaks positions as a function of free-carrier concentration. d) Near-field distribution for the "ON" situation at $\lambda=1290\text{nm}$ and "OFF" situation at $\lambda=1100\text{nm}$.

MAPPING NEAR-FIELD COUPLING EFFECTS IN INFRARED GAP ANTENNAS

P. Alonso-González¹, P. Albella^{1,2}, L. Arzubiaga¹, M. Schnell¹, J. Chen^{1,2}, F. Huth¹, F. Golmar¹, F. Casanova^{1,3}, L. Hueso^{1,3}, J. Aizpurua², and R. Hillenbrand^{1,3}

¹CIC nanoGUNE Consolider, 20018 Donostia-San Sebastián, Spain

²Centro de Física de Materiales (CSIC-UPV/EHU) and Donostia International Physics Center (DIPC), 20018 Donostia-San Sebastián, Spain

³IKERBASQUE, Basque Foundation for Science, 48011 Bilbao, Spain
palonso@nanogune.eu

The vector near-field distribution of infrared gap antennas (linear dipole antennas coupled via a nanometric gap) is mapped by scattering-type scanning near-field microscopy (s-SNOM). The images provide direct experimental evidence of strong in-plane near-field localization inside a gap as small as 50 nm. By measuring the gap fields as a function of the total antenna length (near-field spectroscopy), we observe a clear resonance shift compared to uncoupled linear dipole antennas, thus verifying strong near-field coupling via the gap. We also find significant differences between near-field and far-field spectra of the antennas and discuss their implications.

Vector near-field imaging of the infrared antennas [1, 2] was carried out with s-SNOM where s-polarized laser light is used for antenna excitation. A dielectric Si tip scatters the local near fields of the antennas. Interferometric and polarization-resolved detection of the tip-scattered light yields amplitude E and phase ϕ of the in- (x) and out-of-plane (z) near-field components (E_x, ϕ_x) and (E_z, ϕ_z).

Fig. 1 shows the near-field patterns obtained for a single gap antenna with a gap width of about 50 nm. The out-of-plane near-field component (E_z, ϕ_z) shows large near-field amplitudes at both sides of the gap, while a phase jump of about 180° occurs at the gap center [3]. The in-plane near-field component (E_x, ϕ_x), in contrast, is strongly enhanced exactly inside the gap and directly verifies field concentration inside the gap.

To provide experimental evidence of near-field coupling in the infrared gap antennas, we perform near-field spectroscopy. We fabricate gap antennas of different total length (but constant gap size) and measure the in-plane gap field as a function of the antenna length. A comparison with near-field spectra of single dipole antennas (continuous nanorods) shows a pronounced resonance shift, which clearly verifies near-field coupling across the antenna gap.

Our results show that vector near-field mapping is a powerful tool for measuring spectral resonance shifts in the near field of infrared antennas, in both amplitude and phase. This enables detailed studies of near-field coupling signatures, including the mapping of strongly localized field enhancement (“hot spots”) and resonance shifts of near-field spectra, which are not accessible by far-field spectroscopy.

References:

- [1] Schnell, M.; García-Etxarri, A.; Alkorta, J.; Aizpurua, J.; Hillenbrand, R. *Nano Lett.*, 10 (9) (2010), 3524–3528.
- [2] Olmon R. L., Rang, M.; Krenz, P. M.; Lail, B. A.; Saraf, L. V.; Boreman, G. D.; Raschke, M. B. *Phys. Rev. Lett.*, 105 (2010), 167403.
- [3] Schnell, M.; García-Etxarri, A.; Huber, A. J.; Crozier, K.; Aizpurua, J.; Hillenbrand, R. *Nat. Photonics*, 3 (2009), 287–291.

Figures:

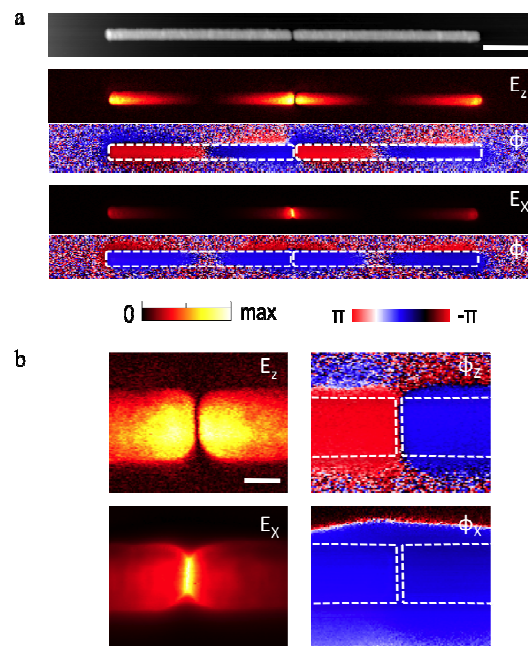


Figure 1: Near-field images of an infrared gap-antenna recorded at $\lambda=11.06\mu\text{m}$. (a) Out-of-plane near-field amplitude E_z and phase ϕ_z (top). In-plane near-field amplitude E_x and phase ϕ_x (bottom). Scale bar is $1\ \mu\text{m}$. (b) Enlarged near-field images of the gap region, showing amplitude and phase of the out-of-plane and in-plane near-field components. Scale bar is $100\ \text{nm}$.

UNUSUAL SPECTRAL RESPONSE OF LOSS-COMPENSATED PLASMONIC NANOPARTICLES IN ACTIVE GAIN MEDIA

A. Veltri, A. Aradian

Centre de Recherche Paul Pascal - CNRS & University of Bordeaux
115 av. du Dr Schweitzer 33600 Pessac, France
veltri@crpp-bordeaux.cnrs.fr; aradian@crpp-bordeaux.cnrs.fr

While based on phenomena recognized and described almost one and a half century ago [1], the physics of plasmons in metal nanoparticles has been recently fueled by the rapid development of new techniques for producing small particles and by the applicability of these structure in the realization of visible range metamaterials. One of the main issues in using metallic nano-structures for metamaterial applications at optical frequencies is their high level of losses. A most promising strategy to circumvent this obstacle is loss compensation, where the structures are coupled to active compounds (such as pumped dye molecules or quantum dots) which are able to transfer them energy and therefore amplify the desired response. Research along this line has recently gained momentum, resulting for example in the first demonstration of a nanoscale spaser using gain-assisted core-shell nanoparticles [2]. In this work, we study the apparently simple situation of a single metallic nanoparticle immersed in a gain medium with a focus on the plasmonic response, and show that interesting effects already arise with surprising modifications of the plasmonic spectral response.

We studied the behavior of a metallic nanosphere of radius r made of a metal of permittivity $\epsilon_1 = \epsilon_1' + i\epsilon_1''$ (based on the experimental data from [3]) surrounded by an active (externally pumped) dielectric host with permittivity $\epsilon_2 = \epsilon_2' + i\epsilon_2''$ (with $\epsilon_2'' < 0$ for gain). We here focus on the polarisability of the particle with respect to the outside medium. In the presence of gain, this is given in the quasi-static limit as:

$$\alpha = \alpha' + i\alpha'' = 4\pi r^3 (\epsilon_2' + i\epsilon_2'') \frac{(\epsilon_1' + i\epsilon_1'') - (\epsilon_2' + i\epsilon_2'')}{(\epsilon_1' + i\epsilon_1'') + 2(\epsilon_2' + i\epsilon_2'')}$$

The plasmon resonance appears at the frequency ω_0 where $2\epsilon_2' = -\epsilon_1'$. As proposed in [4], perfect loss compensation is then obtained when the gain level is exactly adjusted ($2\epsilon_2'' = -\epsilon_1''$) at this same frequency: one then recovers a singular response. It is obviously highly desirable to obtain such a high amplitude plasmon in order to exacerbate the overall metamaterial response. However, our work points out that this singular behavior is intrinsically different from the ideal plasmon obtained from a lossless metal: in the latter case, the imaginary response $\alpha''(\omega)$ is a Dirac peak (resonant losses are confined to a very narrow spectral region), while in the perfectly-compensated plasmon $\alpha''(\omega)$ takes on a spectrally wide, $1/(\omega - \omega_0)$ behavior (Fig. 1-b and 1-f). To the best of our knowledge, this has remained unnoticed but has important implications, since it means that even with perfect loss compensation, resonant losses can be mitigated but they do *not* simply vanish away.

Moving away from the perfect compensation point by adding or removing gain, more unusual, and sometimes surprising features appear. Mathematically, this comes from the fact that the equations for the real and the imaginary part of polarizability are more similar in presence of external gain than in the absence of it, which gives rise to new behaviours. One striking example happens if, at the Plasmon frequency, we have $\epsilon_2''(\omega_0) = -\epsilon_1''(\omega_0)$ as shown in Fig. 1-c and 1-e. In this situation, the real part $\alpha'(\omega)$ takes on a bell shape, while the imaginary part $\alpha''(\omega)$ has a zig-zag shape. This is exactly opposite to the usual plasmon case (Fig. 1-a and 1-d) where – as is well-known from textbooks for any type of passive resonator – the *real* part should be zig-zagging and the *imaginary* part should be bell-shaped. We call this new behavior an “anti-plasmon”.

Beyond the peculiarity of this “anti-plasmon” behaviour, an interesting point is that where the real part of the polarisability is maximum, losses are zero (again in contrast with conventional plasmons, Fig. 1-a and 1-d). In Fig. 1-c, for example, one observes strongly negative response with low loss around the plasmon resonance, a property that could be most interesting if one is interested in metamaterials with negative properties based on such resonant elements. Note that the “anti-plasmons” can have either positive or negative real parts (Fig. 1-e and 1-c): this depends if, for the specific system considered,

the condition for the anti-plasmon ($\epsilon_2'' = -\epsilon_2'$) is met at gain levels higher (Fig. 1, upper row) or lower (lower row) than the condition for perfect loss-compensation ($\epsilon_2'' = -1/2\epsilon_1''$).

Although our approach relies on a very simple theoretical description, it is worthwhile noting that related behaviour appears, although left unnoticed by the authors, in much more sophisticated approaches (full FDTD simulations of split-ring resonators in active medium) [5].

Our work therefore underlines that the behaviours of loss-compensated plasmonic particles can be both unusual and richer than the usual case without gain, and that some of these could find, if confirmed in experiments, some potential applications in metamaterial designs.

This work was supported by the FP7-NMP-2008 European project METACHEM and the SAMM project of the GIS-Advanced Materials in Aquitaine network.

References:

- [1] M. Faraday. Philos. Trans. R. Soc. London, 147 (1857).
- [2] M. A. Noginov et al., Nature, 460 (2009) 1110.
- [3] P. B. Johnson and R. W. Christy, Phys. Rev. B, 6 (1972) 4370.
- [4] N. M. Lawandy. Appl. Phys. Lett., 85 (2004) 5040.
- [5] A. Fang et al., J. Optics, 12 (2010) 024013.

Figures:

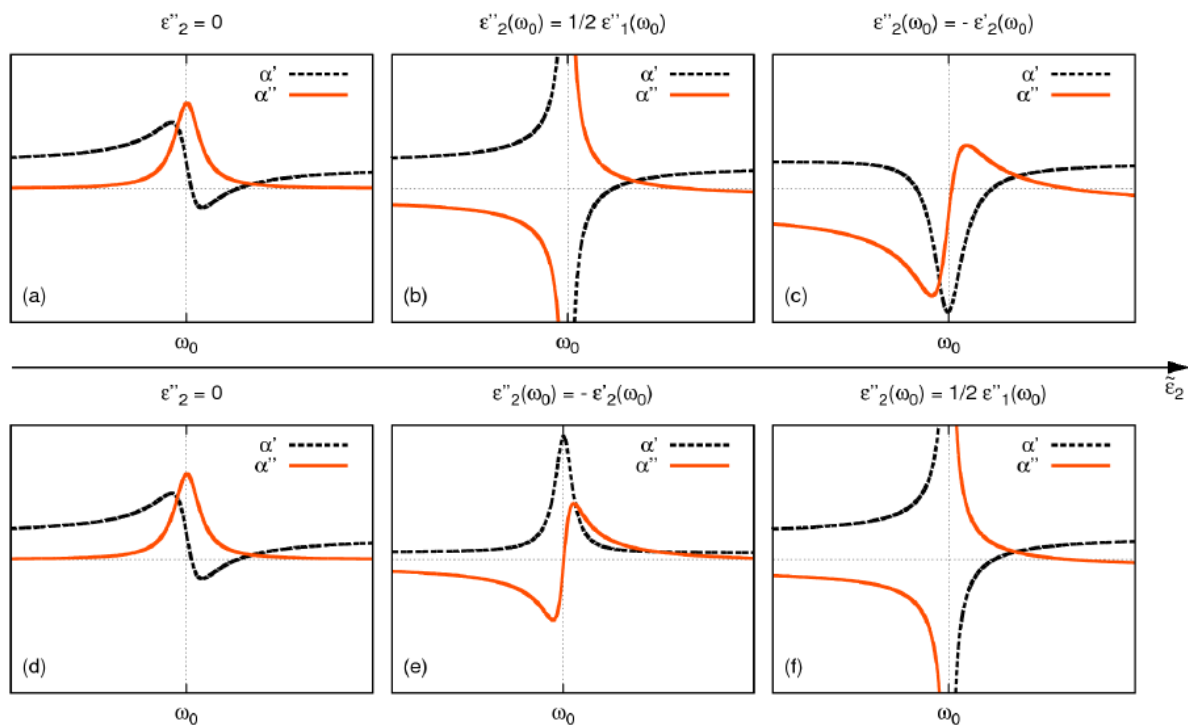


Figure 1: *Polarisability of a spherical nanoparticle in an active gain medium, with increasing gain levels from left to right. (a) and (d): Conventional plasmon resonance without gain. (b) and (f): when perfect loss compensation is obtained a $1/(\omega - \omega_0)$ behavior is obtained both for the real and the imaginary part. (c) and (e): when $\epsilon_2''(\omega_0) = -\epsilon_2'(\omega_0)$ an anti plasmon appear. The sign of the real part of the polarizability in a anti-plasmon resonance depends if it appears after the perfect loss compensation (a-c) or before it (d-f).*

ARTIFICIAL PHOTONIC MATERIALS TO CHALLENGE CONVENTIONAL LIMITS TO LIGHT TRAPPING AND SOLAR ENERGY CONVERSION

Harry A. Atwater, Jeremy N. Munday, Dennis M. Callahan, Emily Kosten

Kavli Nanoscience Institute and Thomas J. Watson Laboratories of Applied Physics,
California Institute of Technology, Pasadena, CA, USA

Solar energy is currently enjoying substantial growth and investment, owing to worldwide sensitivity to energy security and climate change, and this has spurred basic research on light-matter interactions relevant to solar energy. Artificial photonic materials can enhance light-trapping and absorption, as well as increase the open circuit voltage and enhance quantum efficiency in solar photovoltaic structures. We describe photonic approaches for designing thin film and wire array solar cells that have light-trapping intensity and absorption enhancements that can exceed the conventional ergodic light-trapping limit using both wave optics and ray optics methods.

From thermodynamic arguments, Yablonovitch and Cody in 1982 determined the maximum absorption enhancement in the ray optics limit for a bulk material to be $4n^2$, where n is the index of refraction of the absorbing layer [1]. Stuart and Hall in 1997 expanded this approach to study a simple waveguide structure; however, for the waveguide structures they considered, the maximum absorption enhancement was $<4n^2$ [2]. Using a combination of analytical and numerical methods, we describe why these structures do not surpass the conventional ergodic limit, and show how to design structures that can.

We present here a physical interpretation in terms of the waveguide dispersion relations and describe the necessary criteria for surpassing the conventional limit. In particular, the wavevector β needed for a mode to surpass the ergodic limit is given by $\beta > (2n^2h\omega^2)/(\Gamma\pi c^2)$, where Γ is the waveguide confinement factor and h is the waveguide thickness.

Another perspective on this issue is that the conventional light trapping limit can be exceeded in waveguide-like structures when the active region has an elevated local density of optical states (LDOS) compared to that of the bulk, homogeneous material. Additionally, to practically achieve light trapping exceeding the ergodic limit, the modes of the structure must be appreciably populated via an appropriate incoupling mechanism. We find using full wave simulations that ultrathin solar cells incorporating a plasmonic back reflector can achieve spatially averaged LDOS enhancements of 1 to 3, and a metal-insulator-metal (MIM) structure can achieve enhancements over 50 at a wavelength of 1100 nm, the bandedge of Si. Interestingly, incorporating the active solar cell material within a localized metallodielectric plasmonic or metamaterial resonator can lead to nearly spatially uniform LDOS enhancements above 1000 within the active material. We also have examined the possibility of structuring and combining ultrathin solar cells with dispersive dielectric structures such as photonic crystals to exceed the ergodic light trapping limit. We find that LDOS enhancements of ~ 2 -5 inside an untextured, planar solar cell can be achieved by simply placing a photonic crystal above or below the active material.

We have also developed a ray optics model for high aspect ratio wire array light trapping that suggests intensity enhancements within the wires can exceed the conventional limit for arrays with low wire area fractions on a Lambertian back reflector. We have applied this model to wire arrays with area fractions from .1% to 90%, and with aspect ratios between 30 and 200. The intensity enhancement at low wire area fraction can increase cell open circuit voltage, but low wire fraction results in a reduced short circuit current per unit area, and we explore optimizing cell efficiency within this parameter space. We compare with experimental Si wire array optical absorption data for wavelengths between 500 and 1100 nm for Si wires of varying sizes. We find reasonable agreement for large Si wires (radius 4 μ m) but the model underpredicts optical absorption for smaller wires (radius 1 μ m), suggesting that wave optics effects are important for the strong absorption observed in the small wire arrays.

Overall, we find many opportunities for exceeding the previously anticipated intensity enhancement and light trapping factor in dispersive dielectric and metallodielectric photovoltaic structures. These results can guide future solar cell designs that incorporate dispersive dielectric structures, plasmonics and metamaterials to achieve unprecedented light trapping.

References:

- [1] Yablonovitch and Cody. IEEE Trans. Elect. Dev. 29 300 (1982)
- [2] Stuart and Hall J. Opt. Soc. Am A 14 3001 (1997)

TWO-PHOTON LASER FABRICATION OF 3D SILVER NANOWIRE MICROSTRUCTURES AND THEIR PLASMONIC APPLICATIONS

Patrice Baldeck¹, S. Zaiba^{1,2,3}, T. Kouriba¹, O. Stéphan¹, O. Ziane^{1,2}, J. Bosson⁴, G. Vitrant⁵

¹Laboratoire Interdisciplinaire de Physique, CNRS UMR 5588, Université Joseph Fourier Grenoble, BP 87 38220 Saint Martin d'Hères Cedex, France

²Laboratoire d'Electronique Quantique, Faculté de physique, Université des sciences et de la technologie Houari Boumediene, Alger, Algérie

³Université M'hamed Bouguera, Boumerdes, Algérie

⁴Laboratoire de Physique Fondamentale et appliquée, Université d'Abobo-Adjamé, Côte d'Ivoire

⁵IMEP-LACH, CNRS 5130, Grenoble INP Minatec, 38016 Grenoble, France

patrice.baldeck@ujf-grenoble.fr

We have developed a laser photochemistry process to fabricate, by direct writing, 3D metallic microstructures using a two-photon microfabrication machine (<http://www.teemphotonics.com>). In this work we report the optical properties of silver nanowire microstructures. Typical nanowire diameter and length are 300 nanometers and 10 microns, respectively.

In the first part of the presentation we will present the diffraction properties of parallel nanowires with inter-distances in the 0.8 to 4 microns range. The interference of individual interference patterns gives rises to focusing effects that have the characteristics of ideal ultrasmall microlens with focal lengths in the micron range and with resolution limited by diffraction, i.e. in the 300 nm range in the visible. We will show that a 3D arrangement of such nanowires lead to an efficient chromatic spatial dispersion that may open a new route for RGB separation of colors at the micron scale.

In the second part of the presentation we will describe the optical properties of arrays of vertical nanowires with interdistances in the 0.8 to 4 microns range. The re-organized incident electromagnetic field is concentrated along the nanowires as shown by 3D wide-field microscopy and FDTD calculations.

We will present how we have used this electromagnetic field enhancement to improve the detected signals from Raman and fluorescences nanoprobes.

References:

- [1] L. Vurth, P. Baldeck, O. Stéphan, G. Vitrant, "Two-photon induced fabrication of gold microstructures in polystyrene sulfonate thin films using a ruthenium(II) dye as photoinitiator", Appl. Phys. Lett. 92, 171103 (2008)

Figures:

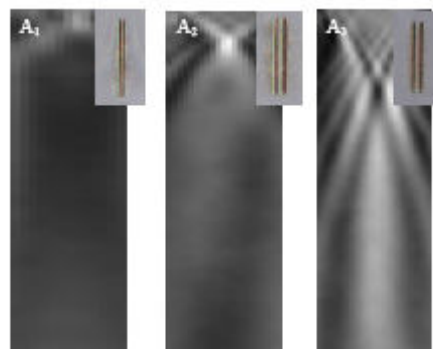


Figure 1: Focusing effects obtained by the diffraction of silver nanowire pairs separated by 1, 2 and 4 microns for A_1 , A_2 and A_3 , respectively

SYNTHETIC OPALS AND SANDCASTLES: EXPLORING WATER AT THE NANOSCALE

Alvaro Blanco, F. Gallego-Gómez, V. Canalejas, C. López

Instituto de Ciencia de Materiales de Madrid and Unidad Asociada CSIC-UVigo, C/ Sor Juana Inés de la Cruz 3, 28049 Madrid, Spain
ablanco@icmm.csic.es

Humid granular media are everyday systems present in pharmaceuticals, construction or agriculture. Sandcastles are built with wet sand, where water forms necks between grains, highly improving their mechanical stability [1]. Synthetic opals can be considered as sandcastles at the nanoscale. It is well known that the amorphous silica surface can adsorb a significant amount of water from the surrounding. The characteristics of systems based on silica structures can be greatly affected by the presence of adsorbed water, like the photonic properties of artificial opals formed by silica spheres. Previous work was focused on irreversible change of the water content in the spheres (e.g., by annealing at high temperatures) and its influence on the resulting silica opal [2]. However, studies on in situ water changes in the opal by e.g. due to alterations of the operating temperature or humidity are missing.

In this direction, we have performed a complete characterization of water content in silica artificial opals for different conditions of composition, temperature and growth. We investigate the reversible modification of the water content in the opal (principally by moderate heating but also in vacuum) and the simultaneously changes in the photonic bandgap (PBG). We observe, due to removal of interstitial water, large blue-shifts up to 30 nm and a predominantly decrease of the bandgap width up to 7%. In this study, we make a novel use of the optical properties of the opal to infer quantitative information about water distribution within silica beads and dehydration phenomena from simple reflection spectra. Taking advantage on the well-defined opal morphology, our approach offers a simple tool for straightforward investigation on generic adsorption-desorption phenomena, which might be extrapolated to other humid granular media.

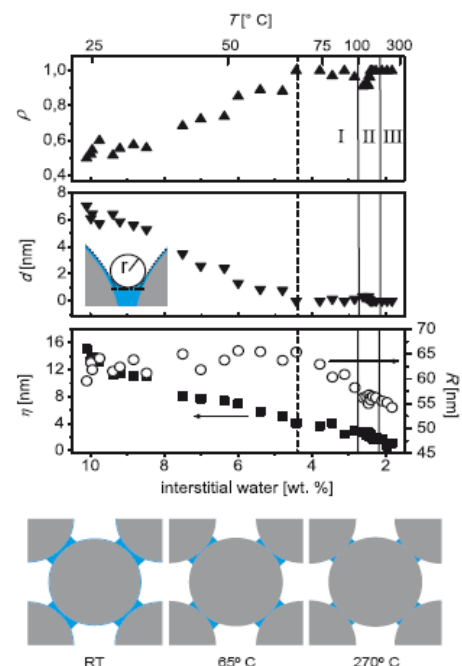
In addition, we also demonstrate that photoswitching can be induced by low cw-visible-irradiation in lightabsorbing hydrophilic silica opals due to local heating, in which large and fast bandgap shift (15 nm in 5 milliseconds) is obtained (Figure 1) [3]. This very simple and cost-effective approach provides high switchability in conventional silica photonic crystals, promising an inexpensive solution for a number of applications.

References:

- [1] D. J. Hornbaker, et al., Nature, 387, 765 (1997).
- [2] H. Míguez et al. Advanced Materials 10, 480 (1998).
- [3] F. Gallego-Gómez et al. submitted (2011).

Figures:

Figure 1: Water distribution as a function of humidity for different temperatures in an artificial opal formed by silica spheres of 335 nm.



INTERNAL ELECTROMAGNETIC FIELD DISTRIBUTION AND MAGNETO-OPTICAL ACTIVITY OF METAL AND METAL-DIELECTRIC MAGNETOPLASMONIC NANODISKS

D. Meneses-Rodríguez, E. Ferreiro-Vila, J.C.Banthí, P. Prieto, J. Anguita, A. García-Martín, M. U. González, J. M. García-Martín, **A. Cebollada**, and G. Armelles

IMM-Instituto de Microelectrónica de Madrid (CNM-CSIC)
Isaac Newton 8, PTM, E-28760 Tres Cantos (Madrid), Spain.
david.meneses@imm.cnm.csic.es

Localized surface plasmon resonances (LSPRs) greatly influence the optical [1-4] and magneto-optical (MO) [5-10] properties of fully metallic and metal-dielectric nanostructures. The observed enhancement in the MO activity when these LSPRs are excited is attributed to the high intensity of the electromagnetic (EM) field inside the global nanostructure when the LSPR occurs [5,11]. Unfortunately, it is not straightforward to experimentally determine the intensity of the EM field inside a nanostructure. Here we show how the EM profile related to the LSPR can be probed locally inside the nanostructure by measuring the MO activity of the system as a function of the position a MO active probe (a Co nanolayer). This will be done in full detail in metallic systems, and preliminary results will also be presented in more complex metal-dielectric magneto-plasmonic nanodisks.

The magnetoplasmonic nanodisk arrays have been fabricated in large area onto glass substrates by combining colloidal lithography with sputter, thermal and electron beam deposition and lift-off techniques. Typical nanodisk structures are Au/Co/Au/Cr and Au/SiO₂/Co/SiO₂/Au/Ti, for the fully metallic and the metal-dielectric structures respectively, with total heights between 50 and 70 nm and diameters between 110 and 140nm (Figure 1(a)). For the sake of comparison, continuous thin films with identical composition have been also prepared.

The MO activity (Φ) has been obtained by measuring the MO Kerr effect in polar configuration upon normal incidence illumination, previously identifying the optical resonances through extinction spectra. In the fully metallic nanostructures, we find a distinctive evolution as a function of Co position of the MO activity in the nanodisks compared with that of the continuous layers, with maximum values when the Co layer is located near the top or the bottom of the disks and minimum values in-between due to the LSPR excitation. This behavior is in contrast with the MO activity exhibited by the continuous films, which increases monotonously as the Co layer becomes closer to the top surface (Figure 1(b)). This indicates that the EM field inside the nanodisks exhibits a nonuniform distribution in plasmon resonance conditions. In fact, the Co layer acts as a probe sensing the EM field within the nanodisk, since the MO activity depends on the intensity of such field. Preliminary results on the possible influence of multiple resonances in metal-dielectric magnetoplasmonic nanodisks will be also presented (Figure 1(c)).

This information could be very relevant for the design of magnetoplasmonic systems offering optimum MO enhancement, for instance for sensing applications where maximum sensitivity is expected in the areas with higher EM field.

References:

[1] S. A. Maier, Plasmonics: Fundamentals and Applications (Springer, Berlin, 2007).
 [2] S. A. Maier and H. A. Atwater, J. Appl. Phys. 98, (2005) 011101.
 [3] K.H.Su, Q.H.Wei, and X.Zhang, Appl. Phys. Lett. 88 (2006) 063118.
 [4] T.Pakizeh, A.Dimitriev, M.S.Abrishamian, N.Granpayeh, and M.Häll, J. Opt. Soc. Am. B 25 (2008) 659.
 [5] J. B. González-Díaz, A. García-Martín, J. M. García-Martín, A. Cebollada, G. Armelles, B. Sepúlveda, Y. Alaverdyan and M. Käll, Small 4 (2008) 202.
 [6] G. A. Wurtz, W. Hendren, R. Pollard, R. Atkinson, L. Le Guyader, A. Kirilyuk, Th. Rasing, I. I. Smolyaninov and A. V. Zayats, New J. of Phys. 10 (2008) 105012.
 [7] P.K.Jain, Y.Xiao, R.Walsworth, and A.E.Cohen, Nanolett. 9 (2009) 1644.
 [8] G.X.Du, T.Mori, M.Suzuki, S.Saito, H.Fukuda, and M.Takahashi, Appl. Phys. Lett. 96 (2010) 081915.
 [9] L.Wang, K.Yang, C.Clavero, A.J.Nelson, K.J.Karroll, E.E.Carpenter, and R.A. Lukaszew, J.Appl. Phys. 107 (2010) 09B303.
 [10] G.X.Du, T. Mori, M.Suzuki, S.Saito, H.Fukuda, and M.Takahashi, J.Appl. Phys. 107 (2010) 09A928.
 [11] G. Armelles, A. Cebollada, A. García-Martín, J. M. García-Martín, M. U. González, J. B. González-Díaz, E. Ferreiro-Vila and J. F. Torrado, J. Opt. A: Pure Appl. Opt. 11 (2009) 114023.

Figures:

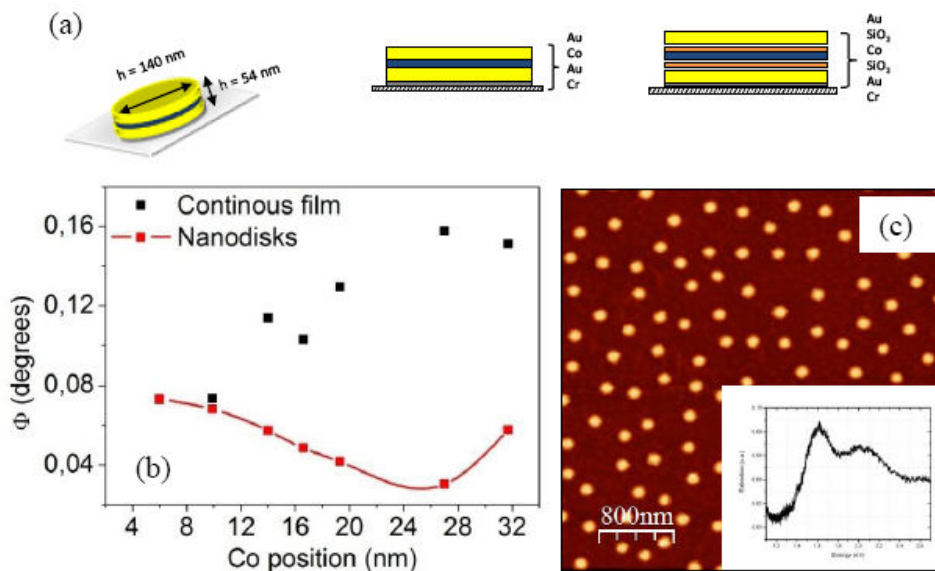


Figure 1: (a) Sketch of the fully metallic and metal/dielectric nanodiscs (b) Maximum magneto-optical activity as a function of the Co position for fully metallic continuous films and nanodisks (c) AFM image of an array of metal-dielectric nanodisc array (Inset: extinction spectrum showing two characteristic peaks).

FERROMAGNETIC PLASMONIC NANOANTENNAS

J. Chen^{1,2}, P. Albella^{1,2}, Z. Pizadeh³, P. Alonso-González¹, F. Huth¹, P. Vavassori^{1,4}, A. Dmitriev³, J. Aizpurua² and R. Hillenbrand^{1,4}

¹CIC nanoGUNE Consolider, 20018 Donostia-San Sebastián, Spain

²Centro de Física de Materiales (CSIC-UPV/EHU) and Donostia International Physics Center (DIPC), 20018 Donostia-San Sebastián, Spain

³Department of Applied Physics, Chalmers University of Technology, 41296 Göteborg, Sweden

⁴IKERBASQUE, Basque Foundation for Science, 48011 Bilbao, Spain

Optical antennas are devices designed to efficiently convert optical radiation into localized energy and vice versa [1]. Currently, there is great interest in the development of magnetic optical nanoantennas that combine optical nanofocusing properties with magnetic functionality. Such antennas would be interesting for bioseparation, drug targeting and cell isolation [2]. However, plasmons in ferromagnetic materials are typically strongly damped. A common strategy to overcome this problem is to develop hybrid structures consisting of noble metals and ferromagnetic materials [3]. Plasmon properties of pure ferromagnetic nanostructures are a widely unexplored terrain, although pure ferromagnetic structures offer the advantage of stronger magnetic polarization and less demanding fabrication.

Here we report an experimental and theoretical study of the optical properties of ferromagnetic nanostructures fabricated purely of nickel. By farfield extinction spectroscopy (Fig. 1a) we provide direct experimental evidence of particle Plasmon resonances in nickel disks and ellipsoids. In order to identify the mode associated with the resonance peak, we imaged amplitude (Fig. 1b) and phase (Fig. 1c) of the vertical near-field component using a scattering-type scanning near-field optical microscope (s-SNOM) operating at 633 nm wavelength. In the amplitude image we observe two bright spots aligned along the polarization direction, which are oscillating out of phase for 180°. Such a near-field pattern provides direct experimental evidence of a dipole mode, which has been observed earlier for plasmon-resonant gold disks [4,5]. We emphasize that we also clearly observe the transverse plasmon mode in the elliptical antenna.

Performing numerical calculations, we find significant differences between far- and near-field spectra of plasmonic nickel antennas, which are indicated experimentally by comparing single wavelength near-field images and far-field spectra. We find that the near-field resonance is dramatically red shifted compared to the far-field resonance. This is a fundamental behavior already reported earlier for gold nanoantennas [6], but which is not fully understood yet. We will discuss these shifts theoretically. We also discuss a simple harmonic oscillator model revealing that a major contribution to the shift between near- and far-field resonances is a consequence of the Plasmon damping.

References:

- [1] Muhlschlegel, P.; Eisler, H. J.; Martin, O. J. F.; Hecht, B.; Pohl, D. W. *Science* 2005, 308, (5728), 1607-1609.
- [2] Insin, N.; Tracy, J. B.; Lee, H.; Zimmer, J. P.; Westervelt, R. M.; Bawendi, M. G. *ACS Nano* 2008, 2, (2), 197-202.
- [3] Levin, C. S.; Hofmann, C.; Ali, T. A.; Kelly, A. T.; Morosan, E.; Nordlander, P.; Whitmire, K. H.; Halas, N. J. *ACS Nano* 2009, 3, (6), 1379-1388.
- [4] Hillenbrand, R.; Keilmann, F.; Hanarp, P.; Sutherland, D. S.; Aizpurua, J. *Appl. Phys. Lett.* 2003, 83, (2), 368-370.
- [5] Esteban, R.; Vogelgesang, R.; Dorfmueller, J.; Dmitriev, A.; Rockstuhl, C.; Etrich, C.; Kern, K. *Nano Lett.* 2008, 8, (10), 3155-3159.
- [6] Bryant, G. W.; De Abajo, F. J. G.; Aizpurua, J. *Nano Lett.* 2008, 8, (2), 631-636.

Figures:

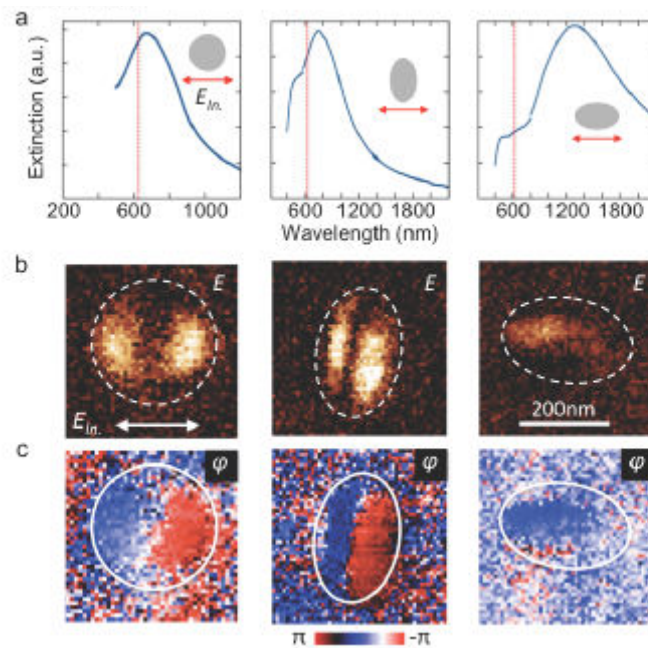


Figure 1: Plasmonic nickel nanoantennas. (a) Extinction spectra of circular and elliptical nickel antennae. The red line in the spectra marks the wavelength $\lambda=633$ nm where near-field imaging was performed. The arrows indicate polarization of incident light. (b) Near-field optical amplitude images E . The arrow and bar denote the polarization of incident laser and scale of the images. (same for all three particles) (c) Near-field optical phase images φ .

MAGNETO-OPTICAL STUDY OF MAGNETIC MICROWIRES: DOMAIN STRUCTURE, DOMAIN WALLS MOTION, MAGNETIZATION REVERSAL

Alexander Chizhik¹, Arcady Zhukov¹, Julián González¹, Juan Mari Blanco²

¹Dpto. Física de Materiales, Fac. de Química, Universidad del País Vasco, San Sebastian, Spain

²Dpto. Física Aplicada I, EUPDS, UPV/EHU, 20018 San Sebastián, Spain

oleksandr.chyzyk@ehu.es

The investigation of the magnetization reversal process, domain structure and domain walls motion in magnetic microwires is one of the most important tasks related to the use of magnetic wires in different technological devices. In particular, intensive studies of magnetic properties of glass coated microwires have been performed to enhance the giant magnetoimpedance (GMI) effect used in magnetic sensing technology.

The present abstract is devoted to the recent results on magneto-optical Kerr effect (MOKE) study of the surface magnetization reversal and surface domain structure in glass covered amorphous microwires.

The full cycle of the magnetization reversal between two circularly magnetized mono-domain states has been fixed using MOKE microscope in longitudinal configuration. The process of circular domains nucleation and propagation strongly depends on the dc external axial magnetic field. The comparative analysis of the magnetometry and optical microscopy results shows that the magnetization reversal consists mainly of the nucleation of circular domains and transformation to multi-domain structure when the dc axial field is relatively small. It was found also that the dc axial field suppresses the nucleation process putting in the forefront the propagation of circular domain walls.

Also the surface domain wall (DW) motion has been studied using the MOKE modified Sixtus-Tonks method when two reflections of the broken laser beam from the microwire surface were used instead of the pickup coils [1].

The surface circular DW motion was induced by the pulsed circular magnetic field. The single domain wall motion along the wire was registered as two successive jumps of the MOKE signal. This motion is associated with the circular magnetic bistability related to the giant Barkhausen jump of circular magnetization. During the experiments our attention was focused of the influence of the dc axial magnetic field on the surface circular DW motion.

It was found the influence of the axial magnetic field on the shape of the MOKE jump. Depending on the value of the axial field there are three stage of the jump transformation. At the first stage, the time duration of the jump decreases with axial field increase. At the second stage, the specific transformation of the shape of the jump was observed. We consider that this transformation is related to the transformation of the form of the DW. Finally, the absolute value of the MOKE jump decreases following by the total disappearance of the MOKE signal. This disappearance is reasonable because the dc axial field of the relatively high value directs the magnetization along the axial direction of the microwire eliminating the transversal projection of the surface magnetization.

Based on the series of the time dependences of the MOKE jumps related to the surface DW motion along the wire, the dependence of the DW velocity on the dc axial field has been plotted (Fig. 1). The results have been obtained for the pulsed circular field of the value of 0.2 Oe.

This dependence has been analyzed jointly with the dc axial field induced transformation of the MOKE jumps. The general growth of the velocity with dc axial field is observed. Nevertheless, three specific parts of the dependence could be marked out. There are two parts with clearly defined increase of the velocity – in the beginning and in the end of the of the curve. Also the local decrease of the velocity value exists in the middle part of the field dependence.

We consider that the first part of the field dependence is related to the DW transformation from inclined one to DW perpendicular to the wire axis, that confirmed by the MOKE signal transformation. When the dc axial field is high enough the magnetization inside the transformed DW is directed

probably more along the axial direction that decelerates the motion of DW between two circular domains. The successive DW acceleration observed in the final part of the curve is clearly related to the field induced decrease of the angle of the turn of the magnetization in the DW. Finally, DW collapses when this angle is reduced to zero.

In frame of the task of the miniaturization of active elements of magnetic sensors the investigation of the magnetization reversal has been performed in nano-scale amorphous microwires for the first time. The arrays of glass covered microwires (nominal composition $(\text{Fe}_{97}\text{Co}_3)_{75}\text{B}_{15}\text{Si}_{10}$, diameter of metallic nucleus 1000 nm) have been studied by magnetic and magneto-optical techniques. The results of PPMS magnetic (4 microwires array) and longitudinal magneto-optic Kerr effect (10 microwires array) experiments are presented in the Figs. 2(a) and 2(b). The clear jumps of magnetization could be observed in volume and surface hysteresis loops. These jumps are related to the giant Barkhausen jumps associated with the magnetization reversal in single microwire as a consequence of the interaction between the microwires. Based on the obtained results we can conclude that the magnetic behaviour of the glass covered microwires with such extremely tiny diameter keeps magnetically bistable and could be considered in the frame of core-shell model.

References:

- [1] A. Chizhik, R. Varga, A. Zhukov, J. Gonzalez, and J. M. Blanco, J. Appl. Phys. 103, 07E707 (2008).

Figures:

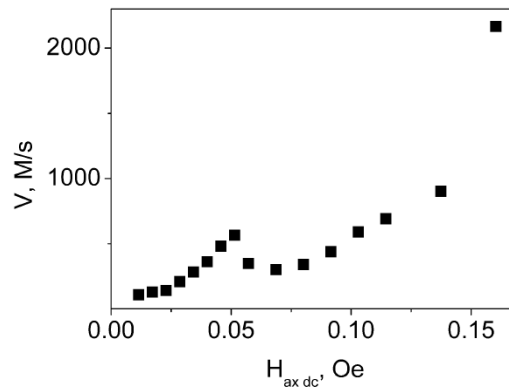


Figure 1: Dependence of the velocity of the circular surface domain wall on dc axial magnetic field. The value of the pulsed circular magnetic field is 0.2 Oe.

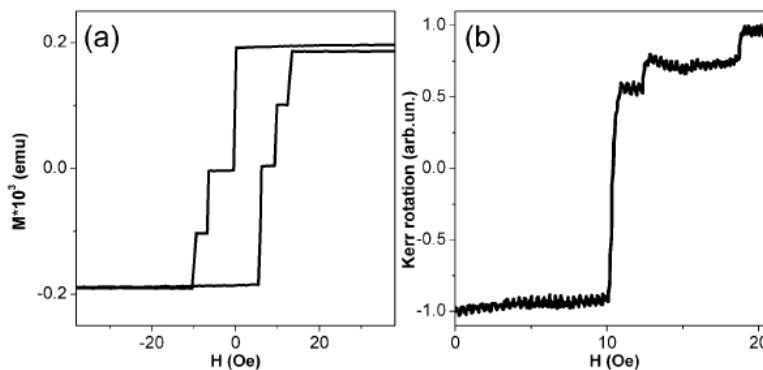


Figure 2: Magnetization reversal curves obtained by magnetic (a) and magneto-optic (b) techniques.

NANOGAP RING ANTENNAE AS PLASMON COUPLED, DICHROIC SERRS SUBSTRATES FOR BIOSENSING

Dr. Alasdair William Clark, Prof. Jonathan M. Cooper

University of Glasgow, Biomedical Engineering, Rankine Building, Oakfield Avenue, Glasgow, UK
alasdair.clark@glasgow.ac.uk

We explore the use of engineered nano-gap plasmonic ring systems in biosensing. By employing cutting edge nanofabrication methods we seek to exploit the extraordinary optical properties of metallic nanostructures in a range of novel ways targeted toward extremely sensitive molecular detection.

Surface enhanced (resonance) Raman spectroscopy (SE(R)RS) is a powerful sensing tool which relies on molecular interaction with the fluctuating plasmon field of a resonating nanoparticle. Using this method it has been shown that SERRS can rival the sensitivity of fluorescence techniques, enabling single molecule detection and characterisation.[1] As nanoengineering techniques have become more advanced in recent years there has been a move toward fabricating ever more complex nanoparticle geometries, with the aim of creating functional, tunable sensing substrates with a uniform distribution of intense localised plasmon fields.

In this work, we explore the use of nano metallic split-ring antenna as powerful, multifunctional biosensors with dichroic optical properties. Fabrication via electron-beam lithography allows for the strict control over structural geometry that is necessary to accurately tune the ring's multiple, polarisation dependant plasmon resonances to particular wavelengths.[2] In doing so, we demonstrate that we can tune their optical response such that they exhibit two independently addressable high frequency plasmon resonance modes, each tuned to the absorption wavelength of a differently coloured Raman reporter molecule and its corresponding laser excitation wavelength (Figure 1).[3, 4] This allows the single geometry ring structures to act as tailored SERRS sensors for low concentration DNA analyses at two distinct wavelengths.[4]

We go on to report on the fabrication, optical characterisation and application of a new generation of ultra-small multiple-split nanoring antenna.[5, 6] Using electron-beam lithography, splits of ca. 6 nm are engineered into silver nanophotonic ring structures to create concentrated areas of localised field coupling, which can be exploited for enhanced plasmonic applications. We compare the plasmonic properties of three devices, containing 3, 4 and 5 splits respectively, which have been spectrally tuned to 532 nm. Using finite element analysis, we explore the distinct plasmonic characteristics of each structure, and describe how variations in surface charge distribution effect inter-segmental coupling at different polarisation angles (Figure 2). The impact these changes have on the sensory functionality of each device was determined by a competitive DNA hybridisation assay measured using surface enhanced resonance Raman spectroscopy. The geometry of these novel, circular, multiple-split rings leads to unique plasmon hybridization between the numerous segments of a single structure; a phenomena we demonstrate is applicable to extreme Raman sensitivity, and may also find use in metamaterial applications.

References:

- [1] S. M. Nie, S. R. Emery, *Science*, 275, (1997) 1102.
- [2] A. W. Clark, A. K. Sheridan, A. Glidle, D. R. S. Cumming, J. M. Cooper, *Applied Physics Letters*, 91 (2007) 093109.
- [3] A. W. Clark, A. Glidle, D. R. S. Cumming, J. M. Cooper, *Applied Physics Letters* 93 (2008) 023121.
- [4] A. W. Clark, A. Glidle, D. R. S. Cumming, J. M. Cooper, *Journal of the American Chemical Society*, 131 (2009) 17615.
- [5] A. W. Clark, J. M. Cooper, *Small*, 7 (2011) 119.
- [6] A. W. Clark, J. M. Cooper, *Advanced Materials*, 22 (2010) 4025.

Figures:

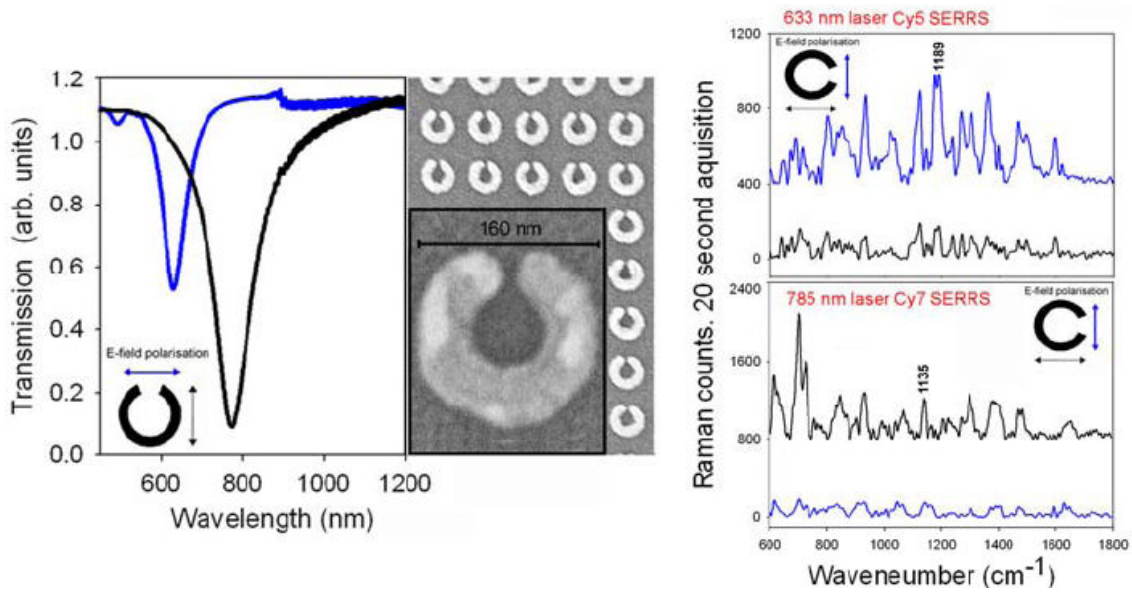


Figure 1: Left – SEM and transmission spectra of an 80 nm radius Ag split-ring resonator sensor array with 2nd and 3rd order resonances tuned to 785 and 633 nm respectively. Right –SERRS from an identical array modified with a 1:1 ratio of Cy5 and Cy7 labelled oligonucleotide sequences hybridized to complimentary strands attached to the sensor surface. Measurements were performed at 633 and 785 nm and data was collected when the electric field vector of each laser was orientated both parallel and perpendicular to the split in the ring geometry.

ImagineNano April 11-14, 2011

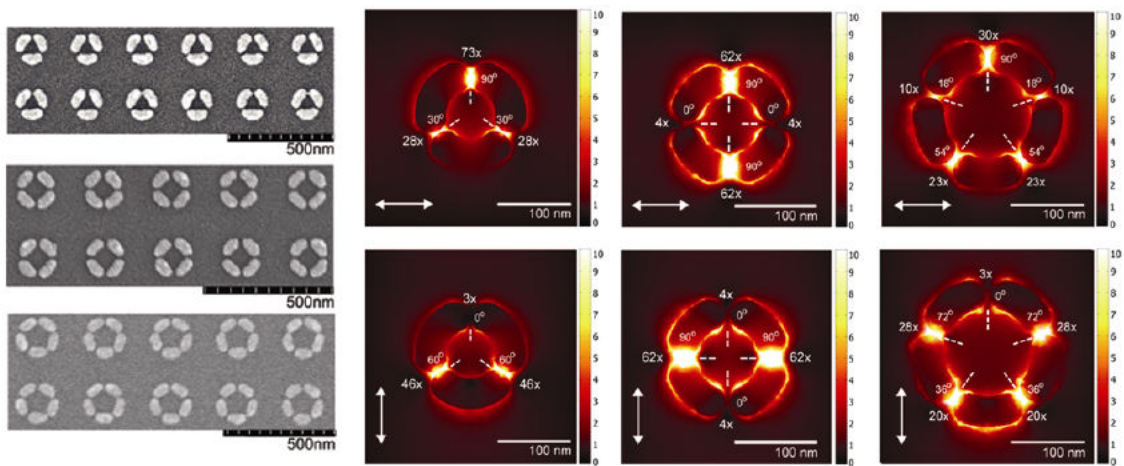


Figure 2: Left – SEM of multiple-split nanoring antenna with average gap sizes of 6nm or less. Right – Finite element analysis of the plasmonic field distribution around each structure at resonance.

PPM2011

COUPLING BETWEEN LOCALIZED SURFACE PLASMON RESONANCE AND MAGNETIC PROPERTIES OF NANOPARTICLES, THE EFFECT IN THE REVERSAL PROCESS

C. de Julián Fernández¹, L. Bogani^{1,2}, L. Cavigli³, R. Novak^{1,4}, F. Pineider^{1,5}, C. Sangregorio^{1,6}, G. Campo¹, G. Mattei⁷, M. Gurioli³, R. Sessoli¹, A. Caneschi¹, P. Mazzoldi⁷ and D. Gatteschi¹

¹INSTM- Università di Firenze, via della Lastruccia 3, 50019 Sesto Fiorentino, Italy; ²Physikalisches Institut, Universität Stuttgart, Pfaffenwaldring 57, 70550, Stuttgart, Germany; ³LENS – Università di Firenze, via G. Sansone 1, 50019 Sesto Fiorentino, Italy; ⁴LPMC-CNRS, Route de Saclay, 91128 Palaiseau, France; ⁵CNR- ISTM, Via Marzolo 1, 35131 Padova, Italy; ⁶CNR-ISTM, Via C. Golgi 19, 20133 Milano, Italy; ⁷Dipartimento di Fisica –Università di Padova, via Marzolo 8, 35125 Padova, Italy
cesar.dejulian@unifi.it

Magneto-optical (MO) techniques are well-established procedures to characterize the dynamics and reversal process of nanostructured materials and surfaces. At the same time MO properties include information on the band structure because MO effects are produced by the spin-orbit coupling. This interaction is largely modified in nanomaterials due to quantum confinement effects, changes in the electronic structure and surface contribution. Electronic plasmon excitations, typical of metal nanostructures, can also affect the MO response and the magnetic dynamics. Moreover the interaction between femtosecond light and magnetic materials can produce changes in the dynamic of the reversal process. As a consequence MO studies are emerging as fundamental methods to investigate the correlations between the magnetic, optical and electronic properties of nano-sized materials with an important role for understanding the possibility of manipulation of the magnetic information with light.

In our presentation we illustrate our research activity on the study on the interactions of the light with magnetic nanomaterials using magneto-optical techniques. We use a home-made magneto-optical set-up built around an optical cryostat with superconducting coils. This allows to measure the magneto-optical signal in the temperature range of 1.5 K to 300 K and with magnetic field of ± 5 T. We record the magnetic Circular Dichroism using beams with discrete wavelengths covering the 400 nm to 1000 nm range. We investigated the wavelength dependence of the MO hysteresis loops and the dynamics of two families of alloy based nanoparticles: Co-Ni alloy nanoparticles prepared by sol-gel route [1] and Fe-Au nanoparticles prepared by ion implantation [2].

Co-Ni nanoparticles with different compositions have been investigated and in general they exhibit MO hysteresis loops larger of the magnetometric one (Figure 1) and mainly the coercive fields are wavelength dependent. The largest effect is observed in nanoparticles with composition Co₃₃Ni₆₆ in which the coercive field decreases from 0.25 T at 904 nm to 0.17 T at 400 nm being the magnetometric value 0.12 T. MO dynamic measurements confirm that near the UV, where Plasmon resonance can be excited in the metallic CoNi nanoparticles, the reversal dynamics is accelerated. Temperature dependence of the MO coercive field experiments exclude that the effect be related to the selectivity of the radiation at different ensemble of nanoparticles. In the case of Au-Fe nanoparticles with composition Au:Fe near SPR appears strongly dumped in the Vis-nIR spectral region due to the electronic hybridization of Au and Fe [3]. In fact pure Fe and AuFe nanoparticles present similar MO lineshape and extinction spectra due to the similarity electronic structure. However experiments made by recording the MO hysteresis loops with light at 632.8nm and simultaneously pumping with the Ar-laser line of 514 nm show one decreasing of the coercive field as function of the pumping power[4].

In both cases we observe changes in the reversal process due to the excitation of localized surface Plasmon excitation in the magnetic nanoparticles. The possible mechanisms and the correlation with the magnetic properties of the nanoparticles are discussed.

It unlocks the possibility of observing spin-plasmonic effects in the visible region, and thus opens a new area of fundamental research and interesting applicative possibilities in all fields requiring the mixing of spin and electronic properties, like magneto-optics, spintronics and spin-plasmonics.

References:

- [1] C. de Julián Fernández *et al.* *Inorganica Chimica Acta* 361 (2008) 4138.
- [2] G. Mattei *et al.* *Nucl. Instr. and Meth. B.* 250 (2006) 225
- [3] C de Julián Fernández *et al* *Nanotechnology* 21 (2010) 165701
- [4] L. Bogani *et al.* *Advanced Materials* 22 (2010) 4054

Figures:

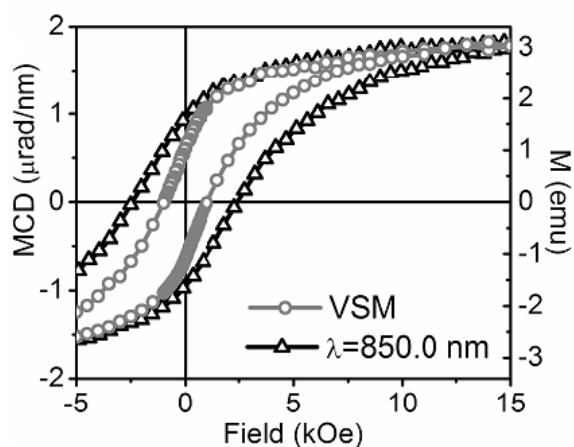


Figure 1: Hysteresis loops recorded by magnetometric (VSM) and MO measurements at 1.5 K.

SIGNATURE OF THE ANISOTROPY OF TWO-PHOTON EXCITED LUMINESCENCE OF NEARLY SPHERICAL GOLD PARTICLES DIFFUSING IN SOLUTION

L Anne Débarre¹, Matthieu Loumagne¹, Priya Vasanthakumar^{1,2}

¹Laboratoire Aimé Cotton, CNRS, University Paris-Sud, Bâtiment 505, Campus d'Orsay, F-91405 Orsay cedex, France.

²Nanolab, Department of Physics "Enrico Fermi", University of Pisa, Largo Bruno Pontecorvo, 3, I-56127 Pisa, Italy
anne.debarre@u-psud.fr

Here, we report on the properties of the two-photon excited luminescence of gold nanobeads dispersed in solution.

Nanometallic objects derive their optical properties from an ability to support collective electronic excitations, known as surface plasmons. In the case of gold, a further interest of the particles is their biocompatibility and their ability to be suitable platforms for biophotonics. A lot of studies have been recently devoted to functionalise gold particles to create sensitive hybrid probes for molecular recognition and biosensing. The corresponding approach generally takes advantage of the modulation of the fluorescence properties of a chromophore in close vicinity to the gold core. The emission properties, enhancement or quenching, depend on the photophysical properties of the linked molecules, on the plasmon resonances of the core and on their interaction [1, 2]. The potential of such hybrid probes relies on the tuning the plasmon resonances by shaping the gold core.

Apart from fluorescent functionalisation with linked chromophores, a growing field of research is dedicated to targeted imaging with gold particles as contrast agents because of reduced phototoxicity and versatility of excitation, in particular. The optical process involved in imaging is the emission of luminescence, following either one or two photons absorption. Excitation in the near-infrared domain is the rule under two-photon excitation [3] but it can be used even with one photon excitation in the case of nanorods for example. It combines the advantages of being less toxic for the samples and of deeper penetration into the tissues. Another interesting application is the thermal effect related to absorption when the excitation wavelength is close to their plasmon resonance peaks. The latter has been demonstrated to be of interest for therapeutic purposes [4].

The initial aim of our studies was to determine if the two-photon excited luminescence process could be efficient enough to track small spherical gold nanobeads diffusing in aqueous solutions. It implied to work at the single particle level. In fact, luminescence of gold nanoparticles has been mainly studied on deposited samples, eventually at the single particle level but very few experiments have been performed on liquid samples, generally with a rather high concentration of particles.

To understand the optical behavior of gold nanobeads, we have used Fluorescence Correlation Spectroscopy (FCS) implemented on a two-photon microscope comprising imaging capabilities. As is displayed on the Figure 1, the cross-correlation profile of the two-photon excited luminescence of gold beads of 20 nm diameter presents an unexpected component in the microsecond temporal range. This contribution has been attributed to the signature of the Brownian rotation of the beads, using an original dual method correlating luminescence and Rayleigh scattering signals [5]. We will report on a multiparameter analysis of the two-photon excited luminescence of gold nanobeads, which reveals the role played by the ligands capping the particles in the anisotropy of the emission. The latter is closely related to the temperature increase at the water-ligands interface following absorption. The effects of the polarization and of the excitation wavelength will be discussed.

References:

- [1] Dulkeith E., Morteani A. C., Niedereichholz T., Klar T. A., Feldmann J., Levi S. A., Van Veggel F. C. J. M., Reinhoudt D. N., Möller M. and Gittins D. I., *Phys. Rev. Lett.*, 89 (2002) 203002.
- [2] Loumagne M., Praho R., Nutarelli D., Werts M. H. V. and Débarre A., *PCCP*, 12 (2010) 11004.
- [3] Wang H., Huff T. B., Zweifel D. A., He W., Low P. S., Wei A. and Cheng J.-X., *PNAS*, 102 (2005) 15752.
- [4] Huang X., El-Sayed I. H., Qian W. and El-Sayed M. A., *JACS*, 128 (2006) 2115.
- [5] Loumagne M., Richard A., Laverdant J., Nutarelli D. and Débarre A., *Nano Lett.*, 10 (2010) 2817.

Figures:

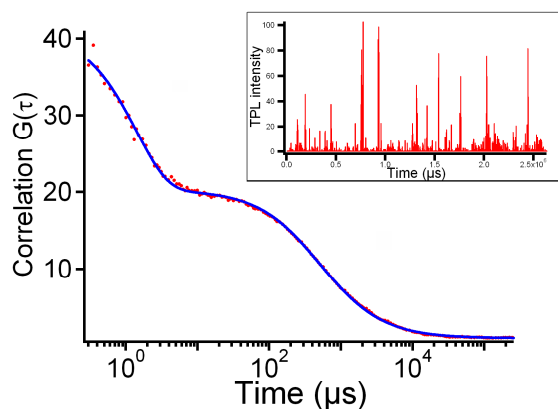


Figure 1: Cross-correlation profile of two-photon excited luminescence of gold beads of 20 nm diameter; excitation wavelength 815nm; power 6mW; In inset, histogram of bursts.

Nader Engheta

University of Pennsylvania, Department of Electrical and Systems Engineering, Philadelphia, PA, USA
Engheta@ee.upenn.edu

In my group, we have been developing the concept of “metatronics”, i.e. metamaterial-inspired optical nanocircuitry, in which the three fields of “electronics”, “photonics” and “magnetics” can be brought together seamlessly under one umbrella – the “Unified Paradigm of Metatronics”. In this optical circuitry, the nanostructures with specific values of permittivity and permeability may act as the lumped circuit elements such as nanocapacitors, nanoinductors and nanoresistors. Nonlinearity in metatronics can also provide us with novel nonlinear lumped elements. We have investigated the concept of metatronics through extensive analytical and numerical studies, computer simulations, and in a set of experiments at the IR wavelengths. We have shown that nanorods made of low-stressed Si_3N_4 with properly designed cross sectional dimensions indeed function as lumped circuit elements at the IR wavelengths between 8 to 14 microns. We have been exploring how metamaterials can be exploited to control the flow of photons, analogous to what semiconductors do for electrons, providing the possibility of one-way flow of photons. We are now extending the concept of metatronics to other platforms such as graphene, which is a single atomically thin layer of carbon atoms, with unusual conductivity functions. We study the graphene as a new paradigm for metatronic circuitry and also as a “flatland” platform for IR metamaterials and transformation optics, leading to the concepts of one-atom-thick metamaterials, and one-atom-thick circuit elements and optical devices. I will give an overview of our most recent results in these fields. For more information, please see the references given below.

References:

- [1] N. Engheta, Physics World, 23 (2010), 31.
- [2] N. Engheta, Science, 317 (2007), 1698.
- [3] N. Engheta, A. Salandrino, A. Alu, Phys. Rev. Lett. 95 (2005), 095504.
- [4] A. Alu, N. Engheta, Nature Photonics, 2, (2008) 307.
- [5] M. G. Silveirinha, A. Alu, J. Li, N. Engheta, J. Appl. Physics, 103, (2008) 064305.
- [6] A. Alu, N. Engheta, Phys. Rev. Lett., 103, (2009) 143902.
- [7] A. Alu, M. E. Young, and N. Engheta, Phys. Rev. B, 77, (2008) 144107.
- [8] A. Alu and N. Engheta, Phys. Rev. Lett., 101, (2008) 043901.
- [9] A. Vakil and N. Engheta, <http://arxiv.org/abs/1101.3585>

NANOSTRUCTURED SILICON SURFACES BY SELF-ASSEMBLED NANOPOROUS ANODIC ALUMINA FOR PHOTONIC APPLICATIONS

Josep Ferré-Borrul, Mohammad Mahbubur Rahman, Abel Santos, Pilar Formentín, Josep Pallarès, Lluís F. Marsal

Universitat Rovira I Virgili, Nano-electronic and Photonic Systems, NePhoS Av. Paisos Catalans 26, ETSE-DEEEA, 43007, Tarragona, Spain
josep.ferre@urv.cat

Nanoporous anodic alumina (NPAA) [1] has become a very interesting material in nanotechnology because of its cost-effective production and its geometrical properties that can be tuned in a wide range. The main application of NPAA is in templating to achieve different nanostructures with different functionalities: [2-4]. Furthermore, the structure of nanoporous anodic alumina is a two-dimensional self-assembled structure with a triangular arrangement of the pores. If no pre-patterning techniques are used, the triangular pore arrangement is broken into domains, giving rise to a quasi-random structure. By adequately tuning the fabrication conditions, the size of the domains can be increased. Such triangular pattern reminds that of a triangular Photonic Crystal [5], although it lacks the perfect periodicity. However, it can be demonstrated [6] that the NPAA pattern can show photonic stop bands in the same way it happens with photonic quasicrystals [7] or even in random structures [8].

Silicon is a good candidate to obtain two-dimensional photonic crystals [9] for different applications, mainly because its compatibility with the wide-spread silicon technology. In order to obtain such photonic crystals, a lithography-based pre-patterning technique and further wet- or dry-etching techniques are required. This makes the cost relatively high, especially if the lattice constants have to be reduced to a few hundreds of nanometers. However, some applications may only need to benefit from the existence of a stop band, and thus, in this case, the NPAA pattern could be adequate.

In this work we focus on the transfer of the NPAA pattern to the silicon surface for further electrochemical etching. Such nanostructured silicon substrate will enable a great variety of applications that take benefit from the existence of a photonic band gap onto a conductive substrate that provides electrical contact: efficient light emitters (both diode or lasers), solar cells with more efficient light harvesting, sensors with enhanced sensitivity. With this aim, the process parameters concerning aluminum deposition, etching conditions and processing steps are optimized. We present results on fabrication and characterization of the structures fabricated. One of the main issues is the optical characterization of the resulting Si nanostructure by angular-dependent reflectance spectroscopy and polarimetry [10,11]. Such measurements require a good surface finish between the pores on the silicon. Consequently the process will be optimized to obtain such a surface quality.

The figures show some of the achievements up to date. Figure 1 shows the current transients and the SEM pictures of the surface and of the cross-section of a NPAA layer grown onto p-Si by a two-step electrochemical etching process with a 0.3 M oxalic acid electrolyte and under potentiostatic conditions with an applied voltage of 40 V. Figure 1a shows the current-time curve for the first and the second steps of the anodization processes, Figure 1b shows an ESEM picture of the sample surface and finally, Figure 1c shows the cross section of the sample, showing the alumina and the silicon regions. Figure 2 shows the same information but for a sample obtained with a 0.3 M phosphoric acid electrolyte and an applied voltage of 160 V.

Acknowledgments

This work was supported by the Spanish Ministry of Science and Innovation (MICINN) under grant number TEC2009-09551, CONSOLIDER HOPE project CSD2007-00007, AECID project A/024560/09 and by the Catalan Authority under project 2009SGR549.

References:

- [1] W. Lee, R. Ji, U. Gosele, K. Nielsch, *Nature Materials*, Vol. 5 (2006) 741.
- [2] A. Santos, L. Vojkuvka, J. Pallares, J. Ferre-Borrull, L.F. Marsal, *Nanoscale Research Letters*, Vol. 4 (2009) 1021.
- [3] b A. Santos, P. Formentin, J. Pallares, J. Ferre-Borrull, L.F. Marsal, *Materials Letters*, Vol. 64 (2010) 371.
- [4] b A. Santos, P. Formentin, J. Pallares, J. Ferre-Borrull, L.F. Marsal, *Solar Energy Materials & Solar Cells*, Vol. 94 (2010) 1247.
- [5] J. D. Joannopoulos, S. G. Johnson, J. N. Winn, R. D. Meade: *Photonic Crystals: Molding the Flow of Light*, Princeton Univ. Press, Princeton, New Jersey (2008).
- [6] M. M. Rahman, J. Ferré-Borrull, J. Pallarès, L. F. Marsal, *Physica Status Solidi-c*, In Press (2011).
- [7] M. E. Zoorob, M.D.B. Charlton, G:J. Parker, J.J Baumberg, M.C Netti, *Nature*, Vol. 404 (2000) 740.
- [8] D. S. Wiersma, A. Lagendijk, *Physical Review E*, Vol. 54 (1996) 4256.
- [9] T. Trifonov, M. Garin, A. Rodriguez, L. F. Marsal, R. Alcubilla, *Physica Status Solidi-a*, Vol. 204 (2007) 3237.
- [10] Z. Kral, L. Vojkuvka, E. Garcia-Caurel, J. Ferre-Borrull, L. F. Marsal, J. Pallares, *Photonics and Nanostructures – Fundamentals and Applications*, Vol. 7 (2009) 12.
- [11] Z. Kral, J. Ferre-Borrull, T. Trifonov, L. F. Marsal, A. Rodriguez, J. Pallares, R. Alcubilla, *Thin Solid Films*, Vol. 512 (2008) 8059.

Figures:

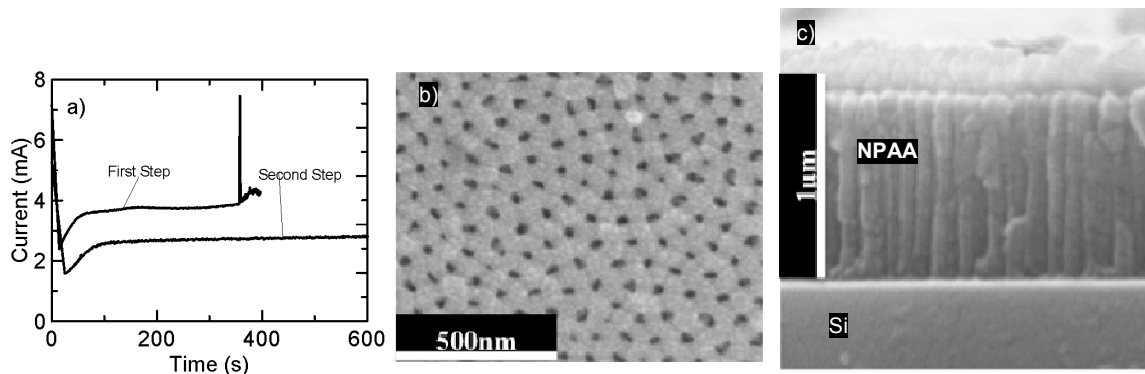


Figure 1: NPAA template on Si obtained with an 0.3 M oxalic acid electrolyte, under potentiostatic conditions with an applied voltage of 40V. a) current-time curve for the first and the second anodization. b) ESEM picture of the sample surface. c) ESEM picture of the sample cross-section.

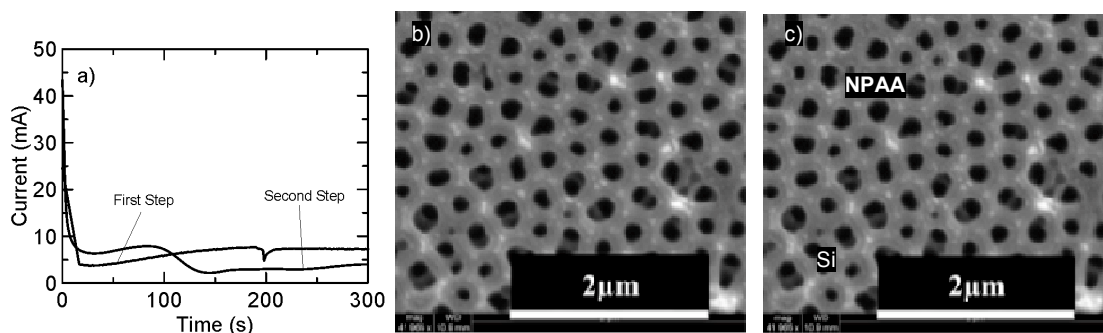


Figure 2: NPAA template on Si obtained with an 0.3 M phosphoric acid electrolyte, under potentiostatic conditions with an applied voltage of 160V. a) current-time curve for the first and the second anodization. b) ESEM picture of the sample surface. c) ESEM picture of the sample cross-section.

LIMITS OF LIGHT FOCUSING THROUGH TURBID MEDIA

Luis S. Froufe-Pérez, J. J. Sáenz

Condensed Matter Dept. Autonomous University of Madrid, Av. Tomás y Valiente 7,
Edificio Ciencias, 28049 Cantoblanco, Spain.
luis.froufe@uam.es

Wave emission and propagation in random media has been a matter of intense research during the last decades. Effects induced by coherent multiple scattering of waves explain to a large extent phenomena such as enhanced coherent backscattering, universal conductance fluctuations, strong Anderson localization of waves and random lasing, to cite a few. [1]

Contrary to what intuition may suggest, the introduction of scattering sources in a system can enhance the focusing ability of an optical system. A simple heuristic argument shows that scattering can efficiently open new propagating channels which are closed otherwise. As has been demonstrated in the microwave regime [2], the inclusion of scatters in the near field of a selected focusing point can even enable subwavelength focusing.

By using wavefront shaping techniques, it has been recently shown [3] in the optical range that, despite experimental limitations, it is possible to achieve the best theoretical focus as predicted by Cittert-Zernike theorem. Using a different approach, it has been shown that the full transmission matrix of a thick turbid medium can be measured both in amplitude and phase [4]. Hence, using an appropriate inversion algorithm, any intensity pattern can be transferred through the sample.

In this work, we theoretically analyze the focusing capabilities of a system with varying amounts of disorder. In particular we shall deal with scalar wave models in confined (guided) geometries.

In this kind of systems, several transport regimes appear depending on the ratio of the system length to the scattering mean free path and the propagating number of channels. For lengths small compared with the mean free path, transport is quasi-ballistic. Diffusive transport is dominant for lengths ranging from about a mean free path up to the so-called localization length. For larger lengths, the system undergoes a crossover to the deep localized regime where transport is exponentially inhibited.

It has been shown [5] that the averaged conductance of the system can account for many transport statistical properties in a universal manner, all the way from quasi-ballistic to deep localization regimes. On the other hand, conductance can be properly defined not only in electronic systems but on optical ones [6]. Being hence conductance a key parameter describing the optical transport properties of a disordered system.

By generating random scattering matrices corresponding to previously defined number of propagating channels, scattering mean free path and system length [7]. We are able to determine all the relevant optical transport parameter of the system. Also, through the use of different inversion algorithms, we can determine the set of appropriate incoming amplitudes for each channel in order to focus light at the other side of the system. In figure 1 we show an example of diffraction-limited focusing by using a Montecarlo algorithm through a system of one mean free path thickness.

It can be shown that, if incoming amplitudes can present an arbitrary dynamic range while keeping a sufficiently small signal-to-noise ratio, focusing is diffraction limited for any transport regime including localization. Nevertheless, the amount of transmitted power is strongly reduced as the scattering increases. It is worth stressing that the transmittance in the focusing mode is much smaller than the channel-averaged transmittance of the sample. Hence, one of the limitations we find is that the transmitted power can be negligible even prior to the onset of localization. As can be seen in figure 2.

On the other hand, if we consider a finite signal-to noise ratio for the incoming amplitudes, focusing ability deteriorates as scattering increases.

In conclusion, we show that, although some amounts of disorder provide an effective coupling to new propagating channels, hence increasing the effective numerical aperture of the optical system.

Focusing capabilities of the system and the effective power transmission are severely reduced if disorder is further increased.

Authors acknowledge fruitful and stimulating discussions with Prof. C. López, Dr. M. Leonetti and Prof. J. S. Dehesa. This work has been supported by the spanish MICINN Consolider Nanolight project (CSD2007-00046).

References:

- [1] P. Sheng, Introduction to Wave Scattering, Localisation, and Mesoscopic Phenomena (Academic Press, New York, 1995).
- [2] G. Lerosey, A. Tourin, and M. Fink, Science 315, (2007) 1120.
- [3] M. Vellekoop, A. Lagendijk, and A. P. Mosk, Nature Photonics 4, (2010) 320.
- [4] S. M. Popoff, G. Lerosey, R. Carminati, M. Fink, A. C. Boccarda, and S. Gigan, Phys. Rev. Lett. 104, (2010) 100601.
- [5] L. S. Froufe-Pérez, P. García-Mochales, P. A. Serena, P. A. Mello, and J. J. Sáenz, Phys. Rev. Lett. 89, (2002) 246403.
- [6] S. Albaladejo, M. Lester, L.S. Froufe-Pérez, A. Garcia Martín y J.J. Sáenz, App. Phys. Lett. 91, (2007) 061107.
- [7] L. S. Froufe-Pérez, M. Yépez, P. A. Mello y J. J. Sáenz, Phys. Rev. E 75, (2007) 031113.

Figures:

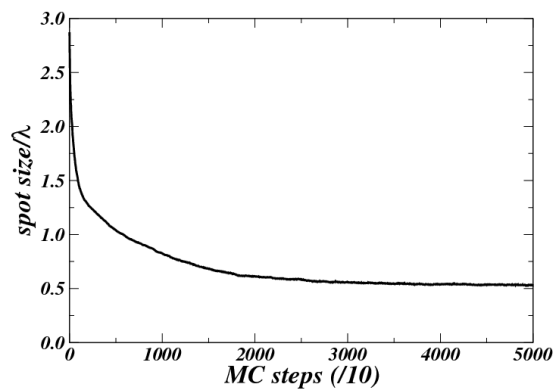


Figure 1: Focusing through a disordered system of 1 mean free path thickness. a) Spot size as a function of the Monte Carlo step. b) intensity map in the focusing plane for a random pattern of incoming field amplitudes. c) intensity map in the focusing plane after incoming amplitudes have been adapted for focusing through a Monte Carlo procedure.

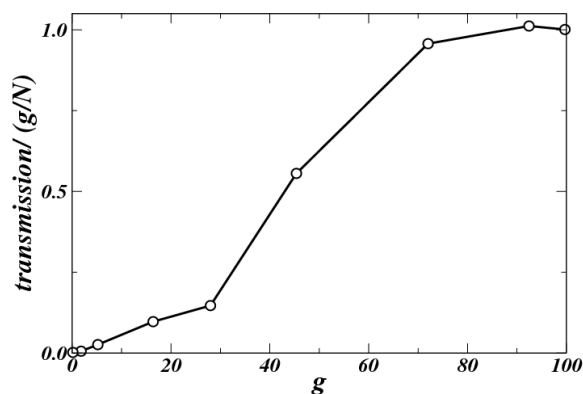


Figure 2: Power transmission of the focused beam normalized to the average one-channel transmittance (conductance divided by the number of channels) as a function of the waveguide conductance.

REAL TIME, MULTIPLEX AND LABEL-FREE BIO-INTERACTION ANALYSIS (BY SURFACE PLASMON RESONANCE IMAGING)

Chiraz Frydman

HORIBA Scientific, Chilly-Mazarin, France
chiraz.frydman@horiba.com

For the last two decades, the Surface Plasmon Resonance (SPR) technology is demonstrated as a powerful tool for the bio-molecular interactions investigations and analysis.

The SPR imaging technology is a ideal solution for rapid, label-free and multiplexed bio-assays and investigations. It's a high sensitive detection method for bio-molecular interactions, using a micro-array biochip format to rapidly monitor multiplex kinetic interactions in real time. This technology allows direct visualization of biomolecular interactions and is suitable for determination of real time physico-chemical interactions and kinetics. Thanks to SPRi, analytes can be detected in the range of the femto-mol.

Surface Plasmon Resonance (SPR) is an optical detection process that can occur when a polarized light hits a prism covered by a thin metal layer. Briefly, a broad monochromatic polarized light (at a specific wavelength) illuminates the whole functionalized area of the SPRi-Biochip™, which is combined with a detection chamber. A CCD video camera gives access to array format by image capture of all local changes at the surface of the SPRi-Biochip™.

SPR imaging has the capacity to record simultaneously the interaction of any ligand to every single spot on the golden surface of the reaction chamber without any label addition. The signals obtained are able to identify, by the spot position in the chip, which probes are recognized by the ligand but also, by analysing the on and off rates of ligand binding, the mean affinity (or avidity) of these ligand to probes can be calculated.

Main applications involve interactions between DNA-DNA, protein-DNA, protein-ligand, peptide-ligand, antibody-cell in the fields of health (aid to diagnosis and treatment), environmental control, new drug discovery and development in pharmaceutical and cosmetic research, quality-control in agro-food etc...

J. F. Galisteo-López¹, M. López-García¹, A. García-Martín², A. Blanco¹, C. López¹

¹Instituto de Ciencia de Materiales de Madrid (ICMM-CSIC), c/ Sor Juana Inés de la Cruz 3, 28049 Cantoblanco, Madrid, Spain

²Instituto de Microelectrónica de Madrid (IMM-CSIC), c/ Isaac Newton 8, 28049 Tres Cantos, Madrid, Spain

galisteo@icmm.csic.es

Self assembly is a well established approach to fabricate photonic structures able to manipulate light propagation and emission at the nanoscale [1]. Beyond its use as a means to fabricate photonic crystals or resonant disordered structures such as photonic glasses, recent reports have shown how self assembly techniques can be used to fabricate hybrid photonic-plasmonic crystals [2, 3] which optical properties allow for a strong modification of the spontaneous emission of internal sources [2]. Further, the sensitivity of their optical response to their environment has been proposed as a means to use this kind of systems of optical sensors [3], and means to control their optical properties by modifying the dielectric components have been demonstrated [4].

In these hybrid structures, where periodic arrays of dielectric colloids are deposited on metallic substrates, electromagnetic fields undergo a strong spatial redistribution and strong field enhancements can be achieved. Depending on the spectral range under consideration electromagnetic fields can be localized close to the metal substrate (plasmon-like modes) or within the dielectric array (waveguidedlike modes) (see Fig. 1a).

Several metallodielectric structures have been fabricated employing gold or silver substrates and their optical response has been compared to reference samples grown on dielectric substrates in order to better appreciate the effect of the metallic component. The dispersion relation of such structures has been probed by means of angle and polarization resolved reflectivity measurements (see Fig. 1b).

As in any photonic structure, losses degrade the optical response of these systems and hence its applicability; therefore knowledge is needed on how such losses can be minimized. In this work we explore the optical response of self-assembled plasmonic-photonic structures having different configurations and fabricated from different materials and explore how one can minimize intrinsic losses due to leakage and absorption. The effect of the optical constants of the metallic substrates has been explored. Further, the role of extrinsic losses originating at residual disorder generated during the growth process is discussed.

References:

- [1] J. F. Galisteo-López, M. Ibisate, R. Sapienza, L. S. Froufe-Pérez, A. Blanco and C. López, *Advanced Materials*, 23 (2011) 30.
- [2] M. López-García, J. F. Galisteo-López, A. Blanco, A. García-Martín and C. López, *Small* 6 (2010) 1757.
- [3] X. Yu, L. Shi, D. Han, J. Zi and P.V. Braun, *Advanced Functional Materials*, 20 (2010) 1910.
- [4] M. López-García, J. F. Galisteo-López, A. Blanco, A. Garcia-Martin and C. Lopez, *Advanced Functional Materials*, 20, (2010) 4338.

Figures:

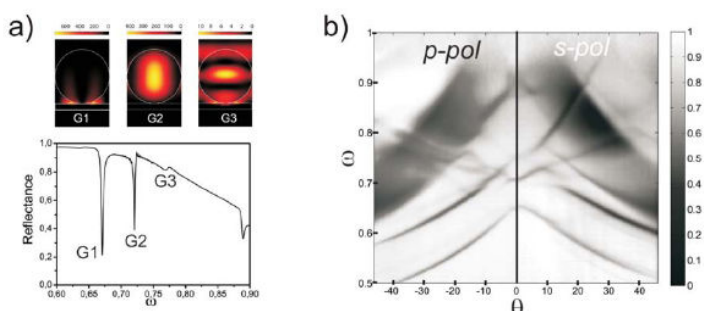
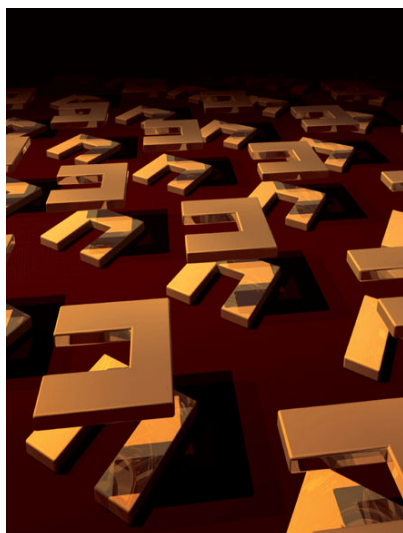


Figure 1: a) Normal incidence reflection spectrum for a dielectric array of 520nm diameter polystyrene spheres deposited on a gold substrate (bottom) and total field intensity profiles of the modes highlighted (top). b) Angle and polarization resolved reflection for the same sample.

THREE-DIMENSIONAL OPTICAL METAMATERIALS AND NANOANTENNAS: CHIRALITY, COUPLING, AND SENSING

Harald Giessen

4th Physics Institute, University of Stuttgart; D-70569 Stuttgart, Germany
giessen@physik.uni-stuttgart.de



Metallic metamaterials have shown a number of fascinating properties over the last few years. A negative refractive index, negative refraction, superlenses, and optical cloaking are some of the ambitious applications where metamaterials hold great promise.

We are going to present fabrication methods for the manufacturing of 3D metamaterials [1]. We are investigating their coupling properties and the resulting optical spectra. Hybridization of the electric [2] as well as the magnetic [3] resonances allows us to easily understand the complex optical properties. Lateral as well as vertical coupling can result in Fano-resonances [4] and EIT-like phenomena [5, 6]. These phenomena allow to construct novel LSPR sensors with a figure of merit as high as five [7].

The connection between structural symmetry and their electric as well as magnetic dipole and higher-order multipole coupling will be elucidated. It turns out that stereometamaterials [8], where the spatial arrangement of the constituents is varied (see figure), reveal a highly complex rotational dispersion. The chiral properties are quite intriguing and can be explained by a coupled oscillator model.

Our three-dimensional stacking approach allows also for the fabrication of 3D nanoantennas, which are favorable for emitting and receiving radiation from quantum systems [9].

References:

- [1] Na Liu, Hongcang Guo, Liwei Fu, Stefan Kaiser, Heinz Schweizer, and Harald Giessen: Three-dimensional photonic metamaterials at optical frequencies, *Nature Materials* 7, 31 (2008).
- [2] N. Liu, H. Guo, L. Fu, S. Kaiser, H. Schweizer, and H. Giessen: Plasmon Hybridization in Stacked Cut-Wire Metamaterials, *Advanced Materials* 19, 3628 (2007)
- [3] Na Liu, Liwei Fu, Stefan Kaiser, Heinz Schweizer, and Harald Giessen: Plasmonic Building Blocks for Magnetic Molecules in Three-Dimensional Optical Metamaterials, *Advanced Materials* 20, 3859 (2008).
- [4] B. Lukyanchuk, N. I. Zheludev, S. A. Maier, N. J. Halas, P. Nordlander, H. Giessen, and C. T. Chong: The Fano resonance in plasmonic nanostructures and metamaterials, *Nature Materials* 9, 707 (2010).
- [5] Na Liu, Stefan Kaiser, and Harald Giessen: Magnetoinductive and Electroinductive Coupling in Plasmonic Metamaterial Molecules, *Advanced Materials* 20, 4521 (2008).
- [6] Na Liu, N. Liu, L. Langguth, T. Weiss, J. Kästel, M. Fleischhauer, T. Pfau, and H. Giessen: Plasmonic EIT analog at the Drude damping limit, *Nature Materials* 8, 758 (2009).
- [7] Na Liu, T. Weiss, M. Mesch, L. Langguth, U. Eigenthaler, M. Hirschner, C. Sönnichsen, and H. Giessen: Planar metamaterial analog of electromagnetically induced transparency for plasmonic sensing, *Nano Lett.* 10, 1103 (2010).
- [8] Na Liu, Hui Liu, Shining Zhu, and Harald Giessen: Stereometamaterials, *Nature Photonics* 3, 157 (2009).
- [9] H. Giessen and M. Lippitz: Directing light emission from quantum dots, *Science* 329, 910 (2010).

INTERFERENCE BETWEEN ELECTRIC AND MAGNETIC DIPOLES IN DIELECTRIC SPHERES: SCATTERING ANISOTROPY AND OPTICAL FORCES

V. R. Gómez-Medina^{1,2}, M. Nieto-Vesperinas¹, J. J. Sáenz²

¹Instituto de Ciencia de Materiales de Madrid, Consejo Superior de Investigaciones Científicas (CSIC),
Campus de Cantoblanco, Madrid 28049, Spain.

² Departamento Física de la Materia Condensada UAM, Madrid 28049, Spain
rgomezmedina@icmm.csic.es

Electromagnetic scattering from nanometer-scale objects has long been a topic of large interest and relevance to fields from astrophysics or meteorology to biophysics, medicine and material science [1-5]. In the last few years, small particles with resonant magnetic properties are being explored as constitutive elements of new metamaterials and devices. Magnetic effects, however, cannot be easily exploited in the visible or infrared regions due to intrinsic natural limitations of optical materials and the quest for magnetic plasmons and magnetic resonant structures at optical frequencies [6] has then been mainly focused on metallic structures. The unavoidable problems of losses and saturation effects inherent to these metamaterials in the optical and near infrared regimes have stimulated the study of high-permittivity particles as their constitutive elements [7-9]: For very large permittivities, small spherical particles present well defined sharp resonances [1]; either electric or magnetic resonant responses can then be tuned by choosing the appropriate sphere radius.

In the presence of both electric and magnetic properties, the scattering characteristics of a small object present markedly differences with respect to pure electric or magnetic responses. Even in the simplest case of small or of dipolar scatterers, remarkable scattering effects of magnetodielectric particles were theoretically established by Kerker et al. [10] concerning suppression or minimization of either forward or backward scattering. Intriguing applications in scattering cancellation and cloaking [11] and magneto-optical systems [12-14] together with the unusual properties of the optical forces on magnetodielectric particles [15-17] have renewed interest in the field.

The striking characteristics of the scattering diagram of small (Rayleigh) magnetodielectric particles [10,18] were obtained assuming arbitrary values of electric permittivity and magnetic permeability. Nevertheless, no concrete example of such particles that might present those interesting properties in the visible or infrared regions had been proposed.

Very recently, it has been shown [19] that submicron silicon spheres present dipolar magnetic and electric responses, characterized by their respective first-order Mie coefficient, in the near infrared, in such a way that either of them can be selected by choosing the illumination wavelength. We will show that Si spheres constitute such a previously quested real example of dipolar particle with either electric and/or magnetic response, of consequences both for their emitted intensity and behavior under electromagnetic forces [16,17]. These properties should not be restricted to Si particles but should also apply to other dielectric materials with relatively moderate refraction index. Furthermore, we will discuss the effects associated to the interference between electric and magnetic dipoles in germanium spheres [20]. As we will demonstrate the extinction cross section and the scattering diagrams of these submicron dielectric particles in the infrared region can be well described by dipolar electric and magnetic fields, being quadrupolar and higher order contributions negligible in this frequency range. Specifically, the scattering diagrams calculated at the generalized Kerker's conditions are shown to be equivalent to those previously reported [10,18] for hypothetical ($\epsilon \neq 1$, $\mu \neq 1$) magnetodielectric particles. Finally we will analyze the consequences of the strong scattering anisotropy on the radiation pressure on these particles showing the electric-magnetic dipolar interaction plays an active role in spinning the particles either in or out of the whirls sites of the interference pattern, leading to trapping or diffusion[17].

References:

- [1] H. C. van de Hulst, *Light Scattering by small particles* (Dover, New York, 1981). C. F. Bohren and D. R. Huffman, *Absorption and Scattering of Light by Small Particles* (John Wiley&Sons, New York, 1998).
- [2] M. I. Mishchenko, L. D. Travis and A. A. Lacis, *Scattering, Absorption, and Emission of Light by Small Particles* (Cambridge Univ. Press, 2002). L. Novotny and B. Hecht, *Principles of Nano-Optics*, (Cambridge University Press, Cambridge, 2006). E. M. Purcell and C. R. Pennypacker, *Astrophys. J.* 186 (1973) 705. B. T. Draine, *Astrophys. J.* 333 (1988) 848.
- [3] S. J Oldenburg, R. D Averitt, S. L Westcott, N. J Halas. *Chem. Phys. Lett.*, 288 (1998) 243.
- [4] P. K. Jain, X. Hunag, I. H. El-Sayed and M. A. El-Sayed, *Acc. Chem: Res.* 41(12) (2008) 1578.
- [5] E. S. Day, J. G. Morton and J. L. West, *J. Biomech. Eng.* 131(7) (2009) 074001.
- [6] A. Alú and N. Engheta, *Opt. Express* 17, 5723-5730 (2009). *Phys. Rev. B* 78 (2008) 085112.
- [7] K. C. Huang, M. L. Povinelli, and J. D. Joannopoulos, *Appl. Phys. Lett.* 85 (2004) 543.
- [8] C. L. Holloway, E. F. Kuester, J. Baker-Jarvis, and P. Kabos, *IEEE Trans. Antennas Propag.* 51 (2003) 2596. M. S. Wheeler, J. S. Aitchison, and M. Mojahedi, *Phys. Rev. B* 72 (2005) 193103.
- [9] V. Yannopoulos and A. Moroz, *J. Phys.: Condens. Matter* 17 (2005) 3717. A. Ahmadi, and H. Mosallaei, *Phys. Rev. B* 77 (2008) 045104. M. S. Wheeler et al, *Phys. Rev. B* 79 (2009) 073103. L. Jylhä, I. Kolmakov, S. Maslovski and S. Tretyakov, *J. Appl. Phys.* 99 (2006) 043102. L. Peng et al, *Phys. Rev. Lett.* 98 (2007) 157403. J. A. Schuller et al., *Phys. Rev. Lett.* 99 (2007) 107401. K. Vynck, et al, *Phys. Rev. Lett.* 102 (2009) 133901.
- [10] M. Kerker, D. S. Wang, and C. L. Giles, *J. Opt. Soc. Am.* 73 (1983) 765767.
- [11] U. Leonhardt, *Science* 312 (2006) 17771780. J. B. Pendry, D. Schurig, and D. R. Smith, *Science* 312 (2006) 17801782. A. Alú and N. Engheta, *J. Nanophoton.* 4 (2010) 041590.
- [12] A. Lakhtakia, V. K. Varadan and V. V. Varadan, *J. Mod. Optics* 38 649 (1991). B. García-Cámara, F. Moreno, F. González and O. J. F. Martín, *Opt. Express* 18 (2010) 10001.
- [13] S. Albaladejo, R. Gómez-Medina, L. S. Froufe-Pérez, H. Marinchio, R. Carminati, J. F. Torrado, G. Armelles, A. García-Martín and J.J. Sáenz, *Opt. Express* 18 (2010) 3556.
- [14] V. V. Temnov, G. Armelles, U. Woggon, D. Guzatov, A. Cebollada, A. García-Martín, J.-M. García-Martín, T. Thomay, A. Leitenstorfer and R. Bratschitsch, *Nat. Phot.* 4 (2010) 107.
- [15] M. Nieto-Vesperinas, J. J. Sáenz, R. Gómez-Medina and L. Chantada, *Opt. Express* 18 (2010) 11428.
- [16] M. Nieto-Vesperinas, R. Gómez-Medina, and J. J. Sáenz, *J. Opt. Soc. Am. A* 28 (2011) 54.
- [17] R. Gómez-Medina, M. Nieto-Vesperinas and J. J. Sáenz, *Phys. Rev. A* (submitted 2010).
- [18] B. García-Cámara, F. Moreno, F. Gonzalez and J. M. Saiz, *J. Opt. Soc. Am. A* 25 (2008) 28752878. *J. Opt. Soc. Am. A* 25 (2008) 2875.
- [19] A. García-Etxarri, R. Gómez-Medina, L. S. Froufe-Pérez, C. López, L. Chantada, F. Scheffold, J. Aizpurúa, M. Nieto-Vesperinas and J. J. Sáenz, *Opt. Express* (submitted 2010), ArXiv:1005.5446v1.
- [20] R. Gómez-Medina, B. García-Cámara, I. Suárez-Lacalle, F. González, F. Moreno, M. Nieto-Vesperinas, J. J. Sáenz, *J. Eur. Opt. Soc, Rapid Publ.* (submitted 2011).

B. Cluzel¹, K. Foubert^{1,2}, L. Lalouat¹, E. Picard², D. Peyrade³, F. de Fornel¹ and **E. Hadji**²

¹LICB/OCP, Unité mixte de recherche n°5209 CNRS - Université de Bourgogne, France

²INAC /SP2M - Laboratoire SiNaPS, UMR-E 9002, CEA-Grenoble, France

³Laboratoire des Technologies de la Microélectronique, CNRS, Grenoble, France

Optical information processing at the chip level has been a long standing dream. However it requires both on chip light generation and manipulation at sub-wavelength scale which remains challenging. In this context, nanobeam cavities appeared as one of the key players thanks to their field confinement capability and their ridge waveguide integrated geometry. In this context, we showed that strong light localization within nanobeam cavities was possible and was moreover tuneable by near-field interaction with an external nanometric tip. We showed as well that twinned high Q nanobeam cavities placed in the near-field of each other can optically couple to form a new optical system with discrete field maps addressable by wavelength selection.

The nanobeam cavities presented here integrate tapered mirrors [2]. Thanks to the mirror Bloch mode - cavity wave guided mode mismatch decrease; they allowed achieving record high Q/V ratios [1]. For those nanobeam cavities, near-field scanning optical microscopy (NSOM) is an effective tool to evidence sub-wavelength sized features in the light localization [3]. But it appeared also as a mean to achieve lossless cavity tuning [4]. The evanescent part of the strongly localized optical field can indeed interact with the NSOM nanometric tip [5]. As a result wavelength shifts larger than the cavity line width were observed under the presence of the NSOM tip leading to drastic change of the cavity transmission at the resonant wavelength. On/off ratios (with and without the tip above the nanobeam cavity) larger than 30 db were observed with Q = 50.000 nanobeam cavities.

Then, if two of these cavities are moved within the near-field of each other, the optical fields can evanescently couple to each other. The easiest way to observe this near-field coupling effect is to fabricate two parallel ridge wave-guides separated by a thin air-slot spacer. A careful recording of optical fields above the structure by NSOM clearly demonstrate the field enhancement in the air slot [6] that result from the coupling effects. Now, if nanobeam cavities, instead of simple optical waveguides, are evanescently coupled, an entirely new optical system can be achieved.

In order to understand the coupling mechanism, we first set two cavities, called twinned cavities since they are strictly identical to each other, at lateral coupling distances ranging from 50 to 500 nm. We observed that the original optical field distribution of one single cavity is now reconfigured over the system made by the twinned cavities. The fundamental mode appears to be splitted into two new modes of different parities [7]. This property means that the light localization within the system of twinned cavities is now wavelength dependent, and thus wavelength addressable.

In order to further exploit this effect, we fabricated structures for which the spacing between nanobeam cavities is maintained constant at 100 nm but the number of coupled cavities is varied from 2 to 4 and 8 cavities.

We then recorded the optical field evolution as a function of the number of coupled cavities and observed that the more we increase the number of cavities the more we generate splitted optical modes [8]. As a result, since each mode carries its own wavelength, we create for n coupled cavities a set of n different field localizations or field maps over the sample, each of them being addressable by a specific wavelength.

So we evidence here that the electromagnetic field distribution within the reported nanosystems can be engineered on demand at the sub-wavelength scale giving access to a whole range of fields map distribution as a function of the input wavelength.

This new architecture offers an unprecedented opportunity to mold on a chip the morphology of the optical field and opens therefore exciting new perspectives for the future development of configurable optical traps, sensors or opto-mechanical oscillators at the nanoscale.

The authors gratefully acknowledge their fruitful discussions with Dr. Philippe Lalanne from Laboratoire Charles Fabry - Institut d'Optique Graduate School, who pioneered the development of the nanobeam cavities.

References:

[1] P. Velha, J. C. Rodier, P. Lalanne, J.P. Hugonin, D. Peyrade, E. Picard, T. Charvolin, E. Hadji, "Ultra-compact silicon-on-insulator ridge-waveguide mirrors with high reflectance", *Appl. Phys. Lett.* 89, 171121 (2006).

[2] P.Velha, E.Picard, T.Charvolin, E.Hadji, J.C.Rodier, P.Lalanne, D.Peyrade, "Ultra-High Q/V Fabry-Perot microcavity on SOI substrate", *Optics Express* 15 (24), 16090 (2007).

[3] L. Lalouat, B. Cluzel, P. Velha, E. Picard, D. Peyrade, J.C Rodier, T. Charvolin, P. Lalanne, F. de Fornel, E. Hadji, "Sub wavelength imaging of light confinement in high Q small V photonic crystal nanocavity", *Appl. Phys. Lett.* 92, 111111 (2008).

[4] B.Cluzel, L.Lalouat, P.Velha, E.Picard, D.Peyrade, J.C Rodier, T.Charvolin, P.Lalanne, F. de Fornel, E. Hadji, "A near-field actuated optical nanocavity", *Optics Express*, 16 (1), 279 (2008).

[5] L.Lalouat, B.Cluzel, P.Velha, E.Picard, D.Peyrade, J.P Hugonin, P.Lalanne, E.Hadji, F. de Fornel, "Near-field interactions between a subwavelength tip and a small-volume photonic-crystal nanocavity", *Phys. Rev. B* 76, 041102 (2007).

[6] K. Foubert, L. Lalouat, B. Cluzel, E. Picard, D. Peyrade, E. Delamadeleine, F. de Fornel et E. Hadji, "Near-field modal microscopy of the subwavelength confinement in multi-mode silicon slot waveguides", *Appl. Phys. Lett.* 93, 251103 (2008).

[7] K. Foubert, L. Lalouat, B. Cluzel, E. Picard, D. Peyrade, F. de Fornel et E. Hadji, "An air-slotted nanoresonator relying on coupled high-Q small-V Fabry Perot nanocavities", *Appl. Phys. Lett.* 94, 251111 (2009).

[8] B. Cluzel, K. Foubert, L. Lalouat, J. Dellinger, D. Peyrade, E. Picard, E. Hadji e t F. de Fornel, "Addressable sub-wavelength grids of confined light in a multi-slotted nanoresonator", *Appl. Phys. Lett.* 98, 081101 (2011).

Figures:

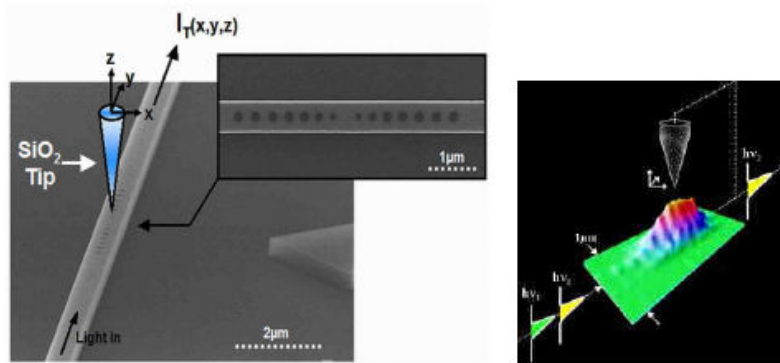


Figure 1: (left) schematic of tip-nanobeam cavity interaction, (inset) details of the nanobeam cavity; (right) resonant optical field as recorded by NSOM.

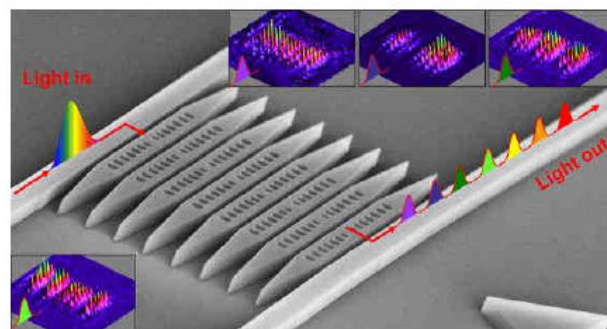


Figure 2: An array of nanobeam cavities generates sub-wavelength grids of confined light. The spatial distribution of the grids can be modified on demand by changing the wavelength in the nanosystem.

GAP-MODE PLASMONIC CAVITIES: ENGINEERING LIGHT-MATTER INTERACTIONS IN METALLIC STRUCTURES

Evelyn L. Hu, Kasey J. Russell, Kitty Yeung, Tsung-Li Liu, Shanying Cui

School of Engineering & Applied Sciences; Harvard University
29 Oxford Street; Cambridge, MA 02138, USA
ehu@seas.harvard.edu

Optical cavities can tightly confine light in the vicinity of optical emitters, enhancing the interaction of light and matter. The modes or optical states of the cavity can be precisely designed and engineered, and in recent years there has been remarkable progress in demonstrations of ‘cavity quantum electrodynamics (cQED)’ in solid state platforms. Such progress has been primarily for cavities fabricated in dielectric materials, with a steady improvement in cavity quality, with quality factors, Q , in excess of $10^4 - 10^6$ realized for cavities with coupled emitters [1],[2]. These high Q -coupled emitter systems have demonstrated heralded single photon emission [3], ultra-low threshold lasing [4] and strong light-matter coupling [5],[6].

Metal-based optical cavities would have inherently lower Q 's (and greater loss) than dielectrics; however, metal cavities utilizing surface plasmon polaritons (SPPs) can have sufficiently small mode volume to produce a substantial Q/V , the quantity relevant for high Purcell factors, a measure of the light-matter interaction. This talk will focus on such *plasmonic cavities*, with optical modes formed within the gap of the two metal layers which defined the cavity [7]. Initial structures comprised silver (Ag) nanowires (NW), 70 nm in diameter and 1 - 3 μm in length, placed into close proximity to a Ag thin film substrate, with the NW axis parallel to the substrate surface. Optically active material was interposed between the nanowire and the Ag substrate: this comprised one to two monolayers of PbS colloidal quantum dots, clad on top and bottom by thin dielectric layers of varying composition and thickness. A representation of the cavity geometry is shown in Figure 1.

The fluorescence spectrum of PbS quantum dots within the gap was strongly modified by the cavity mode, with peak position in quantitative agreement with numerical calculations, and demonstrating Q values of ~ 60 . Figure 2 shows the different modal signatures as a function of nanowire length.

The ability to tune the optical modes into resonance with the emitters is important in achieving the optimal light-matter coupling, and geometry of these cavities lends itself to a relatively simple and straightforward tuning approach. Carefully controlled deposition of dielectric layers formed by Atomic Layer Deposition (ALD) resulted in the systematic shift of the optical modes, as shown in Figure 3.

The high Q/V possible for these cavities, and the range of organic and nanocrystalline emitters they can accommodate make these important building blocks for the exploration of light-matter interaction in the solid state.

References:

- [1] S. Noda, M. Fujita, and T. Asano, *Nature Photonics* 1 (2007) 449.
- [2] B.-S. Song, S.-W. Jeon, and S. Noda, *Optics Letter* 36 (2011) 91.
- [3] P. Michler., et al. *Science* 290 (2000) 2282.
- [4] S. Strauf et al., *Phys. Rev. Lett.* 96 (2006) 127404.
- [5] J. Reithmaier et al.. *Nature* 432(2004) 197.
- [6] K. Hennessy, A. Badolato, et al. *Nature* 445 (2007) 896.
- [7] K. Russell and E. Hu, *Appl. Phys. Lett.*97 (2010) 163115.

Figures:

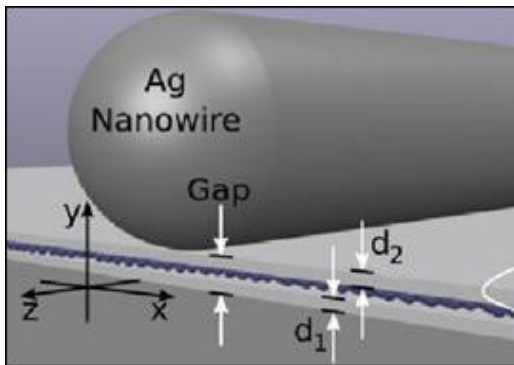


Figure 1: Schematic diagram of plasmonic nanocavity with quantum dot optical emitters (not to scale).

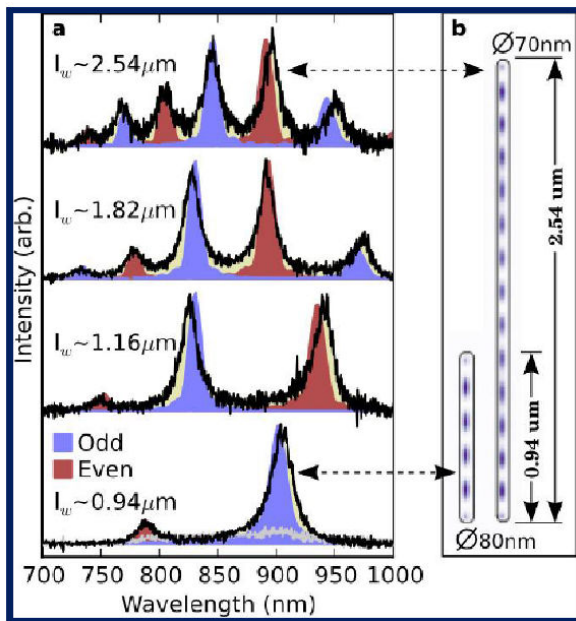


Figure 2: (a) Measured (lines) modes and FDTD calculated resonances (filled curves) from four cavities of different lengths, indicated in (b) Calculated modal profile for the two indicated cavities. The cavity lengths are indicated by the numbers on the upper-left of each spectrum.

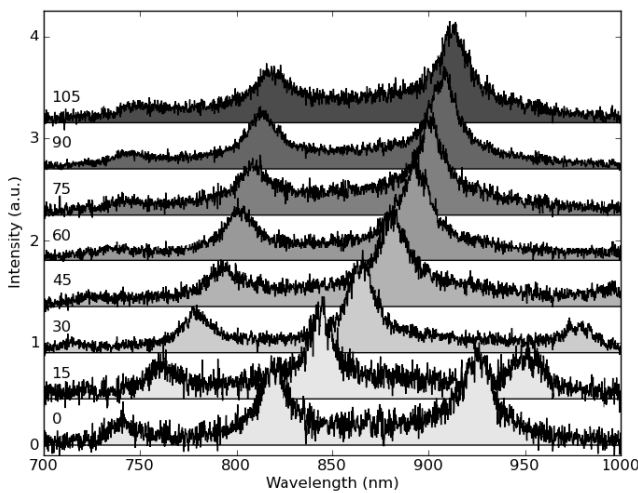


Figure 3: Systematic shift in modes with increased dielectric deposition on cavity. Numbers on the upper left of each spectrum indicate the number of 'cycles' of atomic layer deposition. Approximately 1 nm/cycle of Al_2O_3 is deposited.

BRIGHT CdSe/ZnSe NANOWIRE-QUANTUM DOTS FOR SINGLE PHOTONS EMISSION

S. Bounouar, M. Elouneq-Jamroz, G. Sallen, M. Den Hertog, C. Morchutt, E. Bellet-Amalric, R. André, C. Bougerol, J.P. Poizat, S. Tatarenko and **K. Kheng**

Nanophysics and Semiconductors Group, INAC and Institut NEEL, CEA/CNRS/University Joseph Fourier CEA-Grenoble, 17 rue des Martyrs, 38054 Grenoble, France

kkheng@cea.fr

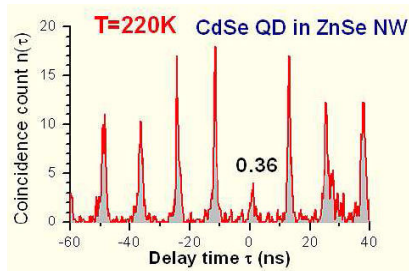


Figure 1: Single photon emission at 220K [2]

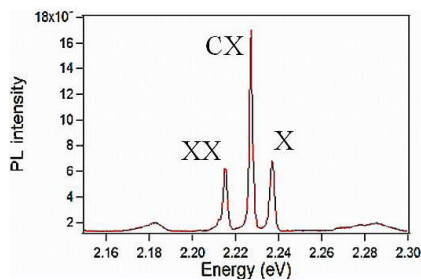


Figure 2: Exciton, biexciton and charged exciton emission in single CdSe/ZnSe NW-QD [3]

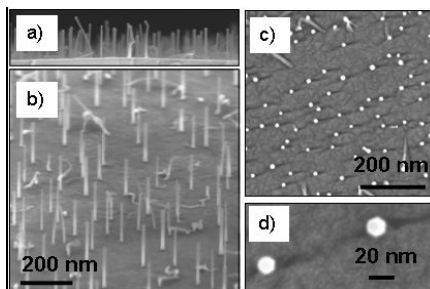


Figure 3: SEM images ZnSe NWs grown on a ZnSe (111)B buffer layer. Side (a,b) and top (c,d) views.

Semiconductor nanowires (NW) are appealing structures that allow designing quantum structure with unprecedented freedom. With NW, new type of quantum dot (QD) heterostructures (NW-QD) can be directly grown on defined positions without the necessity of self-assembly, as well as more complex structures such as coupled QDs or core-shell structure. However, the quantum confinement requires growing NW with very small lateral size (of the order of the Bohr radius) with high crystalline structure and clean surfaces (to prevent quenching of the exciton emission through non radiative recombination).

Using MBE in the vapour-liquid-solid growth mode (VLS) we have developed the growth of very high quality ZnSe nanowire [1] with typical diameter of 10 nm (strong confinement regime). We have demonstrated recently that a single CdSe quantum dot embedded in such a ZnSe NW can emit single photons up to 220K [2]. We will present our recent progress over the growth and optical studies on ZnSe/CdSe NW-QD. The quality of our NW is good enough to allow investigating very fine optical properties in single NWs. In pure ZnSe NW, we can observe the band edge emission at 442nm. In ZnSe/CdSe NW-QD, photon correlations measurements have allowed to unambiguously identify exciton, biexciton and trion [3] as well as to study the dynamics, in the nanosecond scale, of the spectral diffusion mechanism [4].

References:

- [1] T. Aichele et al., Appl. Phys. Lett. 93, 143106 (2008)
- [2] A. Tribu, et al., Nano Lett., 8 (12), 4326 (2008)
- [3] G. Sallen et al., Phys. Rev. B 80, 085310 (2009)
- [4] G. Sallen, A. Tribu, T. Aichele, R. Andre, L. Besombes, C Bougerol, M. Richard, S. Tatarenko, K. Kheng, JP Poizat, Nature Photonics 4, 696 (2010)

Thomas F Krauss

SUPA, School of Physics and Astronomy, University of St Andrews, UK
tfk@st-andrews.ac.uk

Controlling light on the nanoscale is an equally exciting and challenging goal, and it allows us to strongly enhance light-matter interactions. Photonic crystals offer such control without inherent losses; they allow us to slow light down, confine it to wavelength-scale spaces and considerably enhance nonlinear interactions. These abilities are enabled by the careful engineering of the photonic crystal's properties and their nanofabrication. Here, we discuss three examples of enhanced light-matter interaction, namely a) farfield-optimised cavities for harmonic wavelength generation, b) substantial control of defect-based light emission via the Purcell factor and c) the strong confinement of light in air for sensing, all enabled by the photonic crystal toolkit.

I. Cavities. High-Q photonic crystal nanocavities have become very popular in recent years, as they offer a unique way for enhancing light-matter interaction due to their ability of combining very high Q-factors with very small volumes [1] thus allowing us to achieve strong enhancement of optical nonlinearities such as harmonic generation. In particular, we have observed both second and third-harmonic generation using only mW-level diode pump sources [2]. A major issue with the design of such high-Q cavities is their off-plane radiation pattern, which makes vertical in- and out-coupling difficult. We have investigated the possibility of modifying the far-field radiation pattern in order to achieve simultaneously high quality factor and high coupling efficiency to an external laser beam in a vertical-coupling configuration [3].

II. Light emission. While studying the nonlinear behaviour of these cavities, we also noted significant levels of light emission in the 1.4 μm - 1.6 μm band, even at room temperature. The emission is understood to arise from the H_2 - based defects, the H_2 being introduced by the implantation process that occurs during SOI manufacturing. We observe sharp and intense photoluminescence peaks that correspond to the resonant modes of the photonic crystal nanocavities, with an up to 300-fold enhancement of the emission from the nanocavity compared to the background, corresponding to a Purcell factor of around 12 [4]. The weak temperature dependence is one of the most striking features, i.e. there is a less than 2-fold reduction between 10 K and room temperature, which makes this approach suitable for the realization of efficient room-temperature light sources at telecom wavelengths as well as providing a quick and easy tool for the broadband optical characterization of SOI-based nanostructures.

III. Slotted cavities. While the above techniques have provided the means for engineering the cavity mode inside the material, they can also be adopted for confining light in air, thus affording opportunities for very strong light-matter interaction in a range of dielectric materials. To this end, we have modified the well-known slotted waveguide configuration [5] and embedded it into the photonic crystal environment. This geometry affords us significant control over the waveguide mode, even outside the dielectric material. As a result, we have been able to achieve confinement in air and reached Q-factors as high as 50,000, which has obvious implications for environmental sensing [6].

In conclusion, it is clear that photonic crystals offer a host of opportunities in confining light at the nanoscale, especially for applications in nonlinear optics, light emission control and environmental sensing.

References:

- [1] Y. Akahane, T. Asano, B-S. Song, S. Noda, "High-Q photonic nanocavity in a two-dimensional photonic crystal", Nature 425 (2003) pp. 944-947.
- [2] M. Galli, D. Gerace, K. Welna, T. F. Krauss, L. O'Faolain, G. Guizzetti, and L. C. Andreani, "Low-power continuous-wave generation of visible harmonics in silicon photonic crystal nanocavities", Opt. Express 18 (2010) 26613.
- [3] S.L. Portalupi, M. Galli, C. Reardon, T. F. Krauss, L. O'Faolain, L. C. Andreani, and D. Gerace, "Planar photonic crystal cavities with far-field optimization for high coupling efficiency and quality factor", Opt. Express 18 (2010) 16064.
- [4] R. Lo Savio, S. L. Portalupi, D. Gerace, A. Shakoor, T. F. Krauss, L. O'Faolain, L. C. Andreani, and M. Galli, "Room-temperature emission at telecom wavelengths from silicon photonic crystal nanocavities", submitted for publication (2011).
- [5] V. R. Almeida, Q. Xu, C. A. Barrios and M. Lipson, "Guiding and confining light in void nanostructure," Opt. Lett. 29 (2004) pp. 1209-1211.
- [6] A. Di Falco, L. O'Faolain and T. F. Krauss, "Chemical sensing in slotted photonic crystal heterostructure cavities," Appl. Phys. Lett. 94 (2009) 063503.
- [7] M. G. Scullion, T. F. Krauss and A. Di Falco, "High efficiency interface for coupling into slotted photonic crystal waveguides" IEEE Photonics Journal, in press (2011).

Figures:

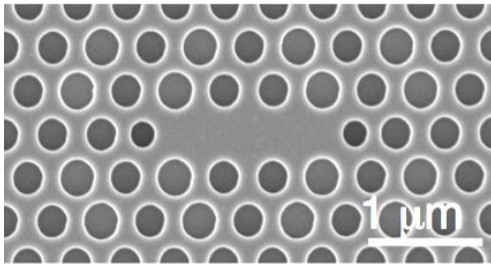


Figure 1: Photonic crystal cavity with farfield engineering. The alternating smaller and larger holes act as a superimposed second order grating that much improves the farfield radiation pattern without overly compromising the Q-factor; in the best case, for example, the Q-factor drops from 120k to 80k while the extraction efficiency increases by an order of magnitude.

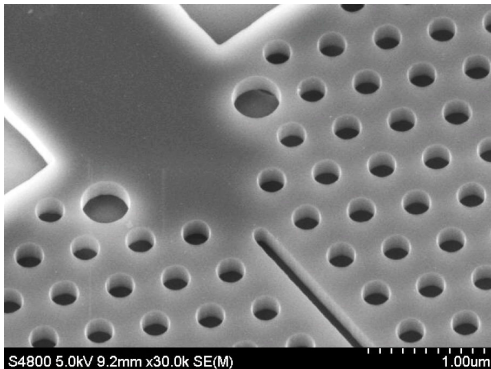


Figure 2: Interface between slotted photonic crystal and conventional waveguide; careful engineering of this interface affords an injection efficiency of better than 1dB. [7].

Christoph Langhammer^{1,4}, Carl Wadell¹, Timur Shegai², Elin M. Larsson^{3,4}, Mikael Käll² and Igor Zoric¹

¹Chemical Physics, Chalmers University of Technology, Göteborg, Sweden

²Bionanophotonics, Chalmers University of Technology, Göteborg, Sweden

³Competence Center for Catalysis, Chalmers University of Technology, Göteborg, Sweden

⁴Insplorion AB, Ekmansgatan 3, 411 32 Göteborg, Sweden

clangham@chalmers.se

Nanosized systems (particles and films) are essential ingredients in many established or envisioned technological applications, including sensors, heterogeneous catalysts, photovoltaics, electronic and photonic devices, batteries and hydrogen storage systems. In many of these applications the nanosized systems are in contact with gaseous or liquid environments and desired (e.g. in catalysis) or undesired (e.g. corrosion) interactions between gas or liquid molecules and the nanosized system may occur. In this context it is of particular importance to develop experimental tools for fast, sensitive and reliable measurements of processes on/in nanosized systems under realistic, close-to-application, conditions. The latter often means working at high temperatures, at ambient or higher pressure and in harsh and corrosive environments. Furthermore, sometimes measurements would preferably be done on a single nanoparticle to avoid ensemble-averaging related effects.

Indirect Nanoplasmonic Sensing (INPS) [1-3] is a novel experimental technique fulfilling the above criteria (in analogy to “traditional” nanoplasmonics for biosensing applications [4]). The remarkably sensitive and very versatile INPS platform consists of plasmonic sensor nanoparticles (Au nanodisks or nanocones, prepared on a transparent substrate by Hole-Mask Colloidal Lithography [5]), covered by a thin dielectric film onto which the nanosized system to be studied is deposited (Figure 1). The key to the sensing is utilization of localized surface plasmon resonances (LSPR) in the Au sensor nanoparticles. The latter, via shifts in their extinction spectra, sensitively measure, for example, changes in the surface coverage of adsorbed reactant species (sensitivity <0.1 ML) on [1], or the formation of new phases in [2,3] the adjacent studied nanosystems on the spacer layer. These already demonstrated examples open a whole new field of nanoplasmonic sensing for nanomaterials science due to the generic nature of the INPS approach.

Here, we demonstrate how INPS, (i) in a simple optical transmission/reflection or (ii) dark-field scattering experiment, can be used to monitor and quantify size effects in metal hydride formation on the particle ensemble (i) and, for the first time, single particle level (ii) in Mg and Pd nanoparticles, ranging in size from 1 nm to 50 nm. The latter are ideal model systems to scrutinize how nano-sizing of the hydrogen storage entities influences phase diagram, thermodynamics and kinetics of nanoscopic metal hydrides. Furthermore, Mg is a very interesting system for commercial solid-state hydrogen storage due to its lightweight and low cost. The versatility of the INPS method in this context is illustrated with the following examples:

- 1) INPS measurements of activation energies for rate limiting steps during hydrogen sorption/desorption in Pd nanoparticles (1-10 nm) illustrate, for the first time, the size dependence of the activation energy for hydrogen diffusion through nanosized Pd hydride and hydrogen desorption from the nanosized Pd particles, respectively. These results are compared to the ab-initio DFTbased calculations for the respective systems.
- 2) Measurements of hydride formation thermodynamics and kinetics in Mg nanoparticles illustrate how complex INPS nanostructures (i.e. Au/Ti/Mg/Ti/Pd layered nanodisks) can be studied quantitatively in a convenient way and how nanosizing can be efficiently used to engineer storage thermodynamics and kinetics in storage systems relevant for applications.
- 3) Single particle dark-field scattering INPS experiments on the two above-described systems, i.e. studies of hydride formation in single Mg and Pd nanoparticles, illustrate the possibility to completely eliminate problems caused by inhomogeneous size-distributions and temperature or mass-transport gradients present in studies of ensembles of nanosized entities.

References:

- [1] E. M. Larsson, C. Langhammer, I. Zoric, B. Kasemo, *Science*, 326 (2009), 1091.
- [2] C. Langhammer, E. M. Larsson, B. Kasemo, I. Zoric, *Nano Letters*, 10 (2010), 3529.
- [3] C. Langhammer, V. P. Zhdanov, I. Zoric, B. Kasemo, *Physical Review Letters*, 104 (2010), 135502.
- [4] J. N. Anker, W. P. Hall, O. Lyandres, N. C. Shah, J. Zhao, R. P. Van Duyne, *Nature Materials*, 7 (2008), 442.
- [5] H. Fredriksson, Y. Alaverdyan, A. Dmitriev, C. Langhammer, D. S. Sutherland, M. Zaech, B. Kasemo, *Advanced Materials* 19 (2007), 4297.

Figures:

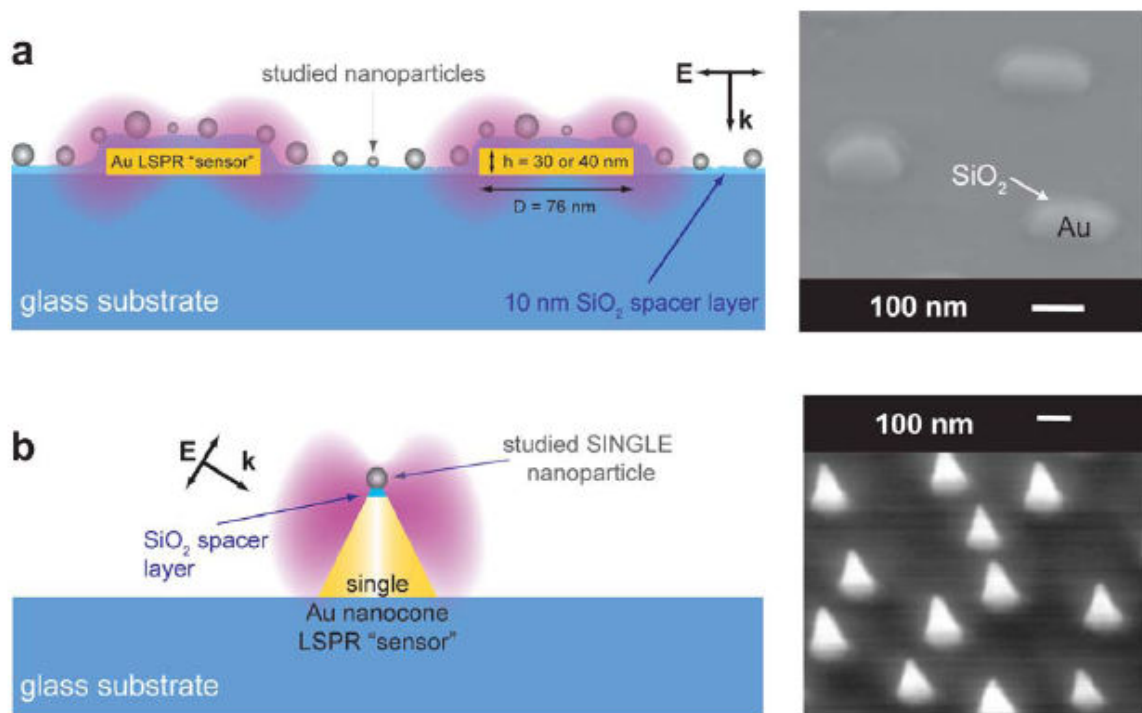


Figure 1: Schematic depictions of (a) a standard INPS platform and (b) single-particle nanocones sensors. The SEM pictures to the right show the respective real nanostructures.

MEASURING LIGHT DIFFUSION IN THIN LEAKY SYSTEMS

Marco Leonetti, Cefe López

ICMM, Sor Juana Inés de la Cruz, 3, Cantoblanco, 28049 Madrid, Spain
marco.leonetti@icmm.csic.es

We developed a new experimental technique that allows to study light diffusion in thin leaky systems, allowing to estimate transport mean free path in samples previously inaccessible.

When a pencil of light shines in a white material (a disordered material with no absorption like e.g. a foam), photons entering in different point of the sample follow different paths and their propagation direction is randomized after a few scattering events. The intensity distribution inside the sample may be predicted in the framework of the diffusion approximation[1] that is, disregarding the ondulatory nature of the electromagnetic field to approximate light like intensity packets performing random walk inside the diffusive material. The critical length describing this phenomena is the transport mean free path ℓ , that is the length after which the packet loses the memory of the incoming direction being completely randomized. A few technique (like Enhanced Backscattering Cone[2] and, total transmission measurement[3]) are able to measure this parameter. Here we propose a new approach that is feasible to measure ℓ in thin (nearly 2d) systems in which light injected in plane and has a large probability of exit on the sides of the sample.

A typical sample consists in a drop of water containing dispersed latex beads, enclosed between microscopy coverslips spaced 100 μm . By using a novel strategy to inject the light between coverslips and collecting side emitted photons as a function of the z coordinate (see figure 1), we obtain a measure of how much deep, diffusing light can penetrate inside the sample before being expelled at the lateral side. By fitting [figure 2] this Lateral Leakage Tail (LLT) with results from random walk simulation we are able to estimate the mean free path of the sample.

ℓ measured by fitting LLT on dispersions of micron sized latex beads, and photonic glasses, are in satisfactory agreement with measurements from literature. Our approach opens the way to new applicative (for example biological and lithographic structures) studies on light diffusion and gives a new instrument to address open fundamental questions on light propagation in disordered structures.

References:

- [1] Sheng P., Introduction to Wave Scattering, Localization and Mesoscopic Phenomena, Springer; 2nd ed. Edition, Berlin (2010)
- [2] Wiersma, D. S., van Albada, Meint P., Lagendijk, Ad, Rev. Sci. Instr., 66 (1995) 5473.
- [3] Garcia N., Genack A.Z, Lisyansky A.A., PRB, 46 (1992) 14475.

Figures:

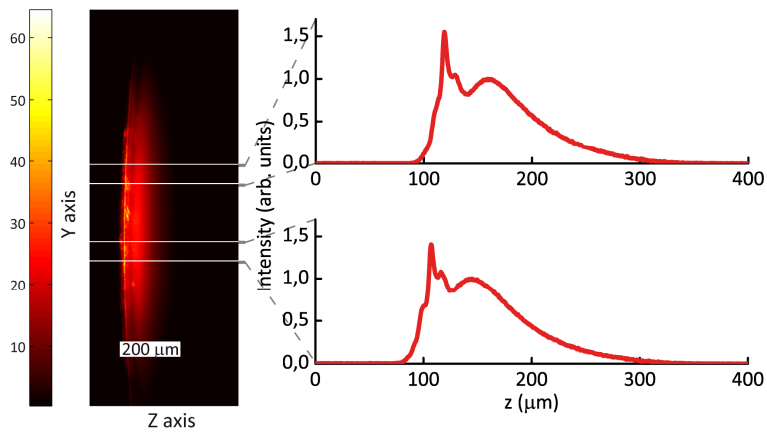


Figure 1: (On the left) Intensity outgoing from the side of the sample, measured by making an image one of the coverslips enclosing the drop of latex particles on a CCD camera. (On the right), the two graphs represent intensity as a function of z retrieved after integrating on the y direction (the integrated area is the one enclosed by white lines on the figure on the right)

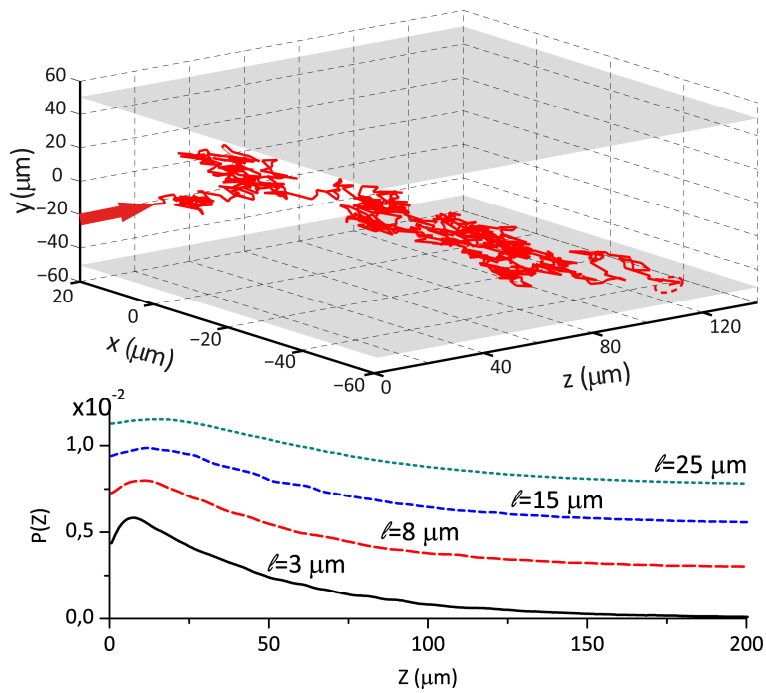


Figure 2: Results from random walk simulations. On the top the trajectory of a single intensity bunch with a random walk step of $R=3 \mu\text{m}$. On the Bottom $P(z)$ (Probability for a diffusive photon Injected at coordinates $(0,0,0)$ photon to exit laterally from the sample at a length Z) calculated for different values of random walk step size for . Graphs are translated vertically of an arbitrary amount.

PHOTOBIOELECTROCHEMICAL SENSORS BASED ON THE COMBINATION OF QUANTUM DOT ELECTRODES WITH ENZYME REACTIONS

F. Lisdat¹, W. Parak², K. Schubert¹, J. Tanne¹

¹Biosystems Technology, Technical University Wildau, Bahnhofstr. 1, 15475 Wildau, Germany

²Biophotonics, Philipps University Marburg Renthof 6, 35032 Marburg, Germany

flisdat@th-wildau.de

Quantum dots, immobilized on electrodes, allow the generation of a photocurrent which is dependent on the applied potential and thus, can work as a light-switchable layer on the sensor surface. The quantum dots can not only interact with the electrode upon illumination but can also exchange electrons with reaction partners in solution allowing the construction of signal chains starting from analyte molecules to be detected [1; 2].

In this work the oxygen dependence of the photocurrent of gold electrodes modified with CdSe/ZnS-quantum dots has been studied. QD immobilisation on the electrode is achieved using a dithiol compound. It has been found that the cathodic photocurrent is enhanced in the presence of oxygen; the current is also influenced by the polarization of the electrode (-500 to +100mV vs Ag/AgCl) and the pH of the solution. It can be also shown that the photocurrent follows the absorption properties of the immobilized QD.

The QD-modified electrode can be used to detect enzyme reactions in solution, this can be shown with lactate dehydrogenase and glucose dehydrogenase [2-4] allowing the analysis of the respective substrate. Here we use the electrode to monitor the activity of the oxygen consuming glucose oxidase (GOD) in solution. Rather small GOD activities (0.025 U/ml) can be detected by photocurrent measurements.

In order to develop a photoelectrochemical biosensor, GOD is immobilized on top of the CdSe/ZnS-electrode. Two different approaches have been followed. The first method is based on the covalent cross-linking of GOD with a bifunctional agent. It can be shown that the consumption of oxygen near the QD surface is a function of the concentration of glucose. The second immobilization strategy uses the layer-by-layer-technique to assemble GOD and poly(allylamin hydrochloride) (PAH). Mass sensitive analysis proves the assembly of [GOD/PAH]_n-layer systems (n=2,4,6) on the surface. Photocurrent measurements demonstrate an increased glucose sensitivity with an increase in the number of GOD layers. High enzyme concentrations results in a well detectable photocurrent change between 100µM and 5mM glucose ([GOD/PAH]₄-layer-QD-electrode). This allows substrate detection by illumination of the respective sensor surface and thus provides the basis for a spatial read out of the sensing electrode.

References:

- [1] C. Stoll, S. Kudera, W. Parak, F. Lisdat, *Small* 2(6) (2006) 741.
- [2] E. Katz, M. Zayats, I. Willner, F. Lisdat, *Chem. Comm.* 13 (2006) 1395.
- [3] C. Stoll, C. Gehring, K. Schubert, M. Zanella, W. Parak, F. Lisdat *Biosens. & Bioelec.* 24 (2008) 260.
- [4] K. Schubert, W. Khalid, Z. Yue, W. J. Parak, F. Lisdat *Langmuir* 26(2) (2010) 1395.

HOT SPOTS AND CONFINEMENT IN METAL NANOPARTICLES AND ASSEMBLIES

Ramón A. Alvarez-Puebla, F. Javier García de Abajo, **Luis M. Liz-Marzán**

Departamento de Química Física and Unidad Asociada CSIC-Universidade de Vigo, Vigo, Spain
lmarzan@uvigo.es

Gold nanoparticles display extremely interesting optical properties, due to their efficient coupling with visible and NIR light, through localized surface plasmon resonances (LSPR). One of the important effects of LSPR is the huge enhancement of the electromagnetic field at the particles surface, which is in turn the main factor behind the so-called surface enhanced spectroscopies (SES) and in particular of surface enhanced Raman scattering (SERS).

It has been predicted that such enhancing ability can be increased at metal surfaces with acute apexes, where LSPR can be strongly confined. Experimental demonstration of this effect has been recently reported, through the colloidal synthesis of so-called gold nanostars, i.e. nanoparticles covered with a significant number of sharp spikes, which display two plasmon resonances, associated to the central core and the spikes themselves. In this talk we shall present a variety of examples regarding the growth of spikes from different gold nanoparticles, as well as their optical characterization (through UV-vis and EELS spectroscopies). Additionally, we have been able to explore the SERS efficiency of these novel nanostructures, through several experiments that demonstrate maximum enhancement when the probe molecules are adsorbed precisely at the tips.

Additionally, examples will be shown of the possibility of creating organized assemblies of metal nanoparticles, with an extremely high density and uniformity of hot spots, in agreement with numerical simulations.

Enrique Maciá

Dpto. Física de Materiales, Facultad CC. Físicas, Universidad Complutense de Madrid,
E-28040, Madrid, Spain
emaciaba@fis.ucm.es

During the last few years a growing number of papers considering the role of deterministic aperiodic order in the optical response of different physical systems has progressively appeared in the literature [1]. Most of these works address the fundamental question concerning whether the specific aperiodic order present in the considered devices results in a better performance than that obtained for more usual periodic arrangements in some specific applications. The inspiring basic principle at work can be easily grasped by considering a layered structure consisting of a number of films aperiodically stacked. In this way, two kinds of order are introduced in the same sample at different length scales. At the atomic level we have the usual periodic order determined by the crystalline arrangement of atoms in each layer, whereas at longer scales we have the quasiperiodic order determined by the sequential deposition of the different layers. This long-range aperiodic order is artificially imposed during the growth process and can be precisely controlled. Since different physical phenomena have their own relevant physical scales, by properly matching the characteristic length scales we can efficiently exploit the aperiodic order we have introduced in the system. Thus, the possibility of growing devices based on an aperiodic stacking of different layers introduces an additional degree of freedom, related to the presence of two different kinds of order in the same sample at different length scales, hence opening new avenues for technological innovation [2]. For instance, one can use sandwiched arrays of aperiodic dielectric multilayers to design optical microcavities [3-5], omnidirectional mirrors [6], multi-stop band filters [7,8], photonic bandgaps [9-12], waveguide structures [13] and many other optical systems of practical interest.

In the case of nonlinear optics, quasiperiodic multilayers can provide more reciprocal vectors to the quasi-phase-matching optical process, and this ultimately results in a more plentiful spectrum structure than that of a periodic multilayer [14,15]. On this basis, the possibility of designing aperiodic structures able to simultaneously phase matching any two nonlinear interactions by properly introducing an aperiodic modulation of the nonlinear coefficient in ferroelectric devices has been proposed in one [16] and two dimensions [17]. The nonlinear properties of optical heterostructures can also be used to fabricate compact-sized compressors for laser pulse. This compression is physically determined by the group velocity dispersion in the material, so that one can expect that by adding more layers to a periodic multilayer one should obtain narrower optical bands and the compression effect will be increased. However, this is inevitably accompanied by an increase of the total thickness of the structure, which is undesirable. In this context, the recourse to aperiodic structures, exhibiting a significantly larger fragmentation of their optical spectrum for similar system sizes, appears as a natural choice.

New approaches in order to obtain innovative optical systems are also based on the construction of modular devices composed of both periodically and aperiodically arranged multilayers. Such devices can be viewed as hybrid order systems made of two different kinds of subunits, each one exhibiting a different kind of topological ordering [18]. The introduction of these subunits endows the system with an additional design parameter, bridging the gap between the atomic level characteristic of the microstructural domain of each layer and the mesoscale level associated to the long-range order of the entire device as a whole [19-21].

References:

- [1] E. Maciá, "Aperiodic Structures in Condensed Matter: Fundamentals and Applications" (CRC Press, Boca Raton, FL, 2009).
- [2] E. Maciá, Rep. Prog. Phys. 69 (2006) 397
- [3] Maciá E, Appl. Phys. Lett. 73 (1998) 3330.
- [4] V. Agarwal, M. E. Mora-Ramos, and B. Alvarado-Tenorio, Photon. Nanostruct. 7 (2009) 63
- [5] S. V. Zhukovsky and S. V. Gaponenko, Phys. Rev. E 77 (2008) 046602
- [6] A. G. Barriuso, J. J. Monzón, L. L. Sánchez-Soto, and A. Felipe, Appl. Opt. 46 (2006) 2903
- [7] S. Golmohammadi, M. K. Moravvej-Farshi, A. Rostami, and A. Zarifkar, Appl. Opt. 47 (2008) 6477
- [8] Y. Trabelsi, M. Kanzari, and B. Rezig, Optica Applicata 39 (2009) 320
- [9] P. W. Mauriz, M. S. Vasconcelos, and E. L. Albuquerque, Phys. Lett. A 373 (2009) 496
- [10] V. R. Tuz, J. Opt. Soc. Am. B 26 (2009) 627
- [11] J. A. Monsoriu, R. A. Depine, and E. Silvestre, J. Eur. Opt. Soc. 2 (2007) 07002; J. A. Monsoriu, R. A. Depine, M. L. Martínez-Ricci, E. Silvestre, and P. Andrés, Opt. Lett. 34 (2009) 3172
- [12] X.-H. Deng, J.-T. Liu, J.-H. Huang, L. Zou, and N.-H. Liu, J. Phys.: Condens. Matt. 22 (2010) 055403
- [13] Zhu S N, Zhu Y Y, Qin Y Q, Wang H F, Ge C Z, and Ming N B, Phys. Rev. Lett. 78 (1997) 2752
- [14] Y. Sheng, K. Koynov, J. Dou, B. Ma, J. Li, and D. Zhang, Appl. Phys. Lett. 92 (2008) 201113
- [15] Fradkin-Kashi K, Arie A, Urenski P, and Rosenman G, Phys. Rev. Lett. 88 (2002) 023903
- [16] Lifshitz R, Arie A, and Bahabad A, Phys. Rev. Lett. 95 (2005) 133901
- [17] Maciá E, Phys. Rev B 63 (2001) 205421
- [18] Y. Bouazzi and M. Kanzari, Optica Applicata 39 (2009) 489
- [19] J Chen, Bo Qin, H. L. W. Chan, Solid State Comm. 146 (2008) 491
- [20] E. M. Nascimento, F. A. B. F. de Moura, and M. L. Lyra, Photon. Nanostruct. 7 (2009) 101

MAGNETO-PLASMONIC NANOSTRUCTURED MATERIALS FOR GAS SENSORS APPLICATIONS

M.G. Manera^a, G. Montagna^a, R. Rella^a, E. Ferreiro-Vila^b, A. Garcia-Martin^b, G. Armelles^b, A. Cebollada^b, J.M. Garcia-Martin^b, L. González-García^c, J. R. Sánchez-Valencia^c, A. R. González-Elipe^c

^aIstituto for Microelectronic and Microsystems, unit of Lecce, Via Monteroni, 73100 Lecce (Italy)

^bInstituto de Microelectronica de Madrid, Consejo Superior de Investigaciones Científicas, Isaac Newton, Tres Cantos, Madrid, Spain

^cInstituto de Ciencia de Materiales de Sevilla (CSIC-Univ. Sevilla). Avda. Américo Vesputio 49. 41092 Sevilla, Spain

mariagrazia.manera@le.imm.cnr.it

Surface plasmon resonance (SPR) spectroscopy has emerged as a powerful technique which permits real-time monitoring of chemical and bio-chemical interactions occurring at the interface between a thin gold film and a dielectric interface, without the need for labelling of reagents [1]. In recent years it has been used for detection and analysis of chemical and biological substances in many research areas and industrial applications, such as surface science, biotechnology, medicine, environment, and drug and food monitoring. In all these applications, improving the resolution and limits of detection is of vital importance and is the primary goal of the research in this field in the last years.

The sensitivity and limits of detection of the SPR sensors can show variations depending on the method used to excite the surface plasmon (prism coupling, grating coupling, optical fibers etc.). In the widely used Kretschmann configuration, a prism is coated with a metal of suitable thickness. A beam of p-polarized light is allowed to fall on the metal–dielectric interface and the intensity of the reflected light is detected as a function of the angle of incidence. At a particular angle of incidence the resonance condition is satisfied and the resonance is observed as a sharp fall in the reflectivity. The plasmon resonance is extremely sensitive to the changes in the refractive index and the thickness of the dielectric medium adjacent to the metal layer. In the intensity-interrogated configuration, the most widely employed, such changes are monitored by measuring the intensity of the reflected p-polarized monochromatic light at a fixed angle of incidence.

In order to boost up SPR detection sensitivity, various efforts have been made, including construction of SPR equipment and setups with improved measurement modes: incorporation of fluorescent spectroscopy into SPR, signal amplification using functionalized nanoparticles, localized SPR (LSPR) using periodic nanowires and nanoposts, phase-sensitive detection schemes [2-4].

Recently, it has been proposed in the literature a novel Magneto-Optic Surface Plasmon Resonance (MOSPR) sensor [5] which sensor performances can be greatly enhanced with respect to traditional SPR sensors (an improvement by a factor of 3 in the limit of detection is demonstrated). The novel device is based on the combination of the magneto-optic (MO) effects of the magnetic materials and the surface plasmon resonance. This combination can be achieved by realizing a transducing sensing layer constituted by a multilayer Au/Co/Au deposited onto glass substrates. A magnetic actuator is used to control the magnetization state of the magnetic layer in the transversal configuration, and the relative variations of the reflectivity are detected. By this way, a great enhancement of the magneto-optic effects in the p-polarized light is produced when the resonant condition is satisfied. Such enhancement is strongly localized at the surface plasmon resonance and strongly depends on the refractive index of the dielectric medium, allowing its use for optical sensing and to greatly improve the sensitivity with respect to “standard” SPR sensors. Since this MOSPR seems very promising, we have undertaken the analysis of this configuration both for biosensing purposes and for gas sensing (for the first time in a MOSPR sensor).

In this work, some preliminary results for gas sensing scheme are shown. TiO₂ thin film have been deposited by GLAD (Glancing Angle deposition) onto the last gold surface and its interaction with Volatile Organic Compounds has been monitored both in a standard SPR and in MOSPR configurations in order to compare their sensing performances. Measurements performed in controlled atmosphere demonstrate that the sensitivity results greatly improved in MOSPR sensor for ethanol, methanol and isopropanol vapours. These first results represent a good starting point for the demonstration of the use of the prepared magneto-plasmonic materials in thin film form as candidates

for sensitive optical gas sensors, by greatly enhancing the performances of traditional SPR optical sensors operating at the same conditions.

References:

- [1] A J. Homola, S. Yee, D. Myszka, in: F.S. Ligler, C.A.R. Taitt (Eds.), Elsevier, The Netherlands, 207, (2002).
- [2] F. Yu, B. Persson, S. Lofas, W. Knoll, JACS comm, 126, (2004) 8902
- [3] L. Malic, B. Cui, T. Veres, and M. Tabrizian, Opt. Lett. 32 (2007) 3092
- [4] S. Y. Wu, H. P. Ho, W. C. Law, C. Lin, and S. K. Kong, Opt. Lett. 29 (2004) 2378
- [5] B. Sepúlveda, A. Calle, L. M. Lechuga and G. Armelles, Opt. Lett. 31, (2006) 1085.

Figures:

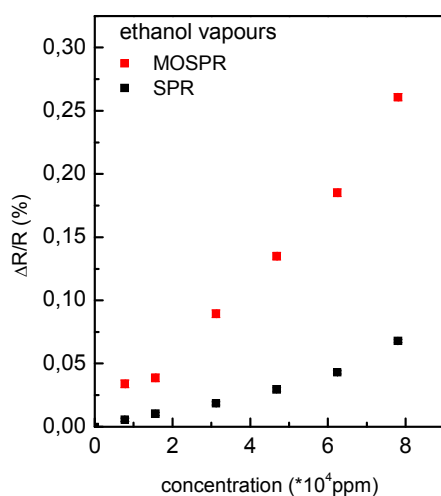


Figure 1: Sensor response towards ethanol alcohol vapours corresponding to the “standard” SPR configuration and to the MO-SPR configuration demonstrating an increase in sensitivity.

STRONG PHOTOLUMINESCENCE ENHANCEMENT OF Si AND SiC QUANTUM DOTS BY THEIR RESONANT COUPLING WITH MULTI-POLAR PLASMONIC HOT SPOTS

Tetyana Nychporuk, Yu. Zakharko, Tetiana Serdiuk, M. Lemiti, Vladimir Lysenko

Lyon Institute of Nanotechnology (INL), CNRS UMR-5270, INSA de Lyon, 7 av. Jean Capelle,
Bat. Blaise Pascal, Villeurbanne F-69621, France
tetyana.nychporuk@insa-lyon.fr

Since the observation in 1990 of strong room-temperature photoluminescence (PL) from nanostructured porous Si [1,2], significant scientific interest has been focused on Si-based nanomaterials (quantum dots (QDs), nanowires, nano-porous layers, etc.) emitting light in a wide spectral range from near infra-red up to ultra-violet regions [3]. However, even for Si QDs of few nanometers with sufficiently broken-down wave-vector selection rules due to spatial and quantum confinements of charge carriers, the luminescence quantum efficiency is rather low (1-10% [4,5,6]) compared to direct band-gap semiconductors [7,8,9], and its considerable enhancement remains an important challenge.

Currently, one of the most intensely studied approaches allowing a significant enhancement of the photo-stimulated emission of various QDs is their localization in the vicinity of metal nanoparticles (NPs) [10,11,12]. Indeed, optically excited collective oscillations of conducting electrons (known also as localized plasmons [13]), appearing in the metal NPs at the spectral ranges corresponding to the plasmon resonance bands allow strong increase of: (i) effective absorption cross-section of the QDs and (ii) their radiative recombination rates. Both reasons provoke an important luminescence enhancement. Moreover, to render much stronger the electrical field in the vicinity of the photoexcited metal NPs and thus to ensure enhancement of the QD photoluminescence intensity by several orders of magnitude, the QDs must be localized in the regions (called hot spots) where the photo-induced electrical fields from several metal NPs are superimposed [14].

Plasmon induced PL amplification was mainly reported for II-VI core/shell QDs [15,16]. In particular, using various configurations of metal (most often: gold and silver) nanostructures, the obtained PL amplification gain varied from 30 to 240 [15,16]. Despite these important recent advances achieved on II-VI QDs, only a seven-fold photoluminescence enhancement was reported for Si QDs [17].

In our present work we show that the plasmon-induced strong local photoluminescence enhancement of Si QDs in SiN matrix can reach 60-fold gain level. This important result was achieved by our team developing original tunable "nano-Ag/SiNX" plasmonic structures. In particular we show that, (i) localization of Si QDs in hot spot regions created by several randomly arranged Ag nanoparticles and (ii) careful tuning of the multi-polar plasmon bands of Ag nanoparticles to match resonantly absorption and emission wavelengths of Si QDs, lead to the important enhancement of their photoluminescence intensity. By exploiting the same physical mechanisms we were also able to achieve high values of PL enhancement of SiC QDs coupled with plasmonic nanostructures, reaching 20-fold level.

References:

- [1] Canham, L. T., Silicon quantum wire array fabrication by electrochemical and chemical dissolution of wafers, *Appl. Phys. Lett.* 57, 1046-1048 (1990)
- [2] Cullis, A. G., Canham, L. T., Visible light emission due to quantum size effects in highly porous crystalline silicon, *Nature* 353, 335-338 (1991)
- [3] Kumar, V., *Nanosilicon*, Elsevier, Oxford, 2007
- [4] Credo, G. M., et al, External quantum efficiency of single porous silicon nanoparticles, *Appl. Phys. Lett.* 74, 1978-1980 (2008)
- [5] Wilson, W. L., et al, Quantum confinement in size-selected, surface-oxidized silicon nanocrystals, *Science*, 262, 1242-1244 (1993)
- [6] Efros, Al. L., et al, Nonlinear optical effects in porous silicon: photoluminescence saturation and optically induced polarization anisotropy, *Phys. Rev. B*, 56, 3875-3884 (1997)
- [7] Talapin, D. V., et al, Highly luminescent monodisperse CdSe and CdSe/ZnS nanocrystals synthesized in a hexadecylamine – triethylphosphine oxide – trioctylphosphine mixture, *Nano Lett.* 1, 207-211 (2001)
- [8] Chan, W. C. W., et al, Quantum dot bioconjugates for ultrasensitive nonisotopic detection, *Science*, 281, 2016-2018 (1998)
- [9] Bruchez, M., et al, Semiconductor nanocrystals as fluorescent biological labels, *Science*, 281, 2013-2016 (1998)
- [10] Schuller J.A., et al, Plasmonics for extreme light concentration and manipulation, *Nature Materials*, 9, 193- 204 (2010)
- [11] Jin, Y., et al, Plasmonic fluorescent quantum dots, *Nature Nanotechnology*, 4, 571-576 (2009)
- [12] Anger, P., et al, Enhancement and quenching of single-molecule fluorescence, *Phys. Rev. Lett.* 96, 113002 (2006)
- [13] Kreibitz, U., Vollmer, M. *Optical properties of metal clusters*; Springer Verlag: Berlin, Heidelberg, 1995
- [14] Bek., A., et al, Fluorescence enhancement in hot spots of AFM – designed gold nanoparticles sandwiches, *Nano Lett.* 8, 485-490 (2010)
- [15] Song, J.-H., et al, Large enhancement of fluorescence efficiency from CdSe/ZnS quantum dots induced by resonant coupling to spatially controlled surface plasmons, *Nano Lett.* 5, 1557-1561 (2005)
- [16] Langhuth. H, et al, Strong photoluminescence enhancement from colloidal quantum dot near silver nano-island films, *J. Fluores.* DOI 10.1007/s10895-010-0740-z
- [17] Biteen, J. S., et al., Spectral tuning of plasmon-enhanced silicon quantum dot luminescence, *Appl. Phys. Lett.* 88, 131109 (2006)

TRANSFORMATION OPTICS AT OPTICAL FREQUENCIES

JB Pendry

Department of Physics, Imperial College, London, SW7 2AZ, UK
j.pendry@imperial.ac.uk

When designing macroscopic optical components such as camera lenses the ray approximation is an excellent design tool. However plasmonic systems function on a scale smaller than the wavelength of light and the ray approximation is of no use to us. In this talk I shall show that the new technology of transformation optics, exact at the level of Maxwell's equations, offers the same intuitive understanding as the ray approximation. The power of the method will be illustrated by showing how to construct 'light harvesting' devices. Starting from a simple well understood system comprising slabs of silver, transformation optics is deployed to generate a whole family of structures that inherit the intrinsic electromagnetic structure of the original but whose geometry is radically transformed from the original.

ULTRAFAST OPTICAL MANIPULATION OF MAGNETIC ORDER: CHALLENGES AND OPPORTUNITIES

Theo Rasing

Department Radboud University Nijmegen, The Netherlands
Institute for Molecules and Materials

The interaction of sub-picosecond laser pulses with magnetically ordered materials has developed into an extremely exciting research topic in modern magnetism and spintronics. From the discovery of sub-picosecond demagnetization over a decade ago to the recent demonstration of magnetization reversal by a single 40 femtosecond laser pulse, the manipulation of spins by ultra short laser pulses has become a fundamentally challenging topic with a potentially high impact for future spintronics, data storage and manipulation and quantum computation.

Recent single-shot pump-probe magneto-optical imaging results show that circularly polarized subpicosecond laser pulses steer the magnetization reversal in a Transition Metal-Rare Earth alloy along a novel and ultrafast route, which does not involve precession but occurs via a strongly nonequilibrium state. However, the nature of this phase and the dynamics of the individual TM and RE moments remained elusive so far. Experiments indicate a possible difference in the dynamics of the TM and RE moments at time scales that are currently limited by the pulse widths of the optical excitations employed (~100fs). To investigate such highly nonequilibrium phases requires both excitation and probing at ultra short time scales and selectivity for the individual moments.

In addition, when the time-scale of the perturbation approaches the characteristic time of the exchange interaction (~10-100 fs), the magnetic dynamics may enter a novel coupling regime where the exchange interaction may even become time dependent. Using ultrashort excitations, we might be able to manipulate the exchange interaction itself. Such studies will require the excitation and probing of the spin and angular momentum contributions to the magnetic order at timescales of 10fs and below, a challenge that might be met by the future fs X-ray FEL's.

References:

- [1] A.V.Kimel, A.Kirilyuk, P.A.Usachev, R.V.Pisarev, A.M.Balbashov and Th.Rasing, Ultrafast nonthermal control of magnetization by instantaneous photomagnetic pulses, *Nature* 435 (2005), 655-657
- [2] C.D.Stanciu, F.Hansteen, A.V.Kimel, A.Kirilyuk, A.Tsukamoto, A.Itoh and Th.Rasing, All-optical Magnetic Recording with Circularly polarized Light, *Phys.Rev.Lett.*99, 047601 (2007)
- [3] A.V.Kimel, B. A.Ivanov, R. V.Pisarev, P. A.Usachev, A.Kirilyuk and Th.Rasing, Inertia-driven spin switching in antiferromagnets, *Nature Physics* 10, 727-731 (2009)
- [4] K.Vahaplar, A.M.Kalashnikova, A.V.Kimel, D.Hinzke, U.Nowak, R.Chantrell, A.Tsukamoto, A.Ithoh, A.Kirilyuk and Th.Rasing, Ultrafast Path for Optical Magnetization Reversal via a Strongly Nonequilibrium State, *Phys.Rev.Lett.*103, 117201 (2009)
- [5] A.Kirilyuk, A.V.Kimel and Th.Rasing, Ultrafast Optical Manipulation of Magnetic Order, *Rev. Mod. Phys.* 82, 2731-2784 (2010)
- [6] I. Radu, K. Vahaplar, C. Stamm, T. Kachel, N. Pontius, H. A. Dürr, T. A. Ostler, J. Barker, R. F. L. Evans, R. W. Chantrell, A. Tsukamoto, A. Itoh, A. Kirilyuk, Th. Rasing and A. V. Kimel, Transient ferromagnetic state mediating ultrafast reversal of antiferromagnetically coupled spins, accepted for *Nature*(2011)

Figures:

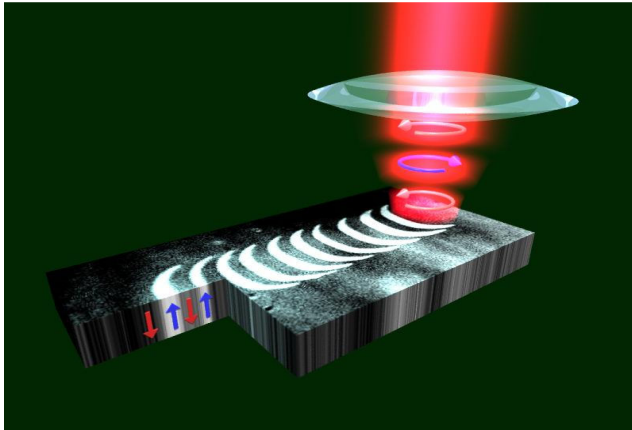


Figure 1: Demonstration of compact all-optical recording of magnetic bits by femtosecond laser pulses. This was achieved by scanning a circularly polarized laser beam across the sample and simultaneously modulating the polarization of the beam between left and right circular. White and black areas correspond to 'up' and 'down' magnetic domains, respectively. How and how fast does this work?

SURFACE ENHANCED RAMAN SPECTROSCOPY OF DIFFERENT CHAIN LENGTH PEP+ MOIETY BOUND TO NANORODS

Ros Ida, Placido T., Comparelli R., Marinzi C., Curri L.; Abbotto A., Bozio R.

University of Padova, via Marzolo 1, Padova, Italy
ida.ros@unipd.it

In recent years, Surface Enhanced Raman Spectroscopy (SERS) has become one of the most important technique for characterizing the chemical structure and monitoring structural changes at the single-molecule level.[1] The key effect for the observation of enhanced Raman signals is the favorable optical properties of metal nanostructures, based on their local surface plasmon. The enhancement depends on the type of metal and nanostructures. Several examples of nanostructures of different shape, metal and, eventually, regularly assembled are reported in the literature, resulting in SERS enhancement factors up to 108.[2-6] For example, rod-shaped nanoparticles present a highly tunable longitudinal plasmon band which should be exploited to amplify both the exciting laser and the scattered field in SERS measurements. Despite the desirable characteristics of metallic nanorods, as SERS substrates, only few reports exist for SERS on nanorods where the Raman excitation occurs at a wavelength that overlaps with nanorod plasmon resonances [7-12].

In this presentation, we report our recent results on the amplification of the Raman signals of 1-(N-methylpyrid-4-yl)-2-(N-methylpyrrol-2-yl)ethylene (**PEP+**) using gold nanorods (NRs) as substrate. The dipolar positively charged dye **PEP+** is a push-pull molecule composed by a π -deficient (pyridinium ion) as acceptor group A and a π -excessive (pyrrole) heterocycle as donor group D.[13] **PEP+** or its derivatives present resonant and non-resonant nonlinear optical properties, such as two-photon absorption or second harmonic generation.[14-15] We have synthesized thiol-acetyl terminated **PEP+** chromophores spaced by two linear alkyl chains of different length, containing 3 or 12 carbon atoms.

The basic idea is to control the intensity of the Raman signals as a function of the distance between the dye and the metallic surface of the metal nanostructure and to study both the effect of the laser resonance with the absorption band of **PEP+** moiety and with the two plasmon modes.

Raman characterization of NRs, functionalized with **PEP+C3SH** and **PEP+C12SH**, both deposited on glass substrates and in solution, is realized using different laser excitation lines. The 488-nm and the 514-nm laser excitation lines are in resonance with the absorption band of the molecules, performing Surface Enhanced Resonance Raman Scattering (SERRS), whereas the 785-nm laser excitation line is out of resonance. Moreover, the 514-nm and the 785-nm lines are resonant with the transverse and longitudinal modes of gold nanorods, respectively, suggesting a further enhancement of the Raman signals.

Comparing Raman spectra, for the same dye bound to NRs, at different laser excitation lines, turns out that data measured by exciting at 514 and 785-nm present a higher signal-to-noise ratio than that at 488 nm. This consideration suggests that the amplification is higher when the laser excitation wavelength is resonant with the two plasmon modes than, exclusively, with the absorption band of the dye, as for the 488-nm radiation.[10] Anyway, the resonance condition of the 514-nm laser excitation with the absorption band of the dye strongly contributes to the amplification of the Raman signal. In fact, DDA calculations, performed on our nanorods, reveal that the local field is about 10 times higher when the longitudinal plasmon mode is excited instead of the transverse one. This means that, in resonance with the longitudinal and transverse plasmon modes, we predict an enhancement of the Raman signal of about 10^4 and 10^2 , respectively, which is not confirmed by the measurements if we don't take into account the resonance with the absorption band of the dye.

To compare the amplification of Raman response when the transverse and longitudinal plasmon modes are excited, we evaluated the enhancement factor (EF) using 4-mercaptopyridine (**4-MPy**) as a standard analyte.[10] **4-MPy**, unlike **PEP+** moiety, is not fluorescent and allows us to perform experiments using both 514 nm and 785 nm laser excitation. At 514-nm laser excitation, no signal is observed for **4-MPy** bound to NRs due to the rather low EF. This result clearly agrees with the DDA model prediction for the local field when the transverse mode is excited and further supports our

hypothesis of a strong contribution to the SERRS response from the resonance with the absorption band of **PEP+** moiety.

On the other hand, some Raman bands of **4-MPy** bound to NRs are strongly amplified when excited with 785-nm laser excitation. Characteristic ring breathing modes are observable at 1004 cm^{-1} ($\nu(\text{C}-\text{C})$ mode) and at 1119 cm^{-1} ($\nu(\text{C}-\text{S})$ mode). The latter is remarkably shifted in **4-MPy** bound to NRs (1094 cm^{-1}) and experiences a dramatic increase in intensity compared with the corresponding Raman signal in solution. The evaluated EF for the $\nu(\text{C}-\text{C})$ ring breathing mode at 1004 cm^{-1} and the $\nu(\text{C}-\text{S})$ ring breathing mode at 1119 cm^{-1} are 4.0×10^4 and 1.2×10^5 , respectively, perfectly comparable with the DDA calculation.

These preliminary results show as it is important to control the resonance condition with both the plasmon mode and with the electronic transitions of the molecules. In this way, it is possible to obtain a higher amplification and to detect lower levels of chemical species required for sensoristic applications.

References:

- [1] Kneipp, K.; Kneipp, H.; Manoharan, R.; Itzkan, I.; Dasari, R. R.; Feld, M. S. *Bioimaging* 6 (1998) 104.
- [2] Kneipp, K.; Kneipp, H.; Kneipp, J. *Acc. Chem. Res.* 39 (2006) 443.
- [3] Diebold, E. D.; Mack, N. H.; Doorn, S. K.; Mazur, E. *Langmuir* 25 (2009) 1790.
- [4] Yan, B.; Thubagere, A.; Ranjith Premasiri, W.; Ziegler, L. D.; Dal Negro, L.; Reinhard, B. M. *ACS Nano* 3 (2009) 1190.
- [5] Yang, M.; Alvarez-Puebla, R. A.; Kim, H. S.; Aldeanueva-Potel, P.; Liz-Marzan, L. M.; Kotov, N. A. *Nano Lett.* 10 (2010) 4013.
- [6] Bechelany, M.; Brodard, P.; Elias, J.; Brioude, A.; Michler, J.; Philippe, L. *Langmuir* 26 (2010) 14364.
- [7] Nikoobakht, B.; Wang, J.; El-Sayed, M. A. *Chem. Phys. Lett.* 366 (2002) 17.
- [8] Nikoobakht, B.; El-Sayed, M. A. *J. Phys. Chem. A* 107 (2003) 3372.
- [9] Orendorff, C. J.; Gole, A.; Sau, T. K.; Murphy, C. J. *Anal. Chem.* 77 (2005) 3261.
- [10] Orendorff, C. J.; Gearheart, L.; Janaz, N. R.; Murphy, C. J. *Phys. Chem. Chem. Phys.* 8 (2006) 165.
- [11] Aroca, R. F.; Goulet, P. J. G.; dos Santos, D. S.; Alvarez-Puebla, R. A.; Oliveira, O. N. *Anal. Chem.* 77 (2005) 378.
- [12] Guo, H.; Ruan, F.; Lu, L.; Hu, J.; Pan, J.; Yang, Z.; Ren, B. *J. Phys. Chem. C* 113 (2009) 10459.
- [13] Bradamante, S.; Facchetti, A.; Pagani, G. A. *Journal of Physical Organic Chemistry* 10 (1997) 514.
- [14] Facchetti, A.; Abbotto, A.; Beverina, L.; Van Der Boom, M. E.; Dutta, P.; Evmenenko, G.; Pagani, G. A.; Marks, T. J. *Chem. Mater.* 15 (2003) 1064.
- [16] Abbotto, A.; Beverina, L.; Bradamante, S.; Facchetti, A.; Pagani, G. A.; Bozio, R.; Ferrante, C.; Pedron, D.; Signorini, R. *Synth. Metals* 136 (2003) 795.

J.J. Sáenz

Departamento Física de la Materia Condensada
Universidad Autónoma de Madrid, Madrid 28049, Spain
juanjo.saenz@uam.es

Electromagnetic scattering from nanometer-scale objects has long been a topic of large interest and relevance to fields from astrophysics or meteorology to biophysics, medicine and material science [1-5]. In the last few years, small particles with resonant magnetic properties are being explored as constitutive elements of new metamaterials and devices. The studies in the field often involve randomly distributed small elements or particles where the dipole approximation may be sufficient to describe the optical response. We will discuss the optical response of disordered nano-materials where the constitutive nanoparticles can have a non-negligible response to static (**Magneto-Optical active nanoparticles**) or dynamic (**Magneto-dielectric nanoparticles**) magnetic fields.

We will first analyse the peculiar scattering properties of single nanoparticles. In particular, we derive the radiative corrections to the polarizability tensor of anisotropic particles, a fundamental issue to understand the energy balance between absorption and scattering processes [1]. As we will show, Magneto optical Kerr effects in non-absorbing nanoparticles with magneto-optical activity arise as a consequence of radiative corrections to the electrostatic polarizability tensor.

We will also explore the properties of high-permittivity dielectric particles with resonant magnetic properties as constitutive elements of new metamaterials and devices [2]. Magnetic properties of low-loss dielectric nanoparticles in the visible or infrared are not expected due to intrinsic low refractive index of optical media in these regimes. Here we analyze the dipolar electric and magnetic response of lossless dielectric spheres made of moderate permittivity materials. For low material refractive index there are no sharp resonances due to strong overlapping between different multipole contributions. However, we find that Silicon particles with index of refraction ~ 3.5 and radius $\sim 200\text{nm}$ present strong electric and magnetic dipolar resonances in telecom and near-infrared frequencies, (i.e. at wavelengths $\approx 1.2 - 2 \mu\text{m}$) without spectral overlap with quadrupolar and higher order resonances. The light scattered by these Si particles can then be perfectly described by dipolar electric and magnetic fields.

As we will see, the striking characteristics of the scattering diagram of small magneto-optical and magnetodielectric particles [3,4] lead to a number of non-conventional effects in the optical response of nanostructured magneto-optical structures.

References:

- [1] S. Albaladejo, R. Gómez-Medina, L. S. Froufe-Pérez, H. Marinchio, R. Carminati, J. F. Torrado, G. Armelles, A. García-Martín and J.J. Sáenz, *Opt. Express* 18 (2010) 3556.
- [2] A. García-Etxarri, R. Gómez-Medina, L. S. Froufe-Pérez, C. López, L. Chantada, F. Scheffold, J. Aizpurúa, M. Nieto-Vesperinas and J. J. Sáenz, *Opt. Express* 19, 4815 (2011)
- [3] M. Nieto-Vesperinas, R. Gómez-Medina, and J. J. Sáenz, *J. Opt. Soc. Am. A* 28 (2011) 54.
- [4] R. Gómez-Medina, B. García-Cámara, I. Suárez-Lacalle, F. González, F. Moreno, M. Nieto-Vesperinas, J. J. Sáenz, to be published (2011).

R. Rodríguez-Oliveros*, R. Paniagua-Domínguez*, F. López-Tejiera*, D. Macías[†], **J. A. Sánchez-Gil***

*Instituto de Estructura de la Materia, Consejo Superior de Investigaciones Científicas,
Serrano 121, 28006, Madrid, Spain

[†]Laboratoire de Nanotechnologie et d'Instrumentation Optique (ICD-LNIO),
Université de Technologie de Troyes, France
j.sanchez@csic.es

Complex metal nanostructures exhibit surface plasmon resonances that play a crucial role in a variety of electromagnetic phenomena relevant to Nanophotonics. We are interested in the electromagnetic properties of metal nanoparticles of complex shape, with localized plasmon resonances (LPR) yielding large local electromagnetic fields or enhanced emission: such as dimers/trimers playing the role of nanoantennas; or nanoparticles of complex shape (nanostars/nanoflowers); both of interest in enhanced optical emission (Raman, fluorescence, photoluminescence,...) [1-5]. In this regard, it is crucial first to fully characterize the LPR for a variety of metal nanoparticles of arbitrary shape. To this end, we have developed an advanced numerical formulation to calculate the optical properties of 2D and 3D nanoparticles (single or coupled) of arbitrary shape and lack of symmetry [6,7]. The method is based on the (formally exact) surface integral equation formulation. Thus the 3D version is based on the same equations as that of Ref. [8]; nonetheless, it has been implemented for parametric surfaces describing particles with flexible shape through a unified treatment (Gieli's formula), which makes it far more versatile [7,9]. On the basis of these methods, we have indeed calculated the scattering cross sections for nanowires [1-4] and nanoparticles [7] of various shapes (triangles, rectangles, cubes, rods, stars, see i.e. Fig. 1), either isolated or interacting, including far-field patterns and spectra, near-field intensity maps (with corresponding enhancement factors), decay rates, and surface charge distributions.

Furthermore, the optimal design of nanoantennas with specific properties is an aspect of the inverse problem that has not received too much attention until recently, despite being crucial from the point of view of applications. In order to find the optimal nanoparticle geometry that maximizes/minimizes a given optical property, we have made use of a bio-inspired stochastic technique based on genetic algorithms [9], which exploits the above mentioned formulations for flexible surfaces [6,7] to solve the direct scattering problem. We show how this stochastic procedure converges to optimized nanoparticles in some configurations of interest in Nanophotonics: nanoflower/nanostar geometry that exhibits a LPR at or near a given wavelength (see Fig. 2) for SERS (surface-enhanced Raman scattering) substrates [9]; dimer nanoantennas that yield maximum field enhancements and radiative decay rates within the gap for enhanced fluorescence/photoluminescence; long nanoantennas with third-order resonances at given wavelengths for non-linear optical processes (SHG, TPL). With regard to the latter, indeed, the occurrence of Fano resonances at the $L \sim 3\lambda/2$ resonance of the nanorod will also be discussed.

The authors acknowledge support both from the Spain Ministerio de Ciencia e Innovación through the Consolider-Ingenio project EMET (CSD2008-00066) and NANOPLAS (FIS2009-11264), and from the Comunidad de Madrid (grant MICROSERES P009/TIC-1476). R. Paniagua-Domínguez acknowledges support from CSIC through a JAE-Pre grant.

References:

- [1] O.L. Muskens, V. Giannini, J.A. Sánchez-Gil, and J. Gómez Rivas, *Nano Lett.*, 7, (2007) 2871-2875.
- [2] V. Giannini, J.A. Sánchez-Gil, O.L. Muskens, and J. Gómez Rivas, *J. Opt. Soc. Am. B*, 26 (2009) 1569-1577.
- [3] V. Giannini, R. Rodríguez-Oliveros, and J. A. Sánchez-Gil, *Plasmonics*, 5 (2010) 99-104.
- [4] V. Giannini, A. Berrier, S. A. Maier, J.A. Sánchez-Gil, and J. Gómez Rivas, *Opt. Express*, 18 (2010) 2797-2807.
- [5] L. Guerrini, I. Izquierdo-Lorenzo, R. Rodríguez-Oliveros, J.A. Sánchez-Gil, S. Sánchez-Cortés, J.V. García-Ramos, and C. Domingo, *Plasmonics*, 5 (2010) 99-104.
- [6] V. Giannini and J. A. Sánchez-Gil, *J. Opt. Soc. Am. A*, 24 (2007) 2822-2830.
- [7] R. Rodríguez-Oliveros, J.A. Sánchez-Gil, "Localized plasmon resonances on single and coupled nanoparticles through surface integral equations for flexible surfaces," submitted to *Opt. Express*.
- [8] A.M. Kern and O.J.F. Martin, *J. Opt. Soc. Am. A*, 26 (2009) 732-740.
- [9] A. Tassadit, D. Macías, J. A. Sánchez-Gil, P.-M. Adam, R. Rodríguez-Oliveros, *Superlattices & Microstructures*, 49 (2011) 288-293.

Figures:

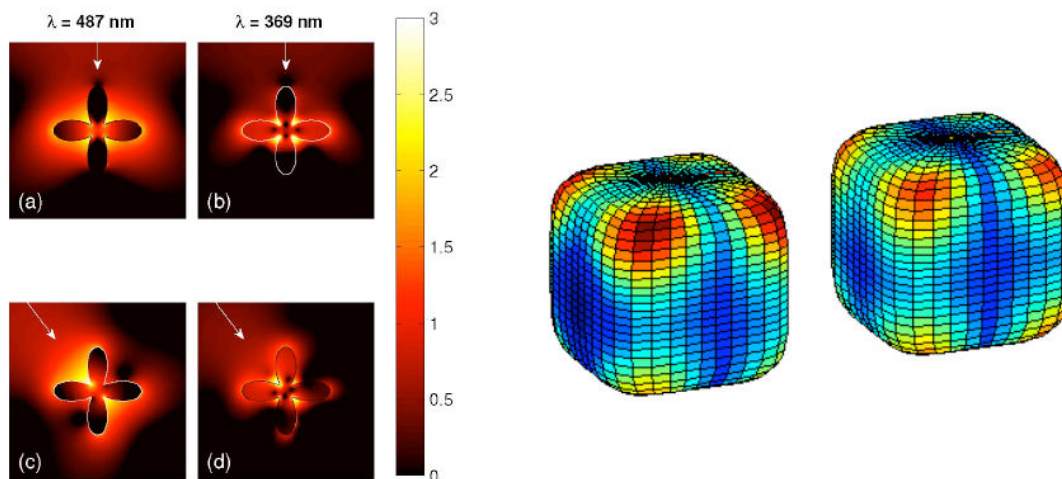


Figure 1: Left-panel: Near-field distributions of the electric field intensities in a log10-scale for the Ag four-petal nanoflower with mean radius $\rho=30 \text{ nm}$ and deformation parameter $\beta=2/3$, illuminated with a monochromatic plane wave with wavelength equal to either one of the two main LPRs (dipolar and quadrupolar, respectively) at $\lambda=487 \text{ nm}$ (a,c) and at $\lambda=369 \text{ nm}$ (b,d): (a,b) $\theta_i=0^\circ$; (c,d) $\theta_i=45^\circ$ [3]. Right-panel: Electric field intensity on the surface of a Ag rounded-cube dimer ($L=30 \text{ nm}$, $\text{gap}=20 \text{ nm}$) with plane wave illumination matching the longitudinal LPR [7].

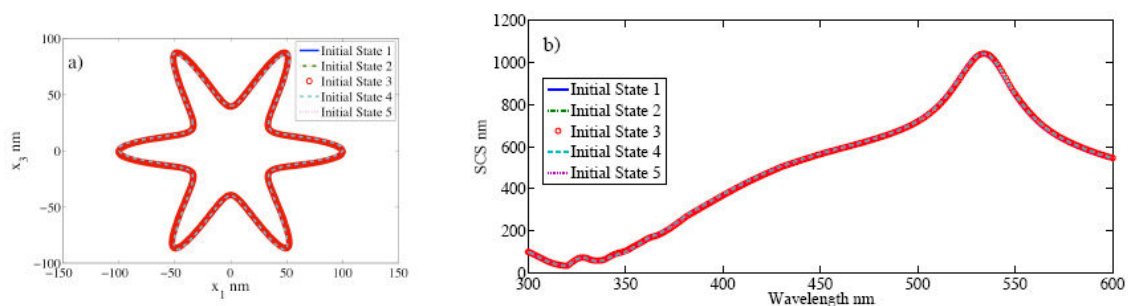


Figure 2: a) Optimized star-like geometries obtained with Gielis' Superformula. Each line corresponds to an initial state of the optimization algorithm. b) SCSs (optimized to yield a maximum at $\lambda=532 \text{ nm}$) for each of the star-like nanostructures depicted in Fig. 2a (same curve styles in both figures) [9].

THE EFFECT OF SHAPE AND STRUCTURE VARIATION OF METALLIC NANOPARTICLES ON LOCALIZED PLASMON RESONANCES

Titus Sandu

National Institute for Research and Development in Microtechnologies, 126A, Erou Iancu Nicolae street, 077190, Bucharest, Romania
titus.sandu@imt.ro

Localized plasmon resonances (LPRs) in metallic nanoparticles have been now studied extensively for more than a decade. They have a wide range of applications like sensing and waveguiding [1,2] or high throughput communications [3] to name a few. To calculate the LPR properties one has to find the solutions of Maxwell's equations with boundary conditions determined by the interface between nanoparticles and the surrounding medium.

Complex computational schemes like discrete-dipole approximation (DDA) [4] or finite-difference time domain (FDTD) [5] are successfully used to predict optical response of arbitrarily shaped nanoparticles. These aforementioned methods offers, however, little insight about the formation, nature, and the behavior of the LPRs with respect to parameters like the shape (geometry) or complex dielectric functions of nanoparticles. To overcome some of these shortcomings, it has been proposed a hybridization model [6], which works very well in the quasi-static limit. On the other hand, in the quasi-static limit, the Maxwell's equations reduce to Poisson equation which can be solved with the Neumann-Poincare operator associated with the Dirichlet and Neumann problems in potential theory [7]. In plasmonic applications, the method based on the Neumann-Poincare operator has been proposed for some time [8]. The method relates the LPRs to the eigenvalues of the Neumann-Poincare operator, but explicit relations are still lacking. Moreover, the method is similar to the operator method applied for calculation of electric polarizability of biological cells in radiofrequency [9].

I use the operator method outlined in Ref. 9 to define the LPRs in metallic nanoparticles. The LPRs are characterized by the eigenvalues of the Neumann-Poincare operator and their weights to the total polarizability of the nanoparticles. Compact formulas, that contain the complex dielectric functions of nanoparticles and the embedding medium, are given not only for homogeneous but also shelled metallic nanoparticles. The effect of geometry is included in both the eigenvalues of the Neumann-Poincare operator and in their weights to the polarizability. Various trends in LPRs, which otherwise are calculated more expensively with DDA and FDTD, are predicted by simple analysis of these formulas. The effect of geometry variation on LPRs is considered by analyzing the variation of the eigenvalues of the Neumann-Poincare operator and their weights to the nanoparticle polarization. Finally, I consider the case of graded nanoparticles, where their complex dielectric function is not homogeneous but may have a space variation.

References:

- [1] P. K. Jain and M. A. El-Sayed, Chem Phys. Lett. 487 (2010) 153.
- [2] S. Lal, S. Link, and N. J. Halas, Nature Photonics, 1 (2007) 641.
- [3] N. Engheta, 317 (2007) 1698.
- [4] B. T. Draine and P. J. Flatau, J. Opt. Soc. Am. A, 11 (1994) 1491.
- [5] C. Oubre and P. Nordlander J. Phys. Chem. B 108 (2004) 17740.
- [6] E. Prodan, C. Radloff, N. J. Halas, and P. Nordlander, Science, 302 (2003) 419.
- [7] O. D. Kellogg, Foundations of Potential Theory, Springer, Berlin, 1929.
- [8] D. R. Fredkin and I. D. Mayergoyz, Phys. Rev. Lett. 91 (2003) 253902.
- [9] T. Sandu, D. Vrinceanu and E. Gheorghiu, Phys. Rev. E 81 (2010) 021913.

Thierry Taliercio¹, Viliame N'tsame Gulengui¹, Jérôme Leon²

¹Institut d'Electronique du Sud, CNRS-INSIS-UMR 5214, Université Montpellier 2,
34095 Montpellier cedex 05, France

²Laboratoire Charles Coulomb, CNRS-UM2 UMR 5221, Département Physique Théorique, CC 070
Université Montpellier 2, 34095 Montpellier cedex 05, France
Thierry.taliercio@univ-montp2.fr

Recent developments of plasmonic have opened new prospects in the control of light-matter interactions. The surface plasmons (SP), at the origin of this new topic, result from the coupling of the electromagnetic wave with the collective oscillation of the electrons supported by the metal/dielectric interface. SP have unique physical properties based on enhanced nanolocalized optical fields. Engineering of surface plasmons using nanostructured materials (nanoparticle, nanostructured film, fishnet etc) made it possible to develop a new range of materials with remarkable properties like, e.g., extraordinary optical transmission (EOT) [1]. A lot of theoretical investigations have been made in the case of one dimensional periodic arrays of slits [2,3]. All these studies focus on the low energy part of the plasmon polariton dispersion, that is, below the plasma frequency. In a recent work [4], we have proposed a model which describes the optical properties of an infinitely periodical nanostructure in a large range of frequencies around the plasma frequency ω_p . The elementary period of the structure, quite similar to a slit, is composed of two layers: a metal, or doped semiconductor, and a dielectric or un-doped semiconductor, considered in its dielectric range (Figure 1). The index of the periodic structure is defined as (1):

$$n^2(z, \omega) = \left\{ \begin{array}{l} \varepsilon_1 \text{ for } z \in [-b, 0] \\ \varepsilon \left[1 - \frac{1}{\omega(\omega + i\gamma)} \right] \text{ for } z \in [0, a] \end{array} \right\} \quad (1)$$

where a Drude dielectric function is used to model the behavior of the doped semiconductor. In this work all frequencies are normalized to the plasma frequency ω_p , the wave numbers to $k_p = \omega_p / c$, the lengths to k_p^{-1} (including spatial variables), and time to ω_p^{-1} . In the range of validity of the long wavelength limit, that is, typically a and $b < 0.1 \lambda_p$, we prove that under transverse magnetic wave (TM) irradiation, the structure can be modeled by means of the following single effective dielectric function of a ionic-crystal type

$$\varepsilon_{eff} = \tilde{\varepsilon} \frac{\omega(\omega + i\gamma) - 1}{\omega(\omega + i\gamma) - \omega_r^2}$$

$$\text{where } \tilde{\varepsilon} = \frac{(a+b)\varepsilon_1\varepsilon}{a\varepsilon_1 + b\varepsilon}, \quad \omega_r^2 = \frac{b\varepsilon}{a\varepsilon_1 + b\varepsilon} \quad (2)$$

where γ is the damping due to losses. In the case of transverse electric (TE) illumination the nanostructure behaves like a metal but with a new plasma frequency, ω_t , which depend on a , b , ε and ε_1 , see ref. [4] for more details.

This work presents original optical properties of the nanostructure for different geometrical or physical parameters. Indeed, by modifying the thickness of both layers and the plasma frequency through electrons density, it is possible to highlight a strong coupling between the incident light and the free electrons of the doped semiconductor. This strong coupling results in a broad photonic band gap ($\Delta\omega = 1 - \omega_t$) near the plasma frequency. Figures 2 and 3 show respectively the reflectance in TE and TM polarization in normal incidence for different values of a and b . The sizes vary from 0.1 to 0.3 μm . ω_p is defined at a value of 54 THz (corresponding to 6 μm) and $\gamma = 0.03 \omega_p$. These values are realistic in the case of a layer of InAs doped by silicon atoms at 10^{20} cm^{-3} . We can see on figure 3 that increasing the ratio between a and b increases considerably the stop band since $\Delta\omega$ (green line) reaches an incredible value of 55 % of ω_p . In the same time, figure 2 shows an increase of ω_t which approaches ω_p . Both behavior are awaited. Indeed a reduction of b versus a corresponds to an increase of the metallic part with respect to the dielectric one. In the extreme case, that is $b = 0 \mu\text{m}$, pure metallic regime is reached. In this case the plasma frequency just depends of the electron density ($\omega_t = \omega_p$) and ω_r reaches 0, we are dealing with a free electron gas. On the contrary, if a/b

decreases, ω_r and ω_p tend respectively towards 0 and ω_p . In the same time $\Delta\omega$ (red line on figure 3) decreases denoting a reduction of the light-matter coupling, that is, the equivalent “oscillator strength”. For a $\sim 0 \mu\text{m}$, the nanostructure gives an optical response similar to that of a dielectric containing oscillators of frequency ω_p .

The interesting aspect of this simple nanostructure is the possibility offered to control the light matter coupling just by adjusting the geometry of the nanostructure or its electrons density. We obtain a metamaterial equivalent to an ensemble of oscillators of which we can control the optical properties, that is, oscillator strength, frequency, broadening, etc. The polaritonic nature of the surface plasmon is at the origin of this specific behavior.

References:

[1] T. W. Ebbesen, H. J. Lezec, H. F. Ghaemi, T. Thio, and P.A. Wolff, Nature 391 (1998) 667.
 [2] J.A. Porto, F.J. Garcia-Vidal, and J.B. Pendry, Phys. Rev. Lett. 83 (1999) 2 845.
 [3] U. Schröter and D. Heitmann, Phys. Rev B58 (1998) 15 419.
 [4] J. Léon and T. Taliercio, Phys. Rev B82 (2010) 195 301.

Figures:

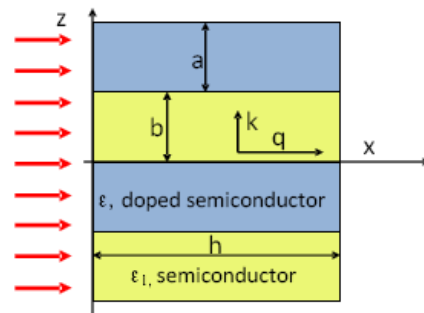


Figure 1: Scheme of the nanostructure, infinitely periodic in direction z and infinite in direction y.

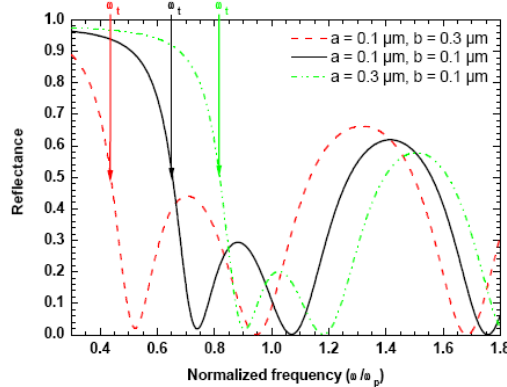


Figure 2: Calculated reflectance spectra in normal incidence and TE polarization for different size of doped (a) and undoped (b) semiconductor layers. The characteristic plasma frequency (ω_r) of the different layers are indicated by the vertical arrows.

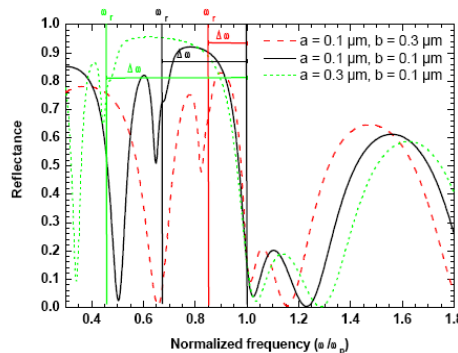


Figure 3: Calculated reflectance spectra in normal incidence and TM polarization for different size of doped (a) and undoped (b) semiconductor layers. The characteristic frequency (ω_r) and stop band ($\Delta\omega$) of the different layers are respectively indicated by the vertical and horizontal bars.

ULTRAFAST ACOUSTO-MAGNETO-PLASMONICS IN HYBRID METAL-FERROMAGNET MULTILAYER STRUCTURES

Vasily Temnov

MIT Chemistry Department, 77 Massachusetts Avenue, 02139 Cambridge, MA, UK
temnov@mit.edu

Nanostructured metal surfaces are presently used to effectively couple light to surface plasmons. This technology is also key to on-chip miniaturization of plasmonic sensors. We present a new plasmonic sensor, based on a tilted slit-groove interferometer, milled into a single noble metal film [1] or into a hybrid metal-ferromagnet structure [2]. Surface plasmons are excited at the groove and propagate towards the slit, where they interfere with incident light (Fig. 1). Due to the tilt angle the optical transmission through the slit shows a pronounced periodic interference pattern. A modulation of the complex surface plasmon wave vector results in a measurable change of the contrast and phase shift of the plasmonic interference pattern [1]. The wave vector of surface plasmons in our hybrid magneto-plasmonic gold-cobalt-gold system can be changed by switching in-plane magnetization using a weak external magnetic field (Fig. 1). Magneto-plasmonic modulation depth of up to 2% is achieved in this geometry. It can be further increased by covering the microinterferometer with high-index dielectric material [3].

When combined with time-resolved optical pump-probe spectroscopy, femtosecond surface plasmon interferometry captures the dynamics of ultrafast electronic excitations and coherent lattice vibrations within $\delta_{\text{skin}}=13\text{nm}$ skin depth in gold with femtosecond time resolution [1]. Using a sapphire/cobalt/gold multilayer structure we generate ultrashort acoustic pulses by thermal expansion of a cobalt film impulsively heated by femtosecond laser pump pulses through sapphire substrate (Fig. 2a). The compressive acoustic pulse propagates through the gold layer at the speed of sound and is converted into a tensile pulse upon reflection from the gold-air interface. The wave vector of femtosecond surface plasmon probe pulses propagating along the gold-air interface serves as a sensitive probe to the local perturbations of the electron density within the skin depth $\delta_{\text{skin}}=13\text{nm}$ induced by the acoustic pulse. Varying the pump-probe delay time makes it possible to monitor the dynamics of acoustic reflection in the plasmonic pump-probe interferogram (Fig. 2c) and extract the pump induced modulation $\delta\varepsilon + i\delta\varepsilon''$ of surface dielectric function ε (Fig. 2d). On top of the slowly increasing thermal background due to the temperature rise of gold-air interface the apparent acoustic echo in $\delta\varepsilon'$ is observed indicating the change of surface plasmon wave vector $\delta k_{\text{sp}} = \delta\varepsilon' / 2|\varepsilon|^2$. Straightforward mathematical analysis delivers the exponential shape of the acoustic strain pulse with the amplitude of $\sim 10^{-4}$. The 300 fs temporal resolution in our experiment is limited by the duration of femtosecond laser pulses and the roughness of the gold surface.

Using much thinner cobalt transducers we were able to generate sub-picosecond acoustic pulses and use them to study the intrinsic ultrasonic attenuation of longitudinal phonons in gold in the THz frequency range. The observed surprisingly long mean free path of THz phonons in gold at room temperature opens the door to the nanometer resolved acoustic microscopy in metals and a new type of acoustic spectroscopy in solids with ultrahigh (μeV) spectral resolution over the entire Brillouin zone [4].

References:

- [1] V.V. Temnov, K.A. Nelson, G. Armelles, A. Cebollada, T. Thomay, A. Leitenstorfer, R. Bratschitsch, *Optics Express* 17 (2009) 8423.
- [2] V.V. Temnov, G. Armelles, U. Woggon, D. Guzatov, A. Cebollada, A. Garcia-Martin, J.M. Garcia-Martin, T. Thomay, A. Leitenstorfer, R. Bratschitsch, *Nature Photonics* 4 (2010) 107.
- [3] D. Martin-Becerra, J.B. Gonzalez-Diaz, V.V. Temnov, A. Cebollada, G. Armelles, T. Thomay, A. Leitenstorfer, R. Bratschitsch, A. Garcia-Martin, M. Ujue-Gonzalez, *Appl. Phys. Lett.* 97 (2010) 183114.
- [4] V.V. Temnov, C. Klieber, K.A. Nelson, T. Thomay, A. Leitenstorfer, D. Makarov, M. Albrecht, R. Bratschitsch (to be published)

Figures:

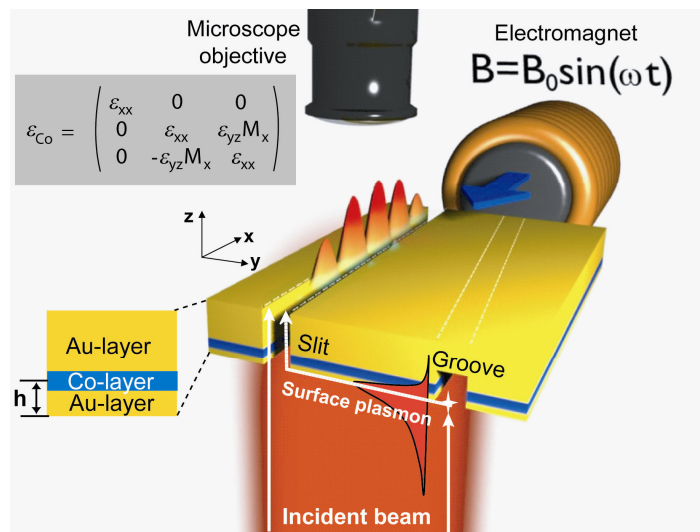


Figure 1: Active magneto-plasmonic interferometry in tilted slit-groove interferometers patterned in Au/Co/Au multilayer structures. The magnetic field of an electromagnet switches the magnetization in a cobalt layer and thus changes the wave vector of a surface plasmon propagating between the slit and the groove, see Ref. [2] for details.

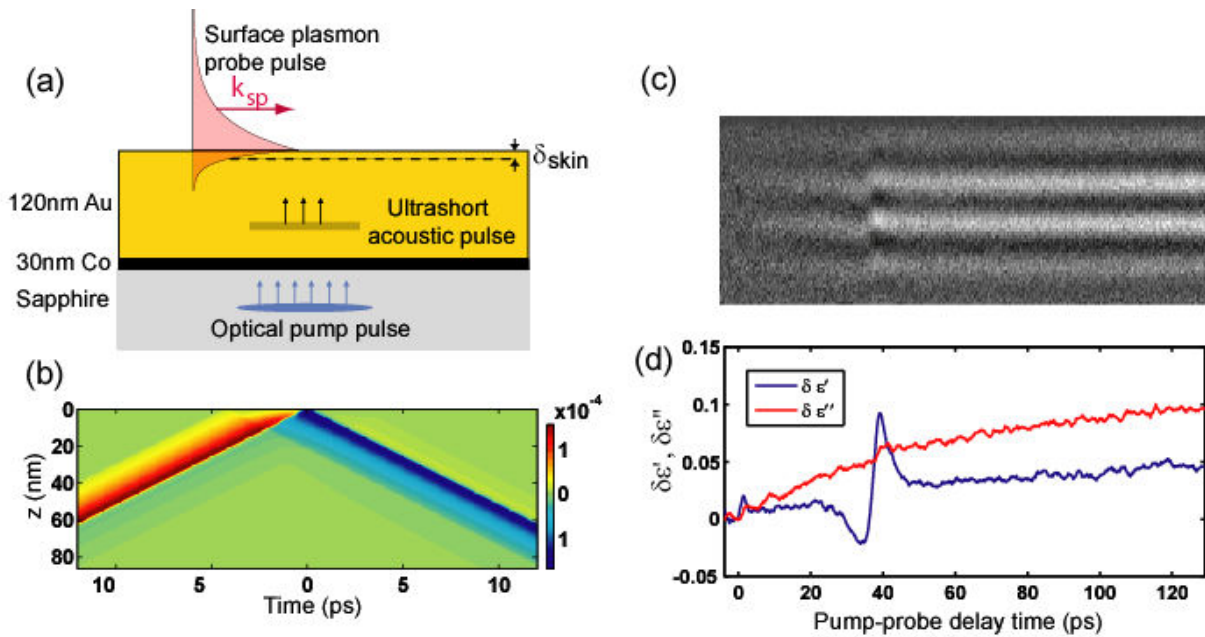


Figure 2: Femtosecond ultrasonics probed with ultrashort surface plasmon pulses. An ultrashort compressive acoustic pulse is generated by thermal expansion of fs-laser heated cobalt transducer and propagates through the gold film at the speed of sound (a). Upon reflection from gold-air interface the compressive acoustic pulse (layer with high electron density) is converted into the tensile pulse (layer with low electron density) (b). The dynamics of acoustic reflection is captured in a plasmonic pump-probe interferogram (c) and results into the pronounced modulation of the wave vector for a time-delayed femtosecond surface plasmon probe pulse (d).

DEVELOPMENT OF HIGH SENSITIVITY BIOSENSORS USING SOI PHOTONIC CRYSTAL WAVEGUIDES

J. García-Rupérez¹, **V. Toccafondo**¹, M. J. Bañuls², A. Griol¹, J. G. Castelló¹, S. Peransi-Llopis² and A. Maquieira²

¹Nanophotonics Technology Center, Universidad Politécnica de Valencia, Camino de Vera s/n, Valencia (Spain)

²Instituto de Reconocimiento Molecular, Dpto de Química, Universidad Politécnica de Valencia, Camino de Vera s/n, Valencia (Spain)
vertocca@ntc.upv.es

Integrated planar photonic devices have become one of the main candidates for the development of high performance lab-on-a-chip devices [1]. Two main advantages of these devices for sensing applications are their high sensitivity and their reduced size, which makes it possible both to detect very small analytes without the need of markers (label-free detection) and to integrate many of these devices on a single chip to perform a multi-parameter detection. Moreover, the CMOS-compatibility when fabricating these planar photonic devices on silicon-on-insulator (SOI) allows a huge reduction of their costs and increase of their production volume.

In this work, we report experimental biosensing results using SOI planar photonic crystal waveguides (PCW). The experimental results comprise refractive index (RI) sensing, label-free detection of antibodies [2] and label-free detection of single strand DNA (ssDNA) [3]. In these experiments, we have used Fabry-Perot fringes appearing in the slow-light regime near the edge of the guided band. These fringes become very sharp as we get close to the band edge, making the determination of their position more accurate, thus allowing a reduction in the limit of detection.

For the refractive index sensing experiments, we flowed several dilutions of ethanol in DIW (Deionized Water), having a RI variation between dilutions of 1.3×10^{-3} RIU (Refractive Index Units). By tracking the shift of one of the Fabry-Perot fringes at the band edge, we have obtained a sensitivity of 174.8nm/RIU and an estimated detection limit of 3.5×10^{-6} RIU (from the noise in the peak position).

For the label-free detection of antibodies, we bio-functionalized the PCW with bovine serum albumin (BSA) antigen probes (we have used 3-isocyanatepropyl triethoxysilane (ICPTES) in vapour phase for the activation of the surface). Then, we flowed the complementary anti-BSA antibody with a concentration of 10 $\mu\text{g/ml}$ during enough time to achieve a monolayer on the top of the BSAfunctionalized chip. From the wavelength shift of the tracked peaks, together with the noise level of the peak position and the surface density for a close-packed anti-BSA monolayer, we have calculated a surface mass density detection limit below 2.1 pg/mm^2 . Concerning the total mass detection limit, if the active region of the PCW is considered, a value of ~ 0.2 fg is obtained.

Finally, for the label-free detection of ssDNA, we used a similar bio-functionalization strategy in order to attach biotinylated ssDNA probes on the PCW surface. Then, we flowed ssDNA 0.5 μM complementary to the probes in the PCW surface. We have measured a peak shift of 47.1 pm. Using the noise level of the peak position, we estimated a detection limit of 19.8 nM for the ssDNA hybridization detection.

Funding from the European Commission under contract FP7-ICT-223932-INTOPSENS and from the Spanish MICINN under contracts TEC2008-06333 and CTQ2007-64735/BQU is acknowledged. Support from the Universidad Politécnica de Valencia through program PAID-06-09 and the Conselleria d'Educació through program GV-2010-031 is also acknowledged.

References:

- [1] X.D. Fan, I.M. White, S.I. Shopova, H. Zhu, J.D. Suter, Y. Sun, *Anal. Chim. Acta*, 620 (2008) 8-26.
- [2] J. García-Rupérez, V. Toccafondo, M. J. Bañuls, J. G. Castelló, A. Griol, S. Peransi-Llopis, and Á. Maquieira, *Opt. Express*, 18 (2010) 24276-24286.
- [3] V. Toccafondo, J. García-Rupérez, M. J. Bañuls, A. Griol, J. G. Castelló, S. Peransi-Llopis, and A. Maquieira, *Opt. Lett.*, 35 (2010) 3673-3675.

Figures:

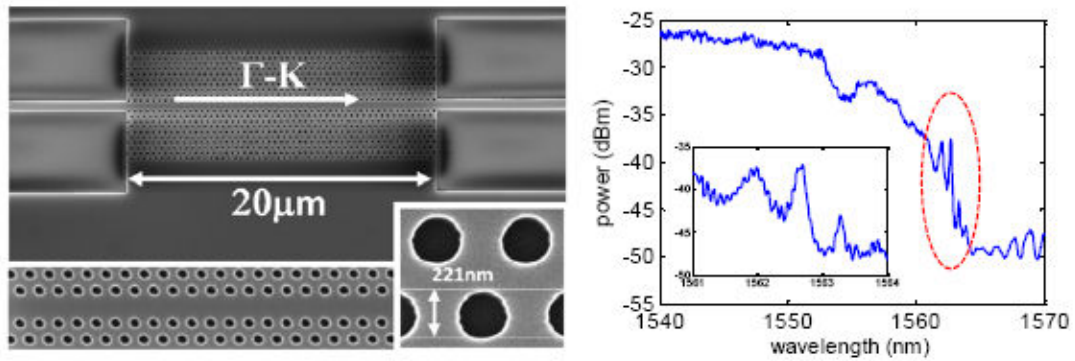


Figure 1: (Left) SEM image of one of the SOI photonic crystal waveguides used in the experiments, where a row of holes is removed in the Γ -K direction (W1-type), with close-up view of the sensor area and photonic crystal holes (insets). (Right) Spectrum of the PCW in the region of the band edge when having DIW as upper-cladding. Fabry-Perot transmission fringes at the band edge are marked with dashed red line and enlarged in the inset.

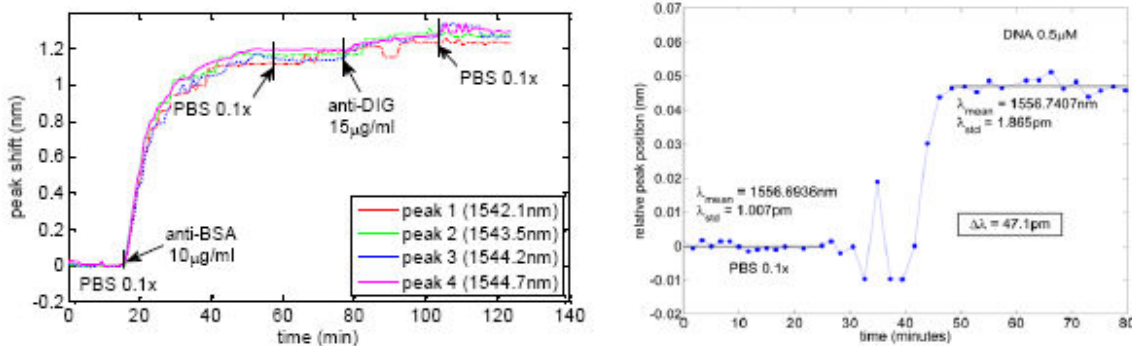


Figure 2: (Left) Wavelength shift vs time for the label-free anti-BSA 10 μg/ml detection experiment. Each line (color and style identified in the legend) correspond to the relative shift of each tracked peak respect its initial wavelength position. (Right) Wavelength shift vs time for the label-free ssDNA 0.5 μM sensing experiment.

MAGNETIC INFORMATION IN THE LIGHT DIFFRACTED BY ARRAYS OF NANOMETER-SCALE MAGNETS

P. Vavassori

CIC nanoGUNE Consolider, Tolosa Hiribidea 76, E-20018, Donostia-San Sebastián and IKERBASQUE, Basque Foundation for Science, E-48011, Bilbao, Spain
p.vavassori@nanogune.eu

A key issue in fundamental physics and data storage technology is to understand and control magnetic phenomena, which appear when systems are confined to the nano-scale. The magnetic properties of nano-scale magnetic materials are continuously investigated using a variety of experimental techniques and the ever-increasing efforts devoted to their study are leading to the development of novel systems.

Magneto-optical measurement techniques, especially the Magneto-Optical Kerr effect (MOKE), are established and widely used characterization techniques for the study of fundamental magnetism issues in thin and ultrathin film/multilayered samples. The basic observation in magneto-optics is that the optical properties of a magnetic material change with an alteration of the magnetization state.

So far the vast amount of work done using MOKE has been in a simple reflection geometry, which limits its applicability to planar structures and physical geometries. Only recently, several successful attempts have been made to extend MOKE to diffraction techniques (see Fig. 1), in order to exploit the interference effects of light being diffracted by arrays of nano-structures. This technique, called diffracted magneto optic Kerr effect (D-MOKE), in conjunction with micromagnetic simulations, demonstrated to be a powerful and non-destructive technique for investigating the spatial correlation of the magnetic spin distribution at the nano-scale in a periodic matrix of nano-structures [1].

D-MOKE has been applied to the study of broad variety of magnetic phenomena occurring in arrays of nano-particles as, e.g.: correlation of the magnetic spins distribution to effects of magnetostatic self energy and dipolar interactions [2]; magnetization reversal path and magnetic configurations in arrays subjected to competing interactions (magnetic frustration) [3].

In this talk, the experimental and theoretical aspects of obtaining the magnetic information carried by laser beams diffracted from an array of nanosized magnetic objects are reviewed. Experimentally it will be shown that MOKE hysteresis loops recorded from diffracted beams (see Fig. 2) are proportional to the magnetic form factor or, equivalently, to the Fourier component of the magnetization corresponding to the reciprocal lattice vector of the diffracted beam. It is finally shown a particular experimental implementation of D-MOKE based on magneto-optical ellipsometry techniques, which allow for the extraction of the unit cell magnetic configuration directly from D-MOKE loops without the aid of micromagnetic simulations. Evidence is given that this recent extension of D-MOKE capabilities provides a vastly improved far-field optical characterization method of the microscopic collective magnetic behavior of arrays of nano-magnets.

We acknowledge funding of the Department of Industry, Trade, and Tourism of the Basque Government and the Provincial Council Gipuzkoa under the ETORTEK Program, Project No. IE06-172, as well as the Spanish Ministry of Science and Education under the Consolider-Ingenio 2010 Program, Project CSD2006-53, IKERBASQUE, the Basque Science Foundation.

References:

- [1] M. Grimsditch and P. Vavassori, J. Phys.: Condens. Matter., 16 R275, (2004).
- [2] P. Vavassori, et al., Phys. Rev. B 67, 134429 (2003); P. Vavassori, et al., Phys. Rev. B 69, 214404 (2004); P. Vavassori, et al., Phys. Rev. B 78, 174403 (2008).
- [3] R. F. Wang et al., Nature 439, 303 (2006).

Figures:

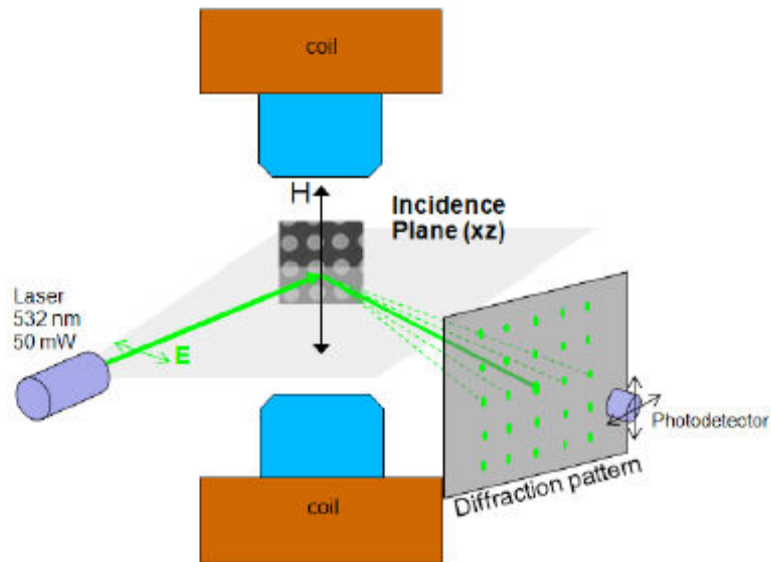


Figure 1: Schematic drawing showing the transverse MOKE configuration for recording magnetization loops at specularly reflected and diffracted beams

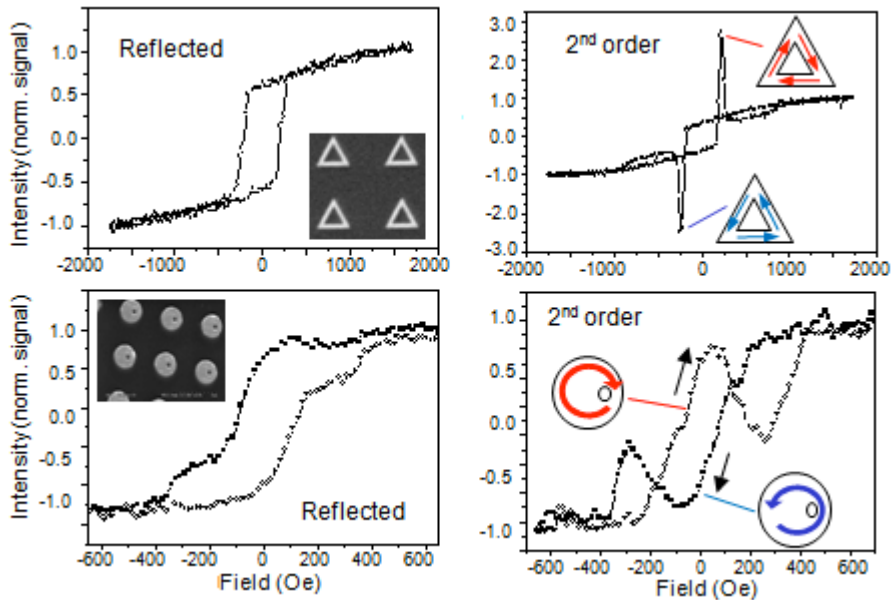


Figure 2: Examples of hysteresis loops from arrays of dots shown in the scanning electron microscopy images in the insets, showing the unusual shapes of D-MOKE with respect to conventional MOKE loops measured from the reflected beam. In the specific cases shown, the unusual shape of D-MOKE loops is related to the nucleation of magnetic vortex states of well defined chirality.

CONTROLLING FLUORESCENCE RESONANT ENERGY TRANSFER WITH A MAGNETO-OPTICAL NANOANTENNA

R. Vincent and R. Carminati

Institut Langevin, ESPCI ParisTech, CNRS, 10 rue Vauquelin,
75231 Paris Cedex 05, France

Energy transfer between a molecule in an excited state (donor) and a molecule in the ground state (acceptor) underlies many significant photophysical and photochemical processes, from photosynthesis to fluorescence probing of biological systems. Depending on the separation between the donor (D) and the acceptor (A), the process can be described accurately by various theories accounting for the electromagnetic interaction between the two species. For a D-A distance range on the order of 2 - 10 nm, which is relevant for photochemical studies and nanophotonics, the well established Förster theory [1] based on quasi-static dipole-dipole interaction has been very successful. It shows that while Förster Resonant Energy Transfer (FRET) is a very useful process which can be used, for example, as a ruler for spectroscopic measurements [2], it is a rather weak process which goes down as the inverse sixth power R^6 of the D-A separation [3].

In the present work, we use an established general framework for dipole-dipole energy transfer between an emitter and an absorber in a nanostructured environment [4]. The theory allows us to address FRET between a donor and an acceptor in the presence of a nanoparticle with an anisotropic electromagnetic response. Using Green function formalism [5], we show that the angular contribution, the distance behavior and the influence of the polarizability tensor of the nanoparticle can be identified and separated.

We also compare the contribution of the different non-radiative energy transfer channels: The direct (standard) Förster transfer and the energy transfer mediated by the nanoparticle. In this comparative study a new distance arise, in the spirit of the Förster radius, named polarization coupling radius R_p , which depends of the polarization properties of the nanoparticle.

We illustrate the formalism for the well known metallic nanoparticle, showing that this formalism could furnish insight in the understanding of the good quantities controlling this process and also for nanoparticle with anisotropic dielectric responses [6], e.g., nanoparticle made of a ferromagnetic material exhibiting a magneto-optical response. For which the degree of anisotropy can be controlled by an external static magnetic field. We discussed potential application for FRET tuning.

References:

- [1] T. Förster, *Ann. Phys.* 437, 55 (1948); *Discuss. Faraday Soc.* 27, 7 (1959).
- [2] L. Stryer, *Annu. Rev. Biochem.* 47, 819 (1978).
- [3] L. Novotny, B. Hecht, *Principles of Nanooptics*, Cambridge University Press, (2006).
- [4] R. Vincent, and R. Carminati, *Magneto-optical control of Förster energy transfer*, *Phys. Rev. B*, in press, (2011).
- [5] R. Carminati, J.-J. Greffet, C. Henkel and J.M. Vigoureux, *Optics Communications*, 261, 2, 368 - 375, (2006).
- [6] S. Albaladejo, R. Gómez-Medina, L. S. Froufe-Pérez, H. Marinchio, R. Carminati, J. F. Torrado, G. Armelles, A. García-Martín, and J. J. Sáenz, *Opt. Express* 18, 3556-3567 (2010).

